**Strathclyde Institute of Pharmacy and Biomedical Science**

# Polymorphism of Polymeric Drug Excipients at High Pressure

Alice Turner 201380816

MRes Drug Delivery Systems

2014

Word Count: 22,220 words

Signed: 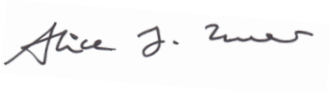 Date: 21/10/14

Alice Turner

This thesis is the result of the author's original research. It has been composed by the author and has not been previously submitted for examination which has led to the award of a degree.



Signed: 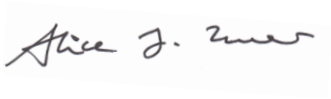 Date: 21/10/14

Alice Turner

## Abstract

The aims of the current study were to investigate the effect of pressure on polyethyelene glycol (PEG4000) to create an effective drug delivery system for poorly water soluble drugs, with a view to increasing their bioavailability. The effect of pressure exerted by a diamond anvil cell on PEG4000 and the model drug respectively, and the polymer and drug together were examined using Raman and infrared spectroscopy. PEG4000 was shown to melt at 5GPa using a diamond anvil cell, as exemplified by flowing. Hydrocortisone does not melt under pressure or physically change and thus could be effectively encapsulated in the PEG at high pressure. Differential scanning calorimetry was carried out on the samples. PEG4000 was observed to melt over an average range of 58.67 to 63ºC and hydrocortisone was observed to melt over an average range of 223.49 to 228.15ºC. The latter was observed to change from a white powder into a marigold yellow liquid. Thermogravimetric analysis revealed degradation occurred at temperatures distinct from the melting range, thus when PEG melts at high pressure it is not degrading. Drug release testing was carried out on the diamond anvil cell samples in simulated intestinal and gastric fluids over 8 hours in a pulsatile fashion, mimicking traditional cortisol replacement therapy but with one administration rather than multiple administrations daily. Scale up using a large volume press was investigated. Drug release occurred over 10 days in a similar pulsatile fashion to the small volume study. Unfortunately due to the highly unstable nature of hydrocortisone in aqueous solutions future work may require the use of stabilisers such as fructose or disodium edentate. Overall PEG does increase the solubility of poorly soluble drugs but further work could be carried out in terms of formulation.

## Contents

# Chapter 1: Introduction

### *1.1 Basic Principles of Poorly Soluble Drugs*

Poorly water-soluble drugs cause a number of problems in drug delivery. Due to their inability to dissolve in the gastrointestinal fluids, they fail to be fully absorbed from the gastrointestinal tract. This can cause inadequate and irregular introduction of the drug into the systemic circulation, resulting in poor bioavailability (Blagden et al., 2007). Currently more than 40% of currently available drugs have this problem (Roberts and Zhang, 2013), including drugs such as griseofulvin, digoxin, phenytoin, sulphathiazole, hydrocortisone and chloramphenicol (Leuner and Dressman, 2000). 70% of drugs being developed in recent years have exhibited poor solubility and thus the problem is on the rise (Ku and Dulin, 2012). This has been attributed to the increasing number of complex synthetic compounds being produced (Kawakami, 2012). These drugs can be characterised by the Biopharmaceutical Classification System.

In the Biopharmaceutical Classification System, drugs are categorised based on their ability to dissolve and be absorbed. These fall into Classes I, II, III and IV. Class I has hydrophilicity and lipophilicity, allowing dissolution and absorption. Class II drugs, or hydrophobic drugs, have a lack of dissolution capability but can be well absorbed. Class III drugs, have the ability to dissolve in the aqueous gastrointestinal fluid, but cannot be absorbed into the surrounding tissues. Class IV lack both dissolution capability and absorption capability. Class II drugs are a greater area of interest in oral drug development currently due to the fact they are inhibited by their inability to dissolve in the gastrointestinal fluid but, unlike Class IV, they can be absorbed once dissolution has been facilitated through formulation (Sant et al., 2004).

Poor solubility causes problems with patient compliance as it can necessitate greater volumes of drug to be administered or shorter dosage intervals (Roberts and Zhang, 2013). This is required as the volume of drug entering the blood stream and thus the blood concentration of the drug needs to be sufficient to be within the therapeutic

index for reasonable pharmacology to occur. This can result in adverse effects due to the higher than normal dose present in the gastrointestinal tract (Kawabata et al., 2011).

### *1.2 Oral Drug Delivery of Poorly Soluble Drugs*

Drug release of hydrophobic agents commonly happens in the particle state, primarily by erosion and as such dissolution largely happens after release of drug particles into the gastrointestinal fluid (Tahara et al., 1996). Oral drug delivery is the preferred method of administering medication as it allows self administration and accurate dosing which makes it a cheaper and easier method of administration than other dosage forms (Vasconcelos et al., 2007). As such it is beneficial to improve the solubility of hydrophobic drugs to allow oral dosing with good bioavailability. The bioavailability of poorly soluble drugs contained in delivery formulation is dependent on the solubility evoked by the drug delivery system as the bioavailability of the drug alone is so poor (Pouton, 2006). As such polymers are a major area of interest for drug delivery of poorly water-soluble drugs.

Polymers are defined as substances consisting of macromolecules, which are constructed from a replicating pattern of smaller molecules, known as monomers, connected with covalent bonds (Jenkins et al., 1996). Polymers were discovered in the early 20$^{th}$ century due to the interest of scientists in the skill of nature to construct substances which were of use to humans, such as cotton, rubber and silk. Initially scientists believed these substances to consist of large structures made up of noncovalently clustered small molecules. However in 1920, Staudinger changed this view dramatically by stating his belief that covalently bonded high molecular weight molecules were in fact the main components of these substances and that this property was essential for the characteristics of the overall structure. Eventually Staudinger's work into synthetic polymers earned him the 1953 Nobel Prize for Chemistry (Serpe and Craig, 2007). Synthetic polymers are now used more frequently than natural ones due to the increasing ability to mimic the properties of their natural counterparts and the ease and cost effectiveness of production in the lab.

Polymers can fall into a number of categories based on their components. A homopolymer is defined as one which consists solely of one type of monomer. A copolymer is one which is made up of multiple types of monomer. This latter category can also be described in terms of the number of monomer types, such as bipolymers for those consisting of two types, terpolymers for those consisting of three types and quaterpolymers for those consisting of four types. There can also be what is described as a pseudo-copolymer. Although this is like a homopolymer in that it consists of only one monomer type, it has a structure more similar to that of the copolymers due to the uneven nature of the macromolecules making up the individual monomers. Likewise they can be defined by the presence of particular types of macromolecules, such as block macromolecules, which can form part of block copolymers. A block macromolecule is defined as groups of many atoms working together, organised as structures known as blocks, which are covalently linked and configured in a linear formation (Jenkins et al., 1996).

Structurally, polymers can also have a number of different architectures, such as linear, graft or brush, hyperbranched, star, block co-polymer and dendrimer (Figure 1).

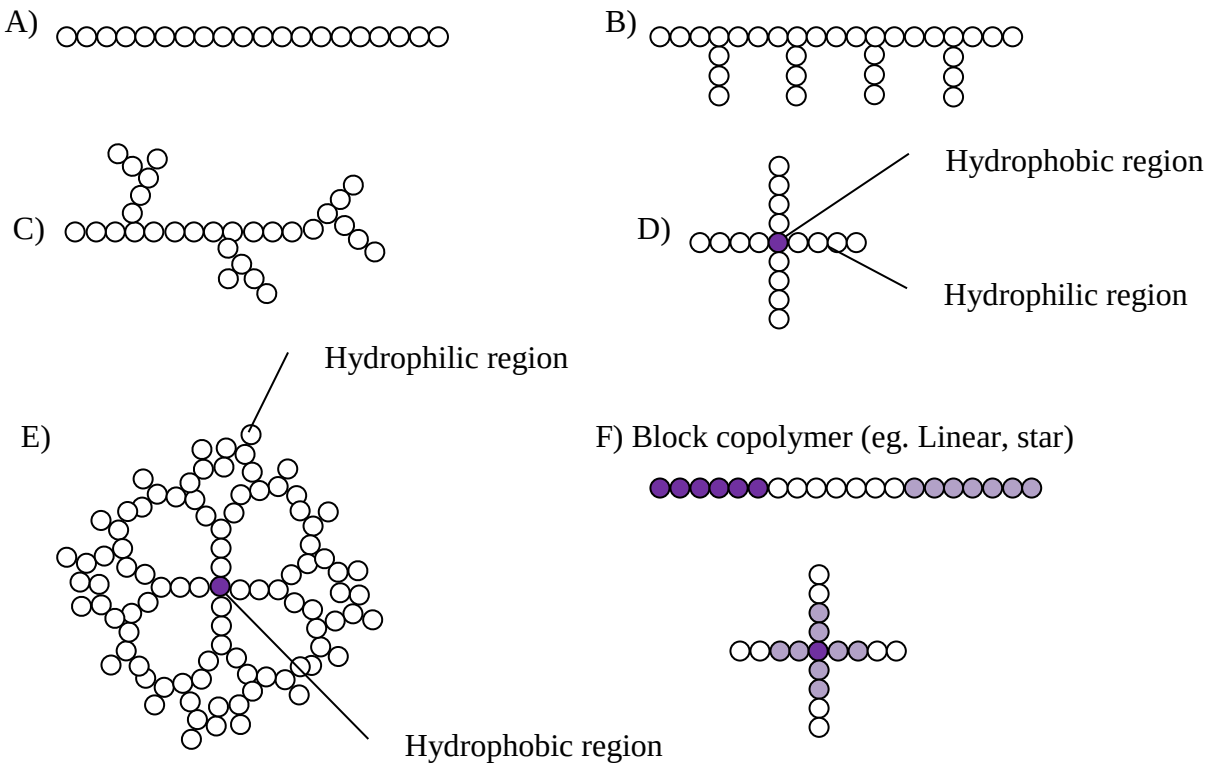


Figure 1: Polymer Architectures: A) Linear polymers, B) Graft polymers, C) Hyperbranched polymers, D) Star polymers, E) Dendrimer polymers and F) block copolymers

The form of a polymeric molecule can dictate its physicochemical properties, such as tolerance to varying pH and temperature, solubility, permeability and viscosity (Qui and Bae, 2006). Linear molecules are the most basic structure, consisting solely of chain with no branches (Jenkins et al., 1996). These have a number of advantages in that they can form random coils and the ability to effectively link drug molecules to the backbone (Qui and Bae, 2006). Polymers can also be branched in nature, as exhibited by a number of structures. A graft structure is made up of polymeric main chain with many polymer side-chains, creating a highly branched structure (Li et al., 2013). Block co-polymers are described as structures with two or more sections in the backbone which can exhibit either solubility or insolubility. However these are less useful as their ability to move is limited (Qui and Bae, 2006). A hyperbranched structure consists of an unsystematically highly branched molecule, with a partially yielding globular configuration, which can covalently bind drugs to its surface (Kolhe et al., 2004, Kirkorian et al., 2012). A star structure exhibits hyperbranched character, consisting of linear arms radiating from a centre point. This central core can exhibit hydrophobic character while the arms tend to be hydrophilic making it useful to carry poorly soluble drugs (Qui and Bae, 2006). A dendrimer exhibits a three-dimensional structure consisting of branching units radiating out from a central point, within which a poorly soluble drug can be contained (Gillies and Fréchet, 2005). Their dimensions can be determined by synthetic methods and other alterations can be used to increase biocompatibility and biodegradability (Suttiruengwong S. et al., 2006). The latter two forms are more efficient methods of transporting hydrophobic drugs as the drug is able to be encapsulated in the centre of the formulation surrounded by a hydrophilic polymer. However, these architectures are only one level of polymer organisation; a further level is observed in the structures they take at a higher level.

Polymers can be used in a number of configurations to create oral formulations such as reservoir, microparticulate, nanoparticulate, micellular and polymer-drug conjugate forms. Reservoir based systems are also a widely used polymeric system. In this formulation type the active pharmaceutical ingredient is contained inside a

polymer barrier layer in the form of a film (Yang and Pierstorff, 2012). This form of system is most commonly used as part of an injectable dosage form or slightly less commonly as part of an implant, however there is recent research into its use orally (Figure 2). Alza Corporation introduced a reservoir oral osmotic dosage form known as OROS®. It consists of a capsule coated with an unyielding semi-permeable membrane with a 0.5-1.4mm laser-drilled hole. Following swallowing, the aqueous gastrointestinal fluid passes through the semi-permeable membrane into the reservoir and the active ingredient leaves the system through the drilled hole as the osmotically active polymers swell (Stevenson et al., 2012). This could potentially be used to improve delivery of poorly soluble drugs.

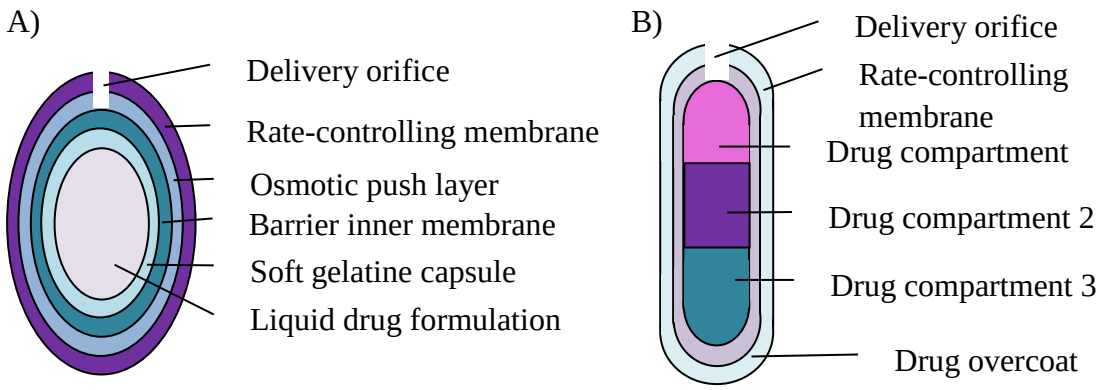


Figure 2: Examples of reservoir systems include A) L-OROS and B) Tri-layer capsules (Stevenson et al., 2012)

Delivery of poorly soluble drugs can also be significantly improved through the use of polymeric nanoparticles and microparticles. The solubility increase in both of these can be greatly attributed to the increase in surface area generated by the reduced particle size (Lee et al., 2010, Kumar et al., 2011). In nano and microparticulate systems the drug can be dispersed throughout the polymer during production of the particles or absorbed on to the surface of the particles by dipping the particles into a concentrated solution of drug (Agnihotri et al., 2004). The active pharmaceutical ingredient can be covalently bound to either type of particle. Nanoparticles are defined as being systems which are largely used at a size range of 3-200 nm, and have the advantage of being able to be altered in size to change rates of release and thus delivery times of drugs (Cho et al., 2008). Nanoparticles can be subdivided into nanocapsules and nanospheres (Figure 3).

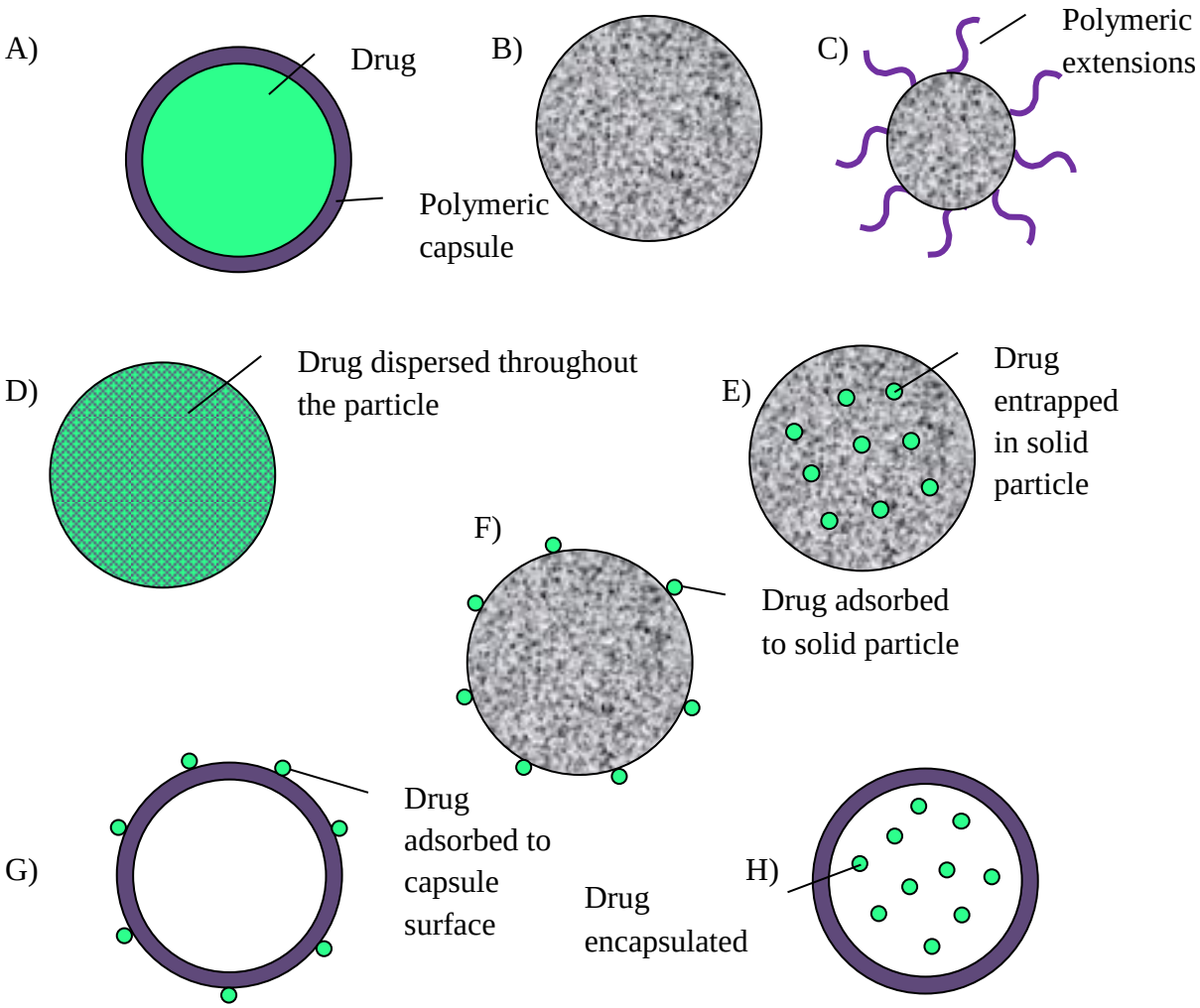


Figure 3: Micro and nanoparticle structures: A) capsule, B) solid particle, C) solid particle with polymeric extensions, D) solid particle with the drug dispersed, E) solid particle entrapping a drug, F) solid particle with the drug adsorbed to the surface, G) capsule with the drug adsorbed to the surface and H) a capsule containing a drug at its core

Nanocapsules (Figure 3A) are vesicle like structures which consist of a polymer layer encapsulating a central hollow where the drug is contained. In nanospheres however the drug is scattered throughout a polymer matrix (Figure 3D) (Soppimath et al., 2001). Nanoparticles should have a net hydrophilic character to allow efficient transport of the drug, which can be achieved through a hydrophilic surface coating, with a polymer such as polyethylene glycol, or using block copolymers with a combination of hydrophobic and hydrophilic properties but the latter having the greatest influence. Examples of polymeric nanoparticle systems include polyglycolic acid (PGA) for use in delivery of camptothecin and N-(2-hydroxylpropyl) methacrylamide (HPMA) for delivery of doxorubicin (Cho et al., 2008).

Microspheres preferably have a particle size lower than 200μm, ranging in dimensions from 0.1-200μm (Madhav and Kala, 2011). Microcapsules have a similar structure to nanocapsules. Microcapsules can have one cavity, known as monocored microcapsules, or more than one cavity, known as polycored microcapsules. They can also have the drug incorporated into the polymeric layer, known as matrix type polymeric microcapsules. As with nanospheres, microspheres exhibit a structure which consists of the active pharmaceutical ingredient being scattered throughout a polymer matrix (Figure 3E). Very different release profiles can be observed in these compared with microcapsules due to their different structures (Kumar et al., 2011). Examples of poorly soluble drugs which can be effectively carried in microparticles include paclitaxel, aclacinomycin and camptothecin (Takale et al., 2012).

Polymeric micelles are useful as another method of delivering a number of drugs (Figure 4). The dosing method is made up of an outer water-soluble layer, surrounding a drug and excipient-based hydrophobic centre, which makes it a highly suitable system for delivery of poorly-soluble drugs (Kim et al., 2009, Kim et al., 2011). Hydrophobic splinters of amphiphilic molecules are found within the central cavity of a micelle, which can be used to increase the solubility of hydrophobic drugs. Hydrophilic polymers such as polyethylene glycol are used to form the outer layer of the micelle, while hydrophobic polymers, such as those consisting of propylene oxide, aspartic acid and spermine monomers, are used to form the central cavity in which poorly soluble drugs can be encapsulated (Torchilin, 2004). Many polymers have been used to construct self-assembled micelles, the majority of which are linear block copolymers. These have main chains consisting of polymers such as polyethylene glycol, poly(N-vinyl-2-pyrrolidone) and poly(vinyl alcohol), with hydrophobic sections consisting of polymers such as polyester and poly(amino acid)s (Guo et al., 2012). An example of micelles used for hydrophobic drugs is detailed in a recent study where the solubility of the poorly soluble anti-cancer agent paclitaxel was improved by encapsulation in a water-soluble polymeric micelle system based on poly(2-(4-(vinylbenzyloxyl)-N,Ndiethylnicotinamide)and polyethylene glycol block copolymers (Huh et al., 2005). Examples of other poorly soluble agents which

have shown improved solubility and delivery capacity on micellation include diazepam, indomethacin, adriamicin and polynucleotides (Torchilin, 2004).

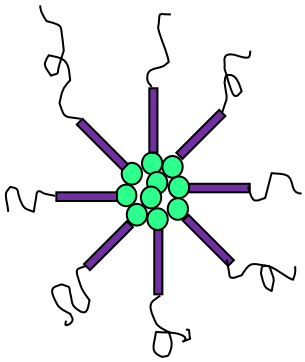

Figure 4: Structure of micelles, with the drug in green encased in a central core surrounded by hydrophobic blocks in purple and hydrophilic blocks represented by the lines extending from these purple blocks.

Polymer-drug conjugates are another effective method of delivering poorly soluble drugs (Figure 5). Generally the conjugated form is a prodrug, which, via acid/base hydrolysis or enzyme cleavage, can release the original drug when required (Kim et al., 2009). The active pharmaceutical ingredient can be attached straight on to a polymeric backbone or indirectly so through a linker, which may or may not be able to be broken down in the body. The polymeric backbone majorly affects the pharmacokinetics and pharmacodynamics of the agent and thus it imparts solubility on the hydrophobic drug (Markovsky et al., 2012). A significant example of this is the use of polyethylene glycol in conjunction with a chemotherapeutic polypeptide molecule as a potential cancer treatment such as PEG-IFN-α (Fox et al., 2009, Narang and Varia, 2011).

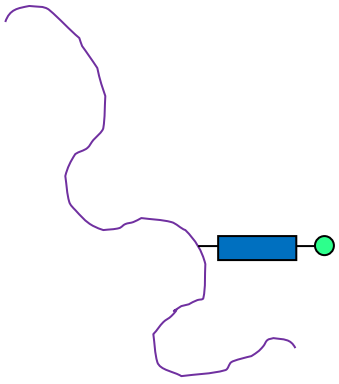

Figure 5: Basic structure of a polymer-drug conjugate, consisting of a polymer backbone in purple, a linker group in blue and a drug molecule in green

Polymers used for oral drug delivery of poorly soluble agents can also be divided up into a number of types at a further level of structural integrity. This level of structure includes diffusion-controlled systems, solvent-activated systems, chemically controlled systems and magnetically controlled systems. The former can be either in the form of reservoir systems (Figure 2) or matrix systems (Figure 6). However due to the risk of rupture and resultant dose dumping, matrix systems are preferred as the drug is evenly distributed throughout the medium and thus the drug is released at a more constant rate.

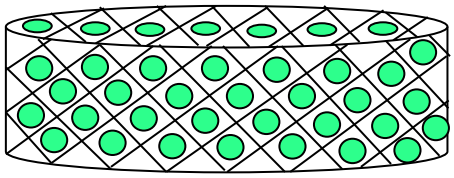

Figure 6: Matrix structure with drug evenly distributed throughout the tablet in green

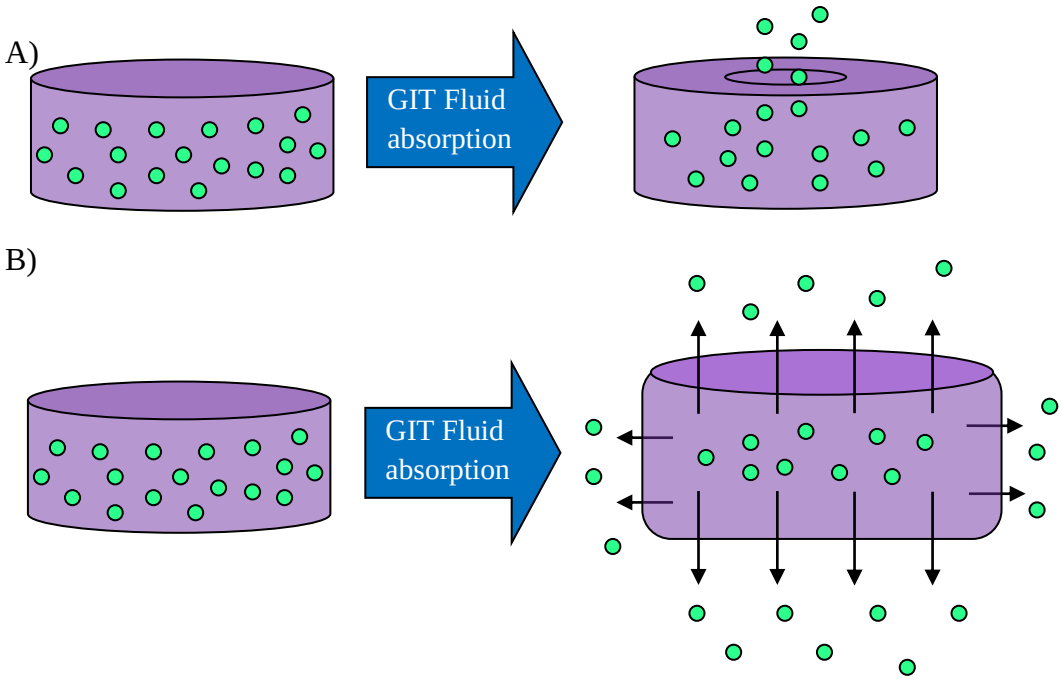


Figure 7: Solvent Activated Systems can be divided into A) Osmotically-controlled and B) Swelling-controlled models. In A) it can be observed that the gastric fluid (shown as blue arrows) forces the drug out of a hole in the tablet surface, and in B) it can be observed gastric fluid is absorbed, causing the system to swell and become permeable to drug release.

Solvent-activated systems can be divided into osmotically controlled systems and swelling-controlled systems (Figure 7). In the former, the gastrointestinal fluid moves from a low concentration of drug out with the system to a high concentration of drug inside the system. The increased fluid inside the system forces the drug out of a crack in the system. In swelling-controlled systems, the
polymer absorbs water, becoming turgid without dissolving in the fluid. The system exhibits permeability which allows the drug to be released through the swollen polymer layer. Magnetically controlled systems are made up of albumin and magnetic microspheres, which give the system a targeting capacity which is useful in cancer chemotherapy.

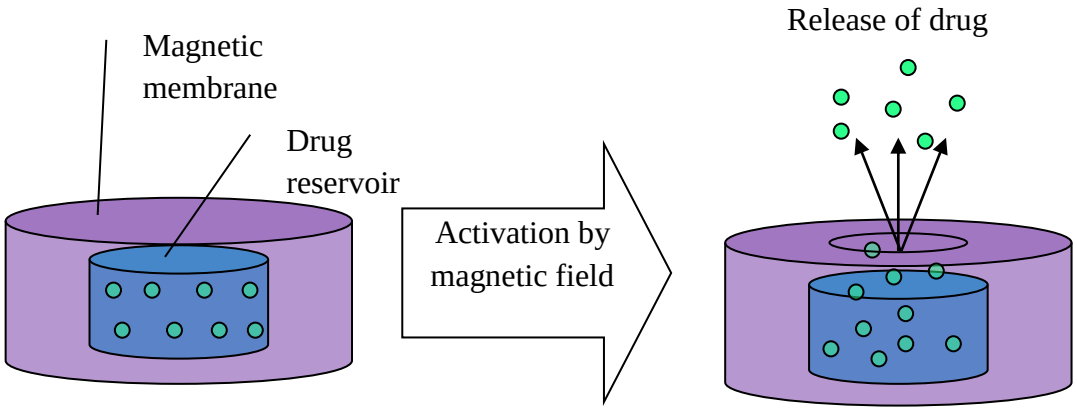


Figure 8: A magnetic field triggers drug release from magnetically controlled systems with the drug illustrated in green and the controlling membrane in purple.

Release of the drug is triggered by a magnetic field (Figure 8). Chemically controlled systems can also be categorised into “pendent-chain” systems and biodegradable systems (Figure 9). The former involves the drug being chemically linked to the polymer backbone, and drug release happens via chemical hydrolysis or enzymatic degradation. In the latter, like the matrix systems the drug is distributed throughout the system and as the polymer breaks down by erosion the drug is gradually released. Due to the fact, unlike some polymer systems (Kopeček, 1990), this form breaks down in the gastrointestinal fluid and does not need to be removed from the body due to potential toxicity and has been shown in the past to be the most effective for delivery of poorly soluble drugs this is very likely to be the main type of system used for this purpose in the future (Ranade and Hollinger, 2004).

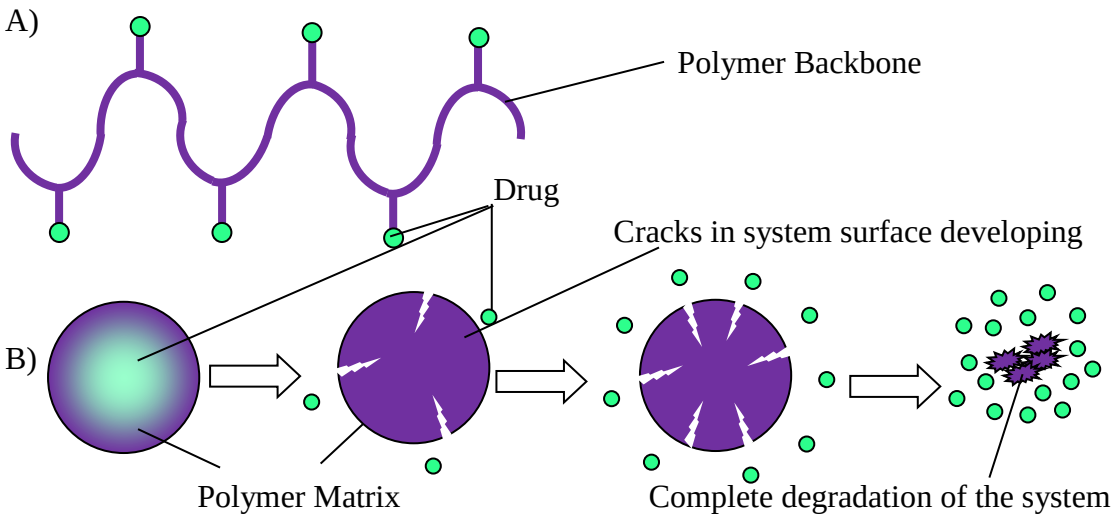


Figure 9: Chemically Controlled Systems fall into two categories A) Pendant chain systems and B) Biodegradable systems

### *1.3 Polyethylene Glycol*

The current study will use the well established hydrophilic polymer polyethylene glycol (PEG, see Figure 10) as a medium for creating a drug delivery system to increase the water solubility of poorly water soluble drugs. PEG has a number of advantages as a currently used excipient and as such is the polymer which is most commonly incorporated into drug delivery systems. These largely include the fact it has been deemed clinically safe, it is not costly to manufacture and it can behave in a stealth-like manner, allowing it to pass through the body without being regarded as foreign by the immune system (Knop et al., 2010).

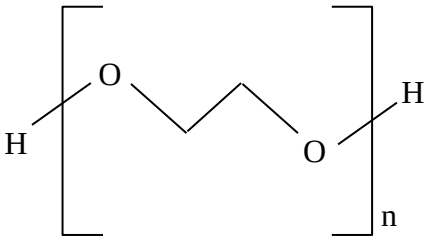


Figure 10: Chemical structure of polyethylene glycol

Polyethylene glycols (PEG) are made up of ethylene oxide monomers (Figure 10) and usually have molecular weights around 200-300,000g/mol. In the context of delivery systems polyethylene glycol is generally applied at molecular weights of

1,500-20,000g/mol. The greater the molecular weight the greater the thickness of the polymer's consistency, which can be a key determinant in the rate of drug release as their solubility is inversely proportional to molecular weight (Leuner and Dressman, 2000). Largely the melting points of polyethylene glycols are less than 65°C, making them suitable for production of delivery systems using melt techniques. For example PEG 1000 has a melting point of 30-40°C, while PEG 20,000 has a melting point of 60-63°C (Price et al., 1994). Ideally for drug incorporation the polyethylene glycol should have a molecular weight that is high enough to impart sufficient water solubility on to the drug without having the issue of water being absorbed and held in the medium and a melting point above 50°C. If a polyethylene glycol with too small a molecular weight is applied, the polymer can exhibit a gummy texture making it difficult to create a suitable formulation. However higher molecular weights have proved more successful in increasing solubility of hydrophobic drugs (Leuner and Dressman, 2000, Li and Jasti, 2005).

It has been shown that the ability of PEG to increase solubility is so great that even quite a soluble agent like aspirin can have its ability to dissolve improved still further by incorporation into polyethylene glycol 6000 (Asker and Whitworth, 1975). In their matrix form they are broken down from the outside in and usually do not puff up or crumble in water-based media, allowing drug release can be regulated relatively simply. It can be used to increase the solubility of hydrophobic drugs because its water soluble polymeric chain has a wide hydrodynamic radius in water-based media, enhancing hydrophilicity (Li and Jasti, 2005). There are a number of examples of using polyethylene glycol to increase water solubility.

The use of polyethylene glycol to improve the solubility of griseofulvin, which is a virtually insoluble drug and useful oral antifungal agent, has been well studied. In an early study incorporation of the drug into solid dispersions with PEG 4000, 6000 and 20,000, was shown to significantly increase drug release and thus dissolution in the gastrointestinal fluids (Chiou and Riegelman, 1969). Gris-PEG is a commercially available griseofulvin preparation which has been released in recent years using PEG 6000 and has been used clinically to great success (Janssens and Van Den Mooter,

2009). In combination with polysorbate 80, PEG 3350, was shown to enhance the bioavailability of a poorly water soluble drug 21-fold relative to the drug alone (Joshi et al., 2004). As mentioned previously dendritic and star polymer architectures form the best carrier structures for hydrophobic drugs. In the context of polyethylene glycol a recent study has shown the poorly soluble anticancer agent paclitaxel and other hydrophobic drugs are solubilised most effectively using these structures (Ooya et al, 2003).

In the current study PEG4000, which has an estimated melting point of 58-61°C, has been selected as a polymer to increase the solubility of poorly soluble drugs. It was shown previously to increase the solubility of the poorly soluble drug Zolpidem® from 0.25mg/ml in a pure drug sample to 1.65mg/ml in a 30:70 PEG:drug solid dispersion (Trapani et al., 1999). Due to this efficiency it is thought PEG4000 will make a suitable polymer to solubilise the model drug in this study.

### *1.4 The Model Drug*

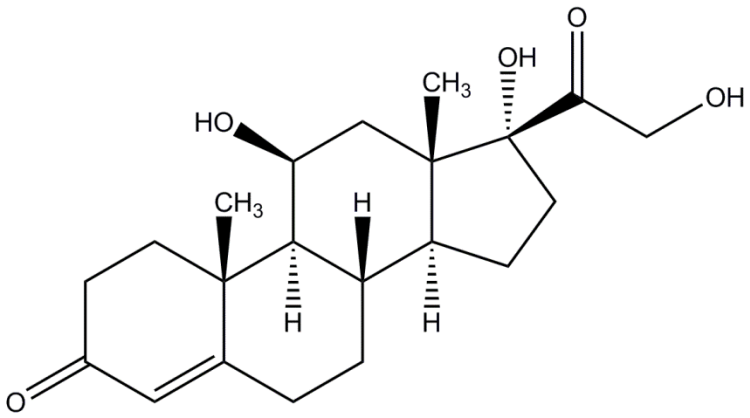


Figure 11: Chemical structure of hydrocortisone

Hydrocortisone (Figure 11) is classified in the British Pharmacopoeia as only slightly soluble in water (0.002M approximately as found by Foroutan and Watson, 1997) and thus is suitable to demonstrate the ability of polyethylene glycol to increase solubility. Hydrocortisone can be used for treatment of acute adrenal insufficiency, chronic primary adrenal insufficiency, secondary adrenal insufficiency and

congenital adrenal hyperplasia. As an extension of this it can also be used for management of rheumatic disorders, kidney conditions, asthma, allergies and other inflammatory conditions (Abad-Santos et al., 2002) as cortisol is vital for intermediate metabolism, the immune system and the muscular-skeletal system (Johannsson et al., 2009). It has also been suggested as a method of treating the depression and anxiety occasionally associated with smoking cessation as there is a marked fall in cortisol in individuals who have given up smoking (Ussher et al., 2011). However its primary use is for issues either at an adrenal or pituitary level.

Adrenal impairment can be caused by primary adrenal malfunction due to autoimmune disease or tuberculosis effects, or as a side effect of adrenal gland removal (Simon et al., 2010). Central reduction in cortisol can also occur as a result of reduced action of the pituitary gland, for example due to tumour growth (Johannson et al., 2009). As a result of this hydrocortisone seeks to mimic natural cortisol release.

Naturally the hypothalamus, mediated by the paraventricular nucleus, would excretes a hormone which would trigger release of corticotrophin from the pituitary, which in turn stimulates release of cortisol from the adrenal glands (Johannsson et al., 2007). Once the cortisol reaches a certain level it exerts negative feedback upon the hypothalamus and pituitary to prevent excess release and development of conditions such as adrenal hyperplasia and excessive testosterone secreation.

One major risk of the use of hydrocortisone as a glucocorticoid replacement therapy is hypercortisolism, which results in reduced glucose tolerance and development of insulin resistance. Oral drug delivery has been suggested for hydorocortisone as it does not raise insulin resistance or reduce glucose tolerance as much as a typical parenteral dose regimen (McConell et al., 2002).

There is much debate about the preferable dose for oral use as cortisol is released naturally on a circadian rhythm with the greatest release occurring on waking and decreasing over time until it reaches its minimum around midnight (Johannsson et

al., 2007). As such a dose regimen of hydrocortisone should try to mimic this as far as possible whether taking the form of a controlled release model or involving multiple dosing. The estimated volume of cortisol released in each individual can vary between approximately 10 and 30mg daily (Abad-Santos et al., 2002). This can vary as a result of genetics as well as stress factors such as exercise, fever, surgery or, mental or emotional stress (Johannsson et al., 2007). Some papers suggest a 30mg dose as standard (Abad-Santos et al., 2002) however some other literature suggests lower doses. For example McConell et al. suggest 15mg in the morning and 5mg in the evening as this lower dose was observed to result in less insulin resistance in patients (McConell et al., 2002). Simon et al. (2010) also suggest a 25mg dose, with around 66% being administered in the morning and around 33% in the afternoon. This will be taken in to account in the current study.

### *1.5 High Pressure Phase Transformation*

There is increasing interest in exposure of polymers to high pressure conditions (Xiong and Kiran, 1998). High pressure can be utilised to bring about a large variety of alterations to the structure of soft material substances, from generating phase transformations in polymers to inducing formation and breakdown of tertiary structures in proteins (Brooks et al., 2010). This study is concerned with the phase transformation of polymers which is associated with polymorphism. Polymorphism is a term which originates from the Greek for being present as numerous different structures. In the context of chemistry and by extension pharmaceutical sciences, polymorphism largely refers to the different crystalline forms a substance can take. Each polymorph of a substance can have very different properties such as melting points, dissolution rate, stability, solubility and density. In the context of pharmaceuticals these properties can have significant effects on drugs' ability to be absorbed, their bioavailability in the body and formulation of effective drug delivery systems to carry them (Fabbiani and Pulham, 2006). In the context of the current study the ideal polymorph for use in a delivery system should possess sufficient water solubility to allow the drug to dissolve and thus should be a less stable polymorph. Solubility is determined by the form the substance takes, because different states of the substance will have distinct energies and thus distinct

solubilities. As an extension of this it can result different bioavailabilities evoked on the encased drug (Threlfall, 1995).

High pressure still continues to be an underused method of inducing phase transformation because of its technical intricacy (Brooks et al., 2010). However it is a growing field. For example high pressure can result in production of a number of different polymorphs from the one original molecule. For example high-pressure recrystallisation of aqueous and methanolic solutions of piracetam (2-oxo-pyrrolidineacetamide) can be carried out in a diamond avil cell at 0.07–0.4 GPa resulting in the production of a novel polymorph of piracetam. Reduction in pressure once more to ambient conditions can result in the generation of a further form via a single-crystal to single-crystal transition (Fabbiani et al., 2005).

Molecular compounds generally stay intact at high pressure. For example Funnell et al. (2011) observed that pressure does not have much of an effect on alanine until it reaches 13.6 GPa. At 15.46 it goes through a phase change from a crystalline to an amorphous state, which, unlike some phase changes, is reversible (Funnell et al., 2011). Another example of high pressure work is the polymerisation of lactide in which the room temperature crystalline state is constant until 17.3 GPa at 26.85°C (Ceppatelli et al., 2011). Polymers also have been previously studied at high pressure (Fang and Kiran, 2006).

The application of pressure can directly influence the properties of polymers as exemplified in a number of studies. For example via X-ray diffraction and differential scanning calorimetry, the crystalline character of low density polyethylene was observed to be enhanced from 42 to 58% when placed under 800MPa using hydrostatic high pressure processing for 5 minutes at 75ºC, and the crystalline character of PETA1Ox was raised from 28.5 to 36.3% to induce hydrostatic pressures of 500MPa for 15 minutes at 50ºC (Fleckenstein et al., 2013). In another study, on exposure to high pressure between 7 to 50MPa, the polymer syndiotactic polystyrene undergoes a liquid-liquid phase separation and forms a range of different crystalline structures (Fang and Kiran, 2009). In a further study,

isotactic poly (4-methyl-1-pentene) in *n*-pentane and, *n*-pentane and carbon dioxide mixtures was found to phase separate at pressures between 10 and 50MPa. Three different polymorphological changes were observed involving solid-solid phase transitions, resulting in a tightly packed crystalline structure formed at the higher end of the pressure range. On addition of carbon dioxide to isotactic poly (4-methyl-1-pentene) a more hollow structure was observed (Fang and Kiran, 2006).

The importance of pressure to the melting points of homo and copolymers such as HDPE, LDPE, PP and ethylene vinyl acetate have also been studied up to 330MPa using nitrogen atmospheric pressure and a high pressure differential thermal analysis cell. It was found the melting point rises proportionally to the pressure induced on the polymers (Seeger et al., 2004). In a further study using high pressure, the water uptake and turgor of poly(*N*-isopropylacrylamide) and poly(*N*-isopropylacrylamide)-poly(*N*,*N*-diethylacrylamide) originated microgels were investigated at high pressure and it was found the turgid state was preferable at high pressure to the deflated state (Pühse et al., 2010).

A previous high pressure study of polyethylene glycol largely focused on the effect of vapour pressure induced by countercurrent circulation system on the polymer's ability to solubilise in carbon dioxide. This study showed it can cause a fall in solubility in proportion to molecular weight (Daneshvar et al., 1990). This may be promising evidence for the current study.

Methods of producing a high pressure environment include distortable diaphragms and rupture disks, pistons and dual cell designs (Xiong and Kiran, 1998). However in recent years most investigations in to phase transformation has been studied using diamond anvil cell (Zarechnyy et al., 2012, Feng et al., 2013). In the current study a Merrill-Bassett model will be used, as it has the advantage of inducing a pressure increase and maintaining it using three screws over the formerly used push method (Merrill and Bassett, 1974). This will be detailed further in chapter 2 of this study.

### *1.6 Aims and Objectives*

The aims of the study are to investigate the effect of pressure on polyethyelene glycol to create an effective drug delivery system for poorly water soluble drugs, with a view to increase their bioavailability. The objectives of the study are to study PEG under high pressure conditions using Raman spectroscopy, and to subject a mixture of poorly soluble drug and PEG to high pressure conditions with the view to generating a drug delivery system capable of releasing the drug in an efficient manner.

# Chapter 2: Materials and Methods

### *2.1 Materials*

The polyethylene glycol 4000 (batch number LOT#BCBG1709V) and hydrocortisone (batch number LOT#SLBD0859V) used were obtained from Sigma-Aldrich (St Louis, Missouri, U.S.A). A drug-polymer mix can be achieved by placing a sample to the total mass of 500mg in a ball mill chamber (Serial number MM400, obtained from Retsch GmbH, Hann, Germany) with 2 metal balls, and shaking the sample for 30 mins at a frequency of 30Hz. Samples of the hydrocortisone to PEG ratios of 10:90, 20:80 and 50:50 were produced for the current study.

### *2.2 Apparatus*

High pressure studies were carried out using a diamond anvil cell obtained from High Pressure Diamond Optics Ltd. (Tucson, Arizona, U.S.A) with gaskets drilled using a Boehler microdriller obtained from Almax EasyLab Group Ltd. (Cambridge, Massachusetts, U.S.A.) with a 0.25mm tungsten carbide rod drill piece. Samples were photographed using a Reichert Polyvar-Met Microscope (obtained from Depew, New York, U.S.A.) Raman spectroscopy was carried out using a Thermo Scientific DXR Raman Microscope (serial number AIY100276) with a 532nm laser obtained from Thermo Fisher Scientific (Waltham, Massachusetts, U.S.A.). Infrared Spectroscopy was carried out using a Thermo Scientific Nicolet ISIO Infrared Spectrometer was also obtained from Thermo Fisher Scientific (Waltham, Massachusetts, U.S.A.). Differential Scanning Calorimetry was carried out using a Metler Toledo Differential Scanning Calorimeter (DSC 822e/400Ro, serial number 5125178759). Thermogravimetric analysis was carried out using a Metler Toledo Thermogravimetric Analyzer (TGA/SDTA851e/LG/Ro, serial number 5125178760). These were both obtained from Metler Toledo Ltd. (Leicester, U.K.). Drug release was analysed using a Dionex High Performance Liquid Chromatography machine (PS80IPE, serial number 1190002) with Chromeleon Data Software obtained from Dionex (Cheshire, U.K.).

### *2.3 Techniques*

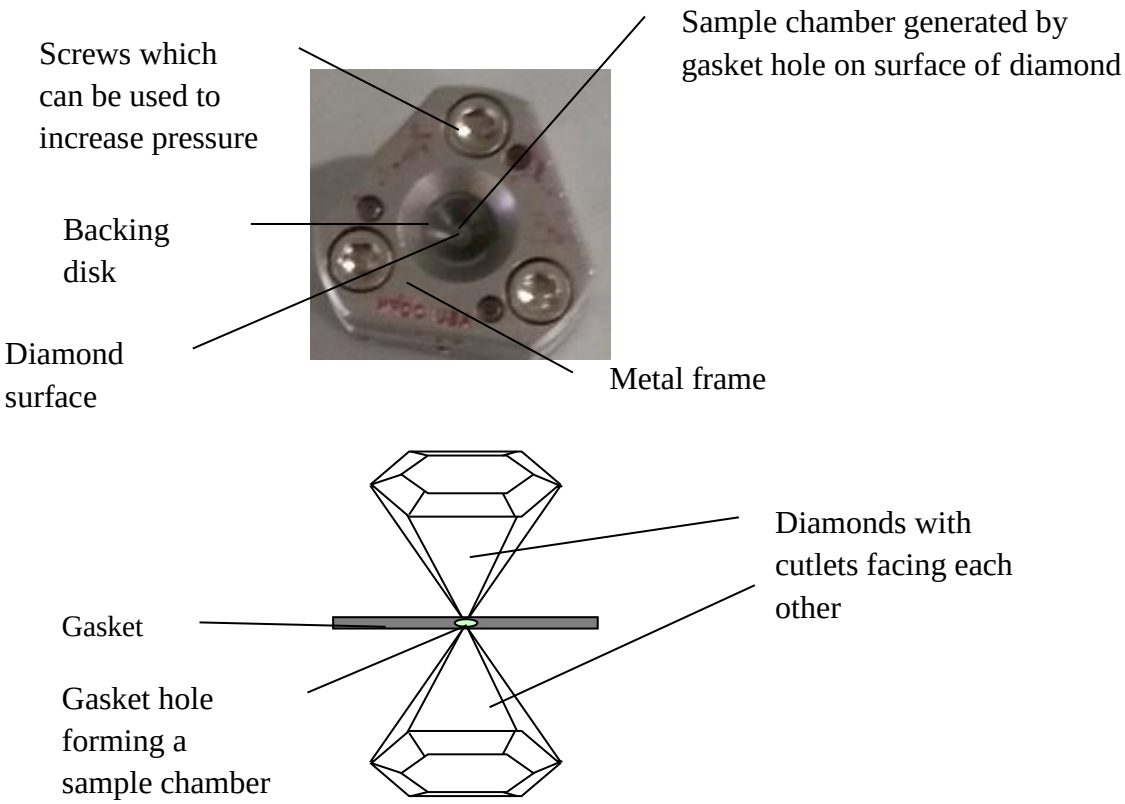


Figure 12: The photographs above portray the exterior of a Merrill-Basset diamond anvil cell, the diagram below them illustrates the orientation of the diamonds and the gasket within.

The diamond anvil cell (Figure 12) is a useful apparatus for investigating the effect of pressure on the physical properties of substances (Liu et al., 2011). This apparatus was introduced in 1958 and caused what has grown to be thought of as one of the greatest advances in the field of high-pressure study as it has delivered the greatest level of pressure ever triggered in a laboratory environment. The basis for the technique was originally inspired by P.W. Bridgman's work with carboloy using a similar anvil structure in 1937(Katrusiak, 2008). However diamond was the crucial component for generating the required level of pressure, which was suggested in a study into high pressure X-ray diffraction 13 years later (Lawson and Tang, 1950). Diamond was not actually recorded as being used part of an anvil cell until 9 years later as part of another X-ray diffraction study (Jamieson et al., 1959) and that same

year as part of an infrared study using diamond anvil cell to create sufficient pressure to allow analysis of $CO_3$ ions (Weir et al, 1959). Jamieson et al. used a clamped right angle arrangement, while Weir et al. used a horizontal configuration (180º) and a spring loaded lever arm. Both the features of the latter study have since become common place in diamond anvil cell apparatus (Jayaraman, 1983). The diamond anvil cell method was developed further with the introduction of the use of a metal gasket to allow creation of a sample chamber and the development of hydrostatic pressure techniques, by encasing aqueous solutions (Valkenburg, 1962). Possibly the greatest advance in the use of the apparatus was the introduction of a way to calibrate the device in the form of ruby-florescence spectroscopy (Forman et al, 1972), as prior to this there was no accurate method of knowing the exact pressure applied to a substance in the cell (Piermarini and Block, 1975).

The principle of the use diamond anvil cell is that by employing moderate axial forces to the region between the points of two diamonds, high pressures can be generated. As one of the hardest substances on earth, diamonds have the power to bear such forces where other substances would fail (Taylor and Pasternak, 1990). The use of diamond also has a number of other advantages including little absorption of short X-rays, its transparency is useful for both visual radiation and analysis using UV, IR and Raman spectrophotometry (Katrusiak, 2008).

The diamond anvil cell creates a pressurised environment when the substance tested is added to a central cavity and the hydrostatic fluid is enclosed and compressed between the diamond tips and the distorted gasket. The pressure generated is highly dependent on the size and shape of the diamond points and the gasket (Katrusiak, 2008). This follows the connection between force and area, and pressure (P=F/A), showing that the greater the force applied to the smaller the area, the greater the pressure generated. Thus the cutlets of the diamonds normally have a diameter of around 1mm, giving a surface area of around $0.8mm^2$ (Smith and Fang, 2009). The force evoked upon the diamonds is controlled by one of two methods, either using screws or a gas membrane. In the former, the energy evoked is generated by tightening screws directly into the apparatus itself or via an arrangement of levers.

The latter generates the required energy by altering the pressure of a gas loading a metallic membrane that thrusts the two halves of the apparatus together. As a whole the screw method is the more straightforward of the two and is therefore more consistent, they can sustain the pressure for longer and they have more predictable effects in response to temperature. As such that is the method which will be applied in the current study (Kantor et al., 2012).

Studies over the years have allowed more and more applications to be discovered, including extensive investigations in to the effects of temperature and pressure on various substances, such as phase transitions, visual effects with polarized light, Xray crystallography and Raman spectroscopic investigations (Piermarini and Block, 1975). It has also allowed complex investigations on microscopic materials and other previously very difficult procedures to become standard practices (Jayaraman, 1983). In the context of polymers diamond anvil cell has allowed analysis of depolymerisation, decomposition, liquefaction, degradation and decholination. Condensation polymers including polyethylene terephthalate and nylon are fully solubilised in aqueous solutions at elevated temperatures initiated by the anvil cell, whereas addition polymers such as polystyrene break down in a heterogeneous manner in the aqueous solution (Smith and Fang, 2009). In a previous study polyethylene terephthalate was found to crystallize at high temperatures, due to the development and supersaturation of oligomers of terephthalic acid, with a greater temperature of dissolution (Fang et al., 1999). Due to the fact polyethylene glycol also undergoes condensation polymerisation, perhaps polyethylene glycol would behave in a similar manner to polyethylene terephthalate. Other evidence for this type of study can be seen in the work of Oswald and Urquart (2011). They studied the polymorphism of acrylic acid and methacrylic acid using diamond anvil cell to induce a high pressure polymer. Using Raman spectroscopy the crystallisation pressures for each of the two polymorphs were found to be 0.65GPa and 1.5GPa respectively before compression to induce polymerisation without the use of heat or initiators (Oswald and Urquhart, 2011). In another study by Oswald and Urquhart in collaboration with Johnston, Marshall and Parsons (2014) acrylic acid was found to

go through a phase change at 0.8GPa and stay intact in that molecular state until 7.2GPa, but it polymerized on complete removal of pressure.

Due to the fact that some polymorphs possess higher melting points, phase transition can require heating. Due to its relatively inert nature diamond can withstand high temperatures and as such diamond anvil cell is highly useful for determination of phase transformations at high temperatures. For example nylon has been found in a previous study to entirely dissolve in water at 331°C (Smith and Fang, 2009). Another example is a diamond anvil cell study which featured heating of polyethylene causing phase transformation. This could be observed in the transition into the liquid phase on a quick increase in temperature, followed by turgidity and colour changes above 450ºC and 570ºC respectively (Fang et al., 2000). Creating a melt can result in phase changes which could not occur from the solid state alone (Oswald and Urquart, 2011). All of the properties of the polymorphs can be analysed via a selection of methods.

## *2.4 Methods*

### *2.4.1 Diamond Anvil Cell*

Initially a tungsten gasket was indented using the diamond cutlets by increasing the pressure on the gasket by tightening the screws until an indent of between 80 and 120μm could be measured and observed through a microscope. This is to support the tip of the diamond which experiences very high pressures. A pilot hole was drilled, using an Almax Easylab gasket drill, to the depth of 100μm at a site distinct from the indent to aid alignment of the instrument. The eye piece was then centred to the pilot hole and the indent lined up to the eyepiece. A hole was drilled through the indented gasket. It was ensured the hole was cleanly cut using a microscope and removing any debris using a needle. The gasket was then replaced in the diamond anvil cell, lining the indent hole up with the diamond face to form a sample chamber. A few rubies were then added to the chamber using a needle. On top of this the sample was added, compressing the powder using the top diamond and adding more sample until the chamber was full. The diamond anvil cell was then reassembled and the pressure was

increased incrementally by tightening the screws one by one in a clockwise fashion. Increasing the pressure applied to the sample in this clockwise gradual fashion allows a more even distribution of pressure. This screw method allows the pressure to be maintained for prolonged periods. For visual representation of this see Figure 12.

*2.4.2 Raman Pressure Studies*

The Raman spectrometer laser was aligned using the alignment tool and experimental window on Omnic, by centring the crosshairs on the pin hole generated by the alignment tool. The instrument was then calibrated using Omnic. The ruby pressure was calibrated by measuring the fluorescence of a number of rubies at ambient pressure on the pressure setting on Omnic. The peak positions of the fluorescence peaks were fitted using a Voigt function. 5 readings were taken and the average was then used to give a mean inital pressure for measurement of the pressure of the diamond anvil cell. To measure the pressure exerted on the diamond anvil cell at each pressure increase, the ruby fluorescence of one of the rubies was taken as above and from this the pressure was calculated using the formula $\frac{\left(\left(\left(\frac{Ruby\ at\ P}{Ruby\ Initial}\right)^{7.665}\right)-1\right)\times 1904}{7.664}$. To ensure consistency in the pressure measurement the pressures were recorded using the same ruby every time. The diamond anvil cell was moved to an area of the sample where no rubies were present to avoid the fluorescence, and the Raman spectrum of the sample was taken. The sample was collected over 10-20s, employing a lower time limit of 10-15s when a flat top was observed for the sample peaks. This was carried out until the pressure reached approximately 8 GPa, as this is reaching the higher pressures seen previously in molecular studies and possibly the upper pressure limit of the cell. The pressure was then gradually released to allow analysis of the Raman spectra on reduction of pressure back to ambient and also to gradually allow the sample to undergo any reverse phase changes. The resultant samples could then be extracted from the gasket sample chamber and photographed using a Reichert Polyvar-Met Microscope analysed by infrared spectroscopy.

*2.4.3 Infrared Spectroscopy*

The pressurised sample was removed from the gasket using a needle and added to the surface of an infrared spectrometer. Infrared spectroscopy was carried out on the sample, taking a background reading to ensure only the sample was measured. The pressurised sample was compared to the ball milled sample, the drug alone and the polymer alone to allow analysis of the effect of pressure on structure of the mixture.

*2.4.4 Drug Release Studies*

The pressurised samples were extracted from the gasket chamber using a needle and weighed, averaging at 30mg per sample. Using eppendorfs with built in filters, in vitro dissolution was carried out on a number of pressurised samples in 1ml simulated intestinal fluid without enzymes, adjusted to pH 6.8 and 1ml simulated gastric fluid without enzymes, adjusted to pH 1.2 at 37ºC±0.5. Both solutions were prepared as detailed in the British Pharmacopoeia (British Pharmacopeia Commission Secretariat of the Medicines and Healthcare Products Regulatory Agency, 2014) minus the addition of pancreatic enzymes or pepsin respectively as these reduced the shelf life of the media. The samples were originally tested in pH7.4 phosphate buffered saline (PBS) however the stimulated fluids were favoured latterly as it was more comparable to oral drug delivery in vivo. The sample was placed within the filtered chamber and allowed to dissolve in the media. 100µl samples were taken from the dissolution chamber and replaced with fresh media at 15 minutes, 30 minutes and at 1 hour time intervals after the 1 hour mark for a further 8 hours, and then at 24 hours to measure drug release over time. 3 replicates were carried out in simulated intestinal and simulated gastric fluids each. For the PBS samples this was analysed using a nanoUV spectrometer however due to issues with the machine, HPLC was used latterly and found to be much more effective. Samples were analysed by HPLC using a UV detector at 246nm. A C-18 silica column was employed and the mobile phase utilised was a 60:40 water:acetonitrile (v/v) solution at a flow rate of 1ml/min as observed in another study (Foroutan and Watson, 1999).This particular method was selected as it gave a readable area under the curve even at the low drug concentrations present initially. The validation could not be carried out by the author personally due to time restrictions and lack of availability of

HPLC machines. However the method was validated and used on a daily basis by other students in the department. Using the equation generated from a hydrocortisone calibration standard curve, the concentration of drug present was calculated from the area under the curve (equation 1 in table 1 taken from Figure 13). The calibration curve was generated using standard solutions of 1µg/ml, 10µg/ml, 100µg/ml and 1mg/ml hydrocortisone in acetonitrile. Acetonitrile was used as dissolution of hydrocortisone alone was not full enough in simulated fluids due to its highly aqueous nature. To account for the removal of drug from the overall solution on replacement of fresh media, equation 2 in table 1 was used to give the overall percentage drug release.

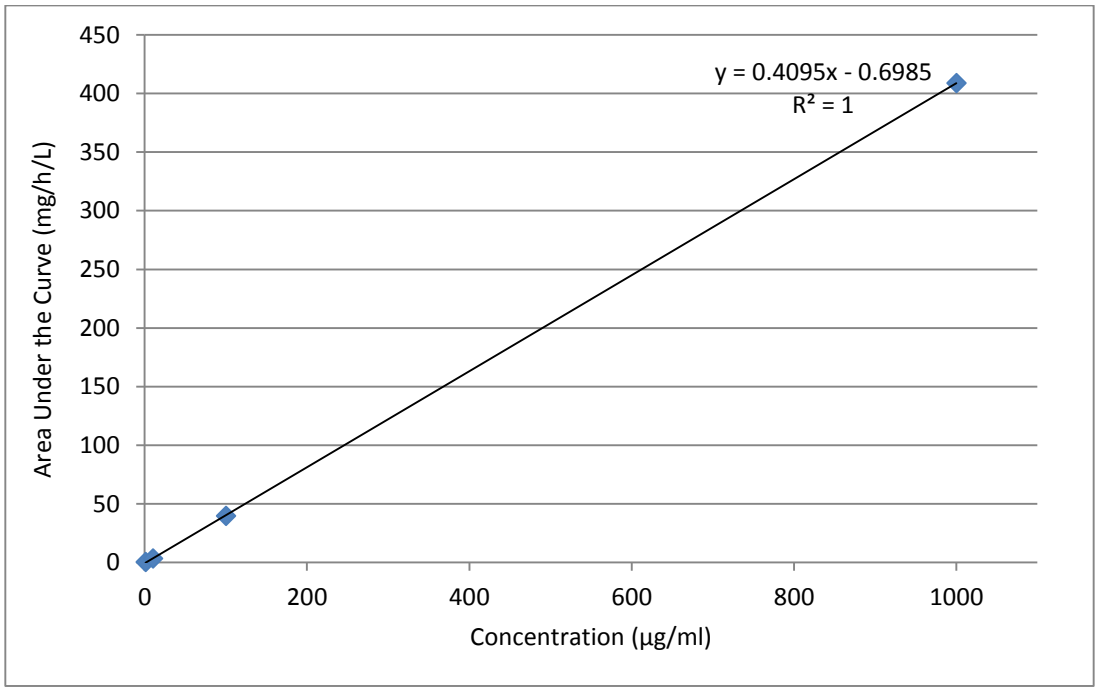


Figure 13: HPLC calibration curve of hydrocortisone taken from the area under the curve values of 1µg/ml, 10µg/ml, 100µg/ml and 1mg/ml samples, where y=4.095x-0.6985 and $R^2$=1

Table 1: Equations used to calculate percentage drug release

| Method | Equation |
|---|---|
| Mass of drug released from DAC samples at each time point | (1)<br>Given the equation of the calibration curve is y=0.4095x-0.6985<br>Where:<br>y = area under the curve (AUC) ($mg.h.L^{-1}$)<br>x= concentration of drug present in solution (µg/ml)<br><br>Concentration of drug released (µg/ml) = (AUC+0.6985)/0.4095 |
| Percentage drug release from DAC samples at each time point accounting for 100µl extracted due to total possible concentration being only 25µg/ml | (2)<br>% drug release = ((A+100µl)/(B/C))x100<br><br>where<br>A= concentration of solution (µg/ml)<br>B= total drug initially present in delivery system (µg)<br>C= total volume of solution (1ml) |
| Mass of drug released from large volume press samples at each time point where a full 1ml sample could be extracted each time due to the greater concentration of drug present | (3)<br>Given the equation of the calibration curve is y=0.4095x-0.6985<br>Where:<br>y = area under the curve (AUC) ($mg.h.L^{-1}$)<br>x= concentration of drug present in solution (µg/ml) |

| | |
|---|---|
| Due to the cumulative nature of this method from the 30 minute reading (second time point) onwards the previous total sample concentration present (P) was added to the concentration measured at the current time point | Initial 15 minute sample:<br>Concentration of drug released (μg/ml) = (AUC+0.6985)/0.4095<br><br>30 minutes onwards:<br>Concentration of drug released (μg/ml) = ((AUC+0.6985)/0.4095)+P<br><br>Where P = previous total sample concentration present<br><br>For example<br>At 15 minutes:<br>Concentration of drug released = ((1.5563+0.6985)/0.4095) =5.51μg/ml (to 2 d.p.)<br><br>At 30 minutes:<br>Concentration of drug released = ((0.6994+0.6985)/0.4095)+ 5.51μg/ml =8.92 μg/ml (to 2 d.p.)<br><br>At 1 hour:<br>Concentration of drug released = ((7.0118+0.6985)/0.4095)+ 8.92μg/ml =27.75 μg/ml (to 2 d.p.) |
| Percentage drug release from large volume press samples | (4) % drug release = (A/B)x100<br><br>Where<br>A= concentration of drug released in solution<br>B= total drug present in delivery system initially |

*2.4.5 Statistical analysis*

The maximum release achieved from the sample in simulated gastric and intestinal fluids was compared by unpaired t-tests. In addition any degradation was analysed by unpaired t-tests comparing pure hydrocortisone present with hydrocortisone plus any derivatives present. A P-value of less than 0.05 was deemed to be statistically significant.

*2.4.6 Differential Scanning Calorimetry (DSC)*

Standard DSC pans were filled with 2-5mg of sample, taking care to avoid contamination from the researcher or the surfaces worked on. The pan lids were punched with a central hole using a needle to prevent rupture at over 80ºC. The pans were then heated over a range of 40-290ºC, using the differential scanning calorimeter detailed in the apparatus section, to allow melting of both PEG (which, from the manufacturer's data, was believed to have a melting point between 58 and 61ºC) and hydrocortisone (which was believed to have a melting point between 211and 214ºC). The resultant curves were then analysed and visual observations on reopening the pans were recorded. Some of the samples were also analysed by infrared spectroscopy to analyse the change in structure of the drug and polymer blend on heating, compared to the ballmilled and pressurised samples.

*2.4.7 Thermogravimetric Analysis (TGA)*

Standard 150µl TGA ceramic covered crucibles were filled with 10-20mg of sample, taking care to avoid contamination or filling the crucibles by more than 75%. The samples were then heated over ranges of 55-500°C for the blends and pure PEG, and 150-550° C for pure hydrocortisone, using the thermogravimetric analyzer detailed in the apparatus section. This allowed analysis of the interactions between PEG and hydrocortisone. The resultant curves were then analysed.

*2.4.8 Temperature vs. Pressure Studies*

The ability of pressure to reduce the temperature required melt polyethylene glycol was hypothesised from the fact a phase change occurs at 25ºC (room temperature) at 5GPa, as demonstrated by the visual transformation of the white powder into a

transparent liquid and changes in the Raman spectra, whereas the above differential scanning calorimetry study identified a higher melting point at ambient pressure (0GPa), with troughs occurring at between 55 and 65°C on the resultant spectra. The diamond anvil cell was loaded with polyethylene glycol. The sample was pressurised and then placed in an oven for 2 hours, starting at 30ºC and increasing the temperature by 5 degrees each time. At each increase in temperature, the effect was measured visually and via Raman spectroscopy. This was carried out at 0.8GPa, 1GPa, 2GPa, 3GPa and 4 GPa, to measure the relationship between pressure and temperature.

*2.4.9 Pressure Scale Up*

A PTFE cell (see Figure 14) was loaded with 50:50 PEG:hydrocortisone mixed with a pressure transmitting medium (water initially and then petroleum ether latterly). The cell was sealed at both ends using plastic caps sealed with PTFE tape. The cell was then placed in a beryllium copper alloy (BERYL CO-25) outer cell and pushed in to place using a tungsten carbide pusher, sealing it with copper rings. A piston was added and vacuum grease applied to lubricate it, before adding a spacer. A retaining nut was then added to the end and a carbon tungsten rod was placed on top of the inner cell. For a visual representation of this cell see Figure 14. Pressure was then exerted on the cell using a hydraulic ram and locked in place by tightening the retaining nut. This pressurising step was repeated until a pressure of 0.8 GPa was achieved. The carbon tungsten rod was then removed and the cell was placed in a 57℃ oven overnight to allow the PEG to fully melt. The pressure was then backed off by reversing the previous steps. The inner cell was then pushed out of the bottom of the outer cell and the sample extracted and allowed to dry. For the sample using water as a pressure transmitting medium, the addition of an ultrafiltration step was required as it generated a very wet sample. Drug release studies were carried out using eppendorfs with filters, but unlike the previous drug release studies the whole 1ml was removed and replaced each time, instead of just 100µl, as the greater mass of drug added allowed this to occur and it was hoped this would reduce degradation of the drug occurring in the stagnant dissolution media. Drug release was calculated

using equations 3 and 4 in table 1, and statistical analysis was carried out as in section 2.4.5.

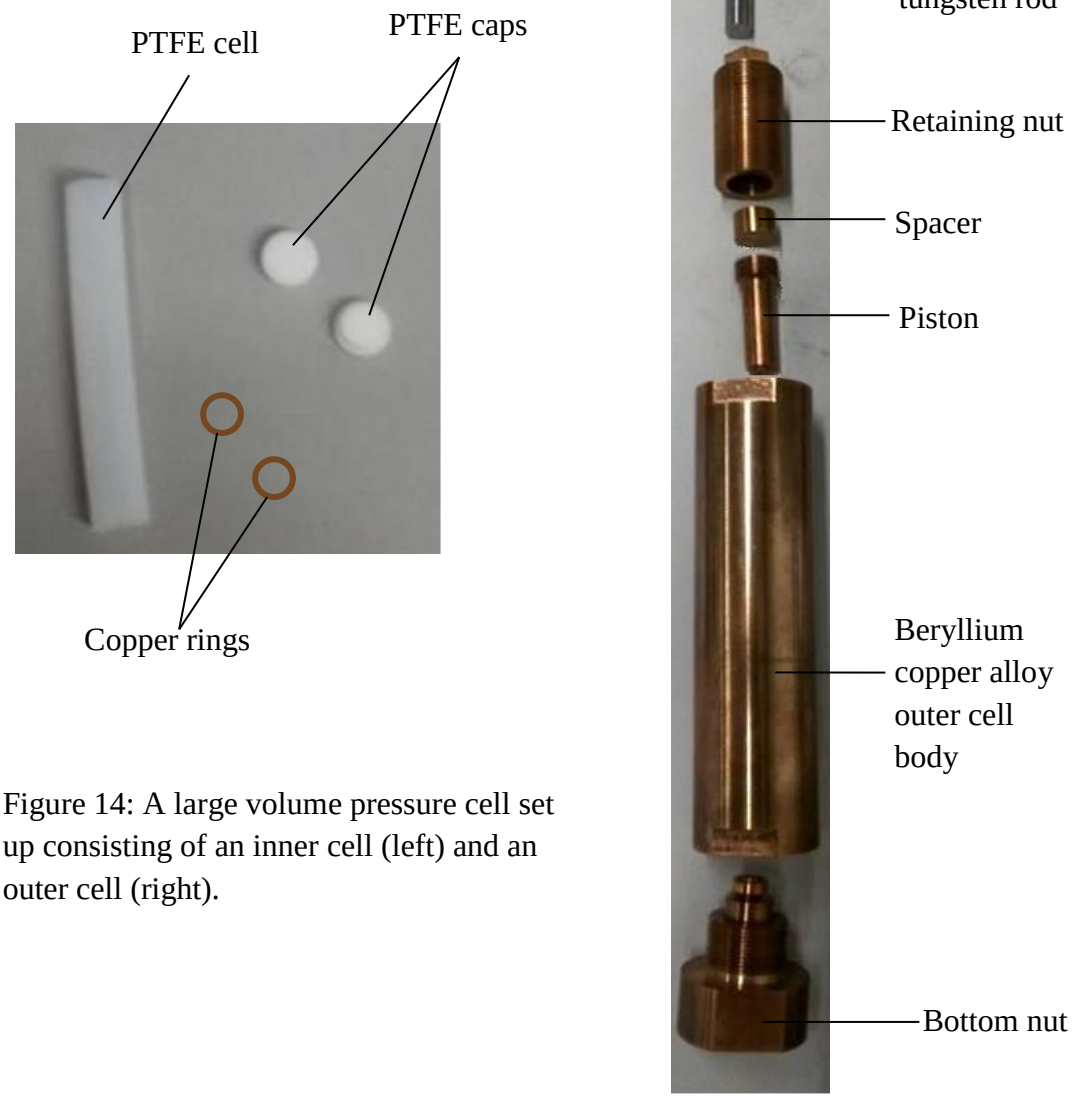


Figure 14: A large volume pressure cell set up consisting of an inner cell (left) and an outer cell (right).

# Chapter 3: Results

## *3.1 PEG*

The effect of pressure from a visual perspective can be seen in Figure 15. The white crystalline powder is observed to change gradually change into a clear liquid as the pressure is increased. The white powder was observed to be fully melted around 5GPa, as marked by a shiny texture through the microscope. On removal of the pressure and reopening of the diamond anvil cell a transparent solid mass is formed as seen in the latter pane of Figure 15. The ragged edges of the samples illustrate the flow that has occurred.

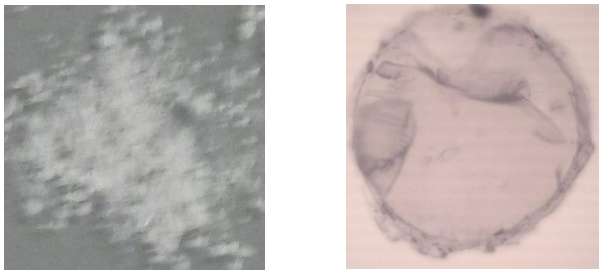

Figure 15: In the left hand pane the initial unpressurised powder can be observed and in the right pane one of the samples generated on taking the pressure exerted up to 5GPa and then returned to ambient.

### *3.1.1 Raman*

In Figure 16 initially at ambient pressure a distinct sizable ridged peak can be seen at approximately 2900 $cm^{-1}$ and a smaller distinct peak with a step like conformation at approximately 844 $cm^{-1}$. The former falls in the CH region of the spectra and thus corresponds to the carbons attached to hydrogen atoms found in the main chain of PEG4000. The latter falls in the C-O-C region of the spectra and thus is the distinct C-O-C bond pattern found in PEG 4000. There are other peaks present in the spectrum but they do not show distinct changes. On application of pressure the ridges of the CH peak are lost and the peak becomes smooth in a gradual manner, becoming completely smooth by 5GPa, signifying the stretching of the CH groups are tending towards a similar energy. The axis breaks are due to the diamond peak being removed from the spectra (~1300 $cm^{-1}$). In Figure 17 shift to higher wavenumber in

this region caused by increasing pressure can be observed. There appears to be a linear relationship between pressure and Raman shift, with the increase in Raman shift being directly proportional to the increase in pressure.

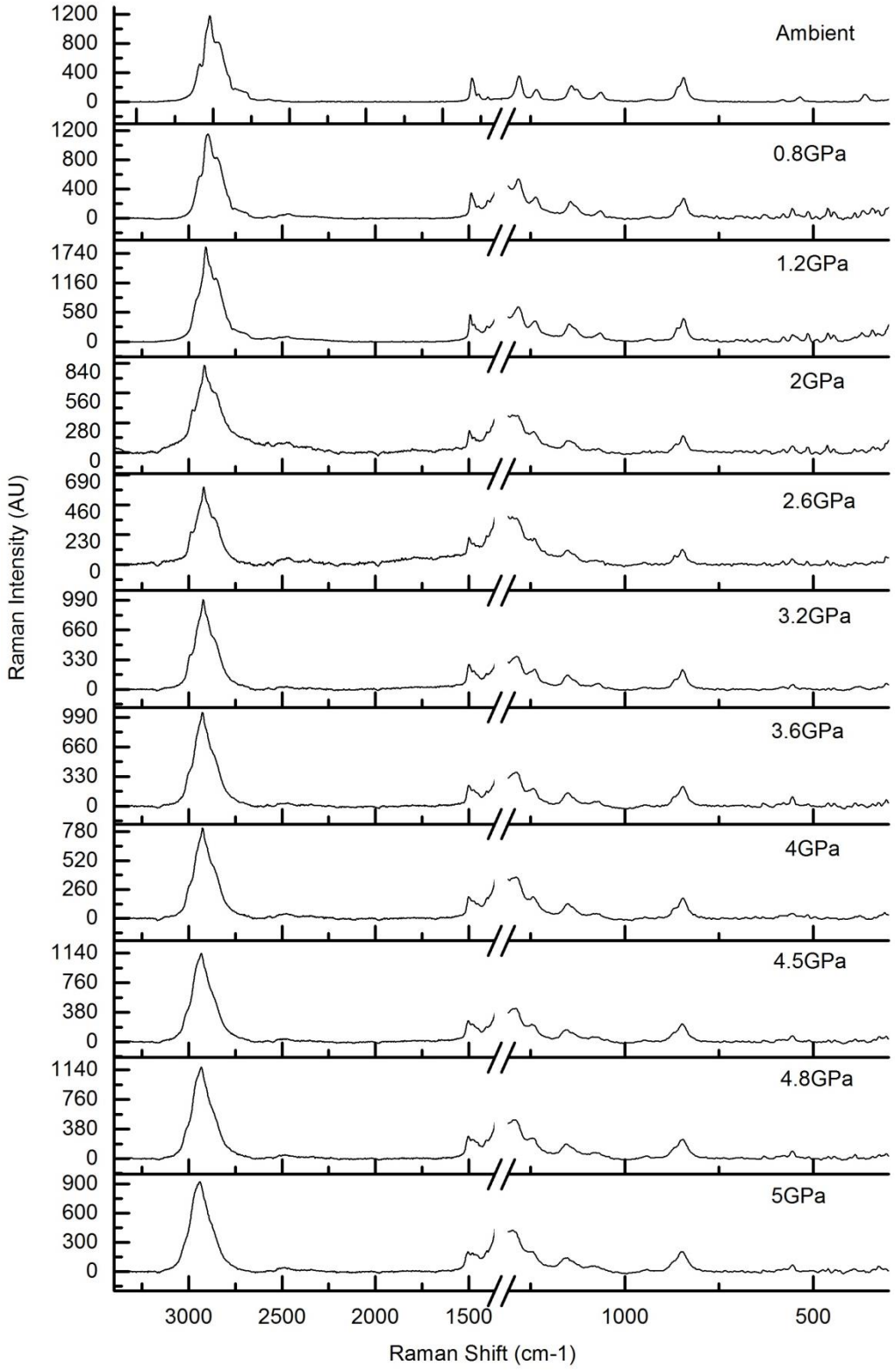


Figure 16: Raman spectra of PEG4000 illustrating the changes occurring on increasing pressure

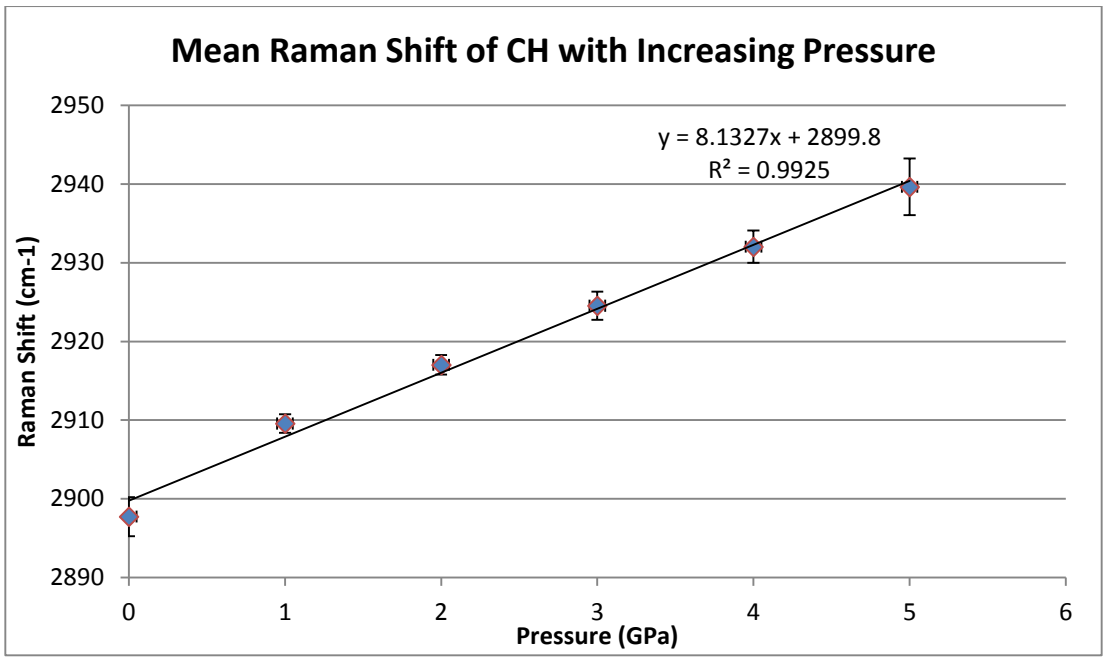


Figure 17: Raman Shift of the CH 2900 $cm^{-1}$ region of PEG4000, occurring with increasing pressure where n=5 SE± 0, 3.31, 2.41, 3.31, 2.41, 3.21, 3.40 and 3.36 $cm^{-1}$ respectively. The horizontal error bars represent the 0.05GPa margin of error of each pressure.

Figure 18 is a zoom in to the C-O-C region. It is observed to consist of a step like peak and as the pressure is increased the lower portion of the peak is seen to gradually diminish, completely disappearing by 5GPa. The Raman shift of the main C-O-C peak is illustrated in Figure 19. The shift to a higher wavenumber and increase in Raman shift is again directly proportional to the increase in pressure, as shown by the fairly linear treadline.

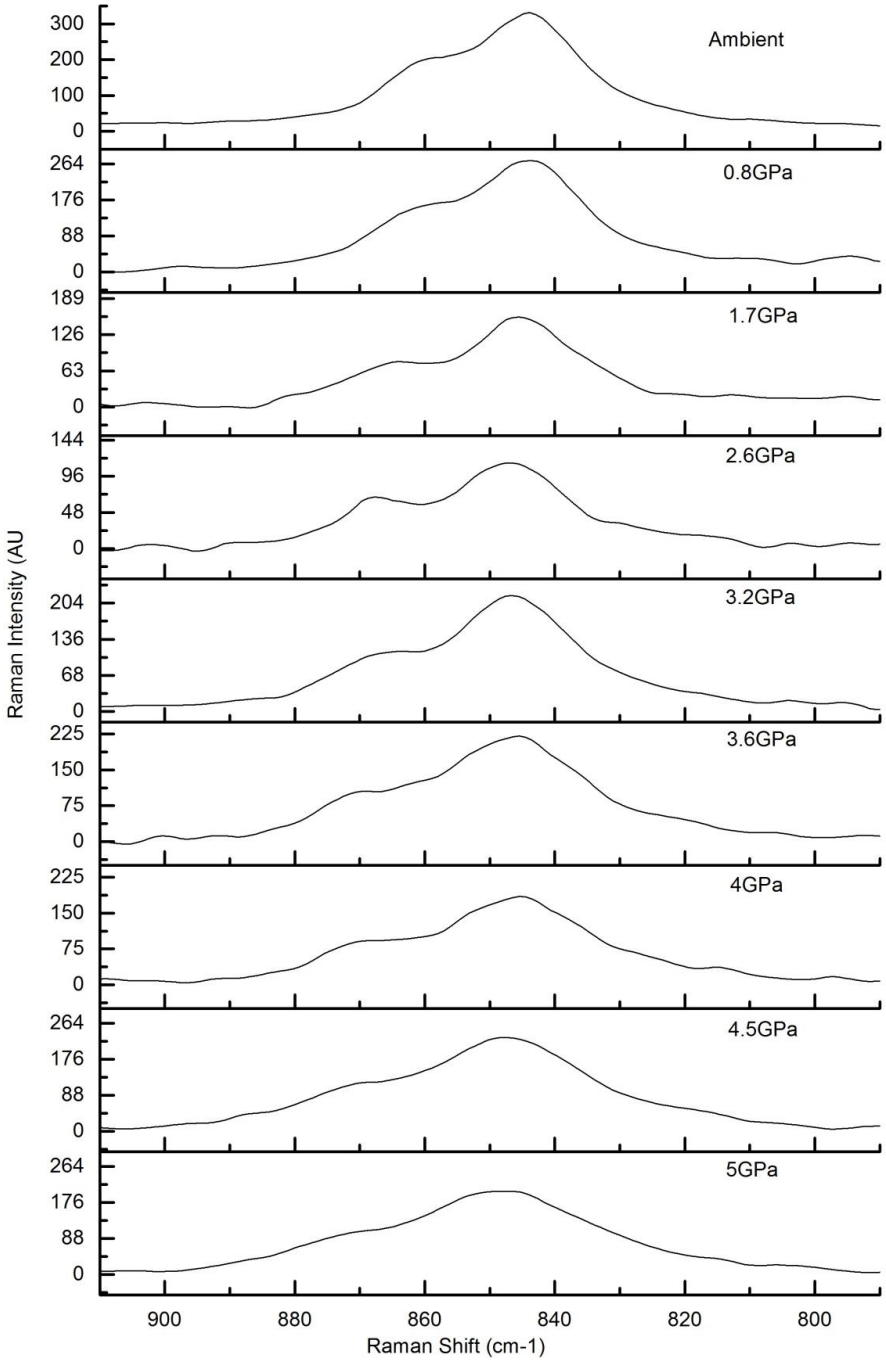


Figure 18: Raman Spectra of the C-O-C region of PEG4000 and the effect of increasing pressure

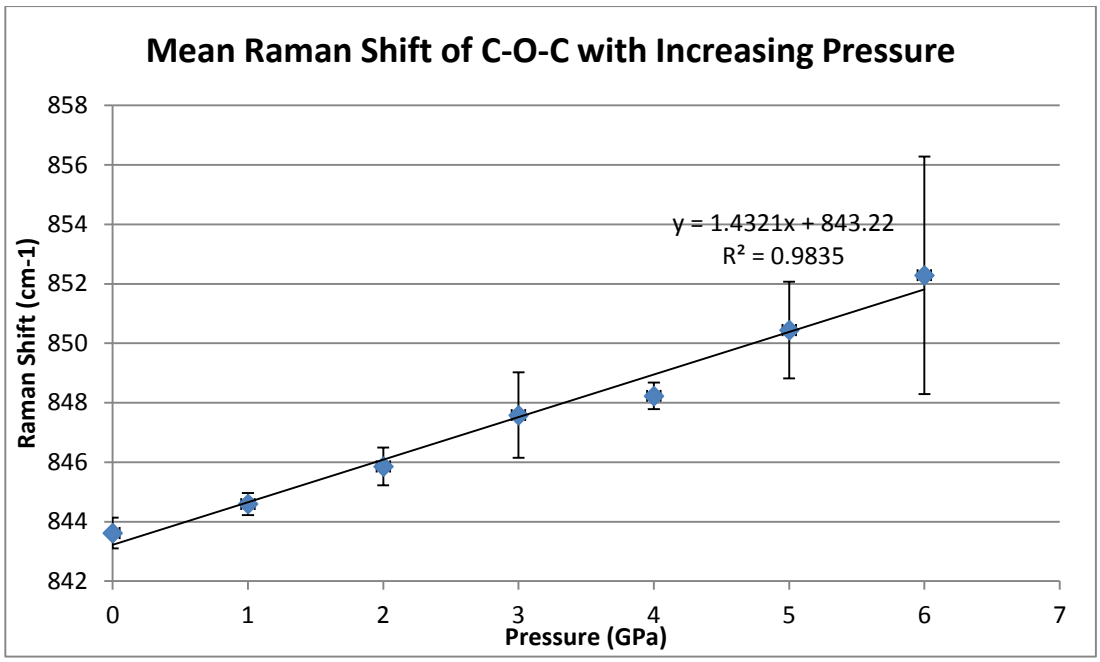


Figure 19: Raman Shift of the C-O-C 844 $cm^{-1}$ region of PEG4000, occurring with increasing pressure where n=5 SE± 0, 0.459295, 0.602906, 1.393178, 0.83855 and 2.029418 $cm^{-1}$ respectively. The horizontal error bars represent the 0.05GPa margin of error of each pressure.

In Figures 20 and 21, the effect of pressure removal is shown. In Figure 20 the smaller step-like feature of the C-O-C region returns on removal of pressure reforms as PEG becomes a solid once more. Likewise in Figure 21 the ridges of the CH region are observed to return, as shown by the fact that once the pressure is removed the spectra in B) returns to more like A) as shown in C).

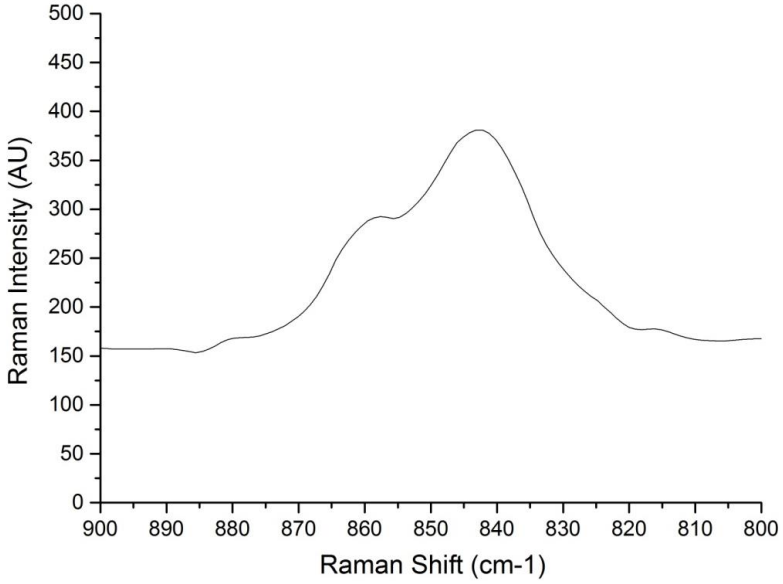


Figure 20: Raman Spectra of the C-O-C region of PEG4000 on removal of pressure.

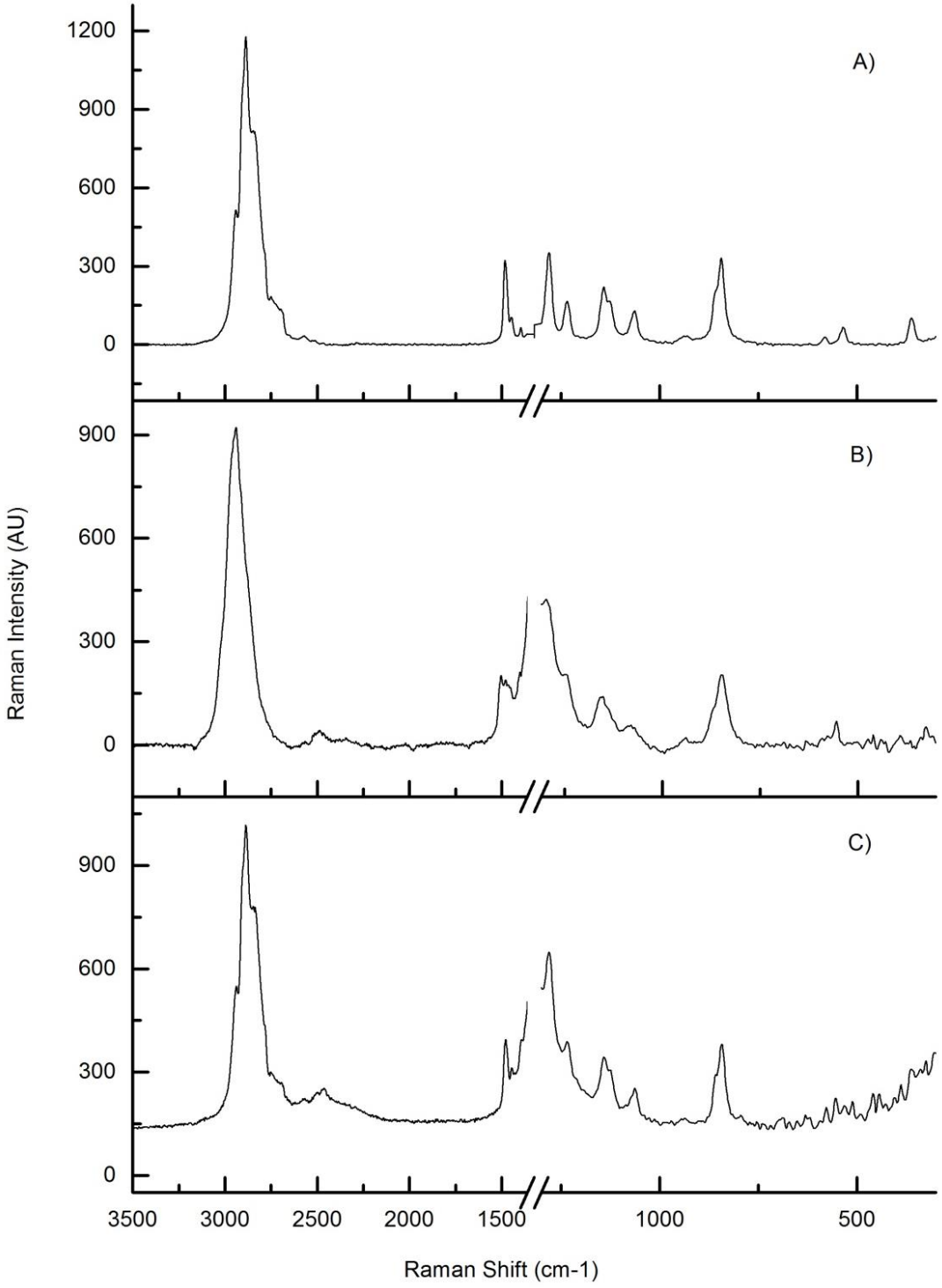


Figure 21: Raman spectra illustrating A) PEG4000 in ambient before pressure, B) PEG4000 at 5.6GPa and C) PEG4000 after the pressure is removed again.

*3.1.2 Infrared Spectroscopy*

In Figure 22, the effect of pressure on the functional groups of PEG4000 can be observed. The 1096 $cm^{-1}$ region corresponds to the C-O-C region. In the ambient sample spectra this peak is approximately 2.4-fold higher than the surrounding peaks, with the next highest peak at the CH group at 841 $cm^{-1}$ reaching 0.276162AU compared to 0.666641AU. Whereas, after pressure, although all the peaks decrease in height, this peak is approximately 1.7-fold higher than the surrounding peaks at 0.01818AU compared with 0.01063AU for the next highest peak. The decrease in proportion of this peak relative to the surrounding peaks may suggest there is less of a prominence of this functional group in the structure which may suggest there is a change in structure. Changes in this particular region support the changes in C-O-C Raman peaks.

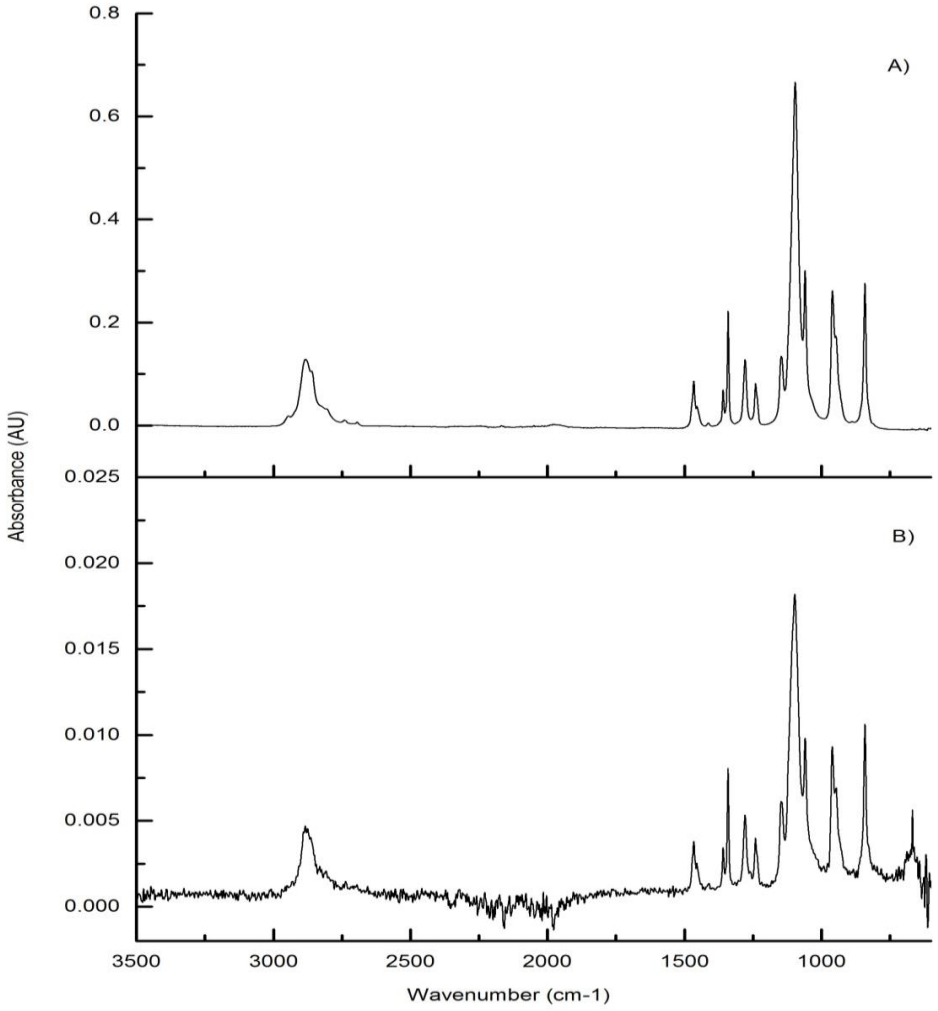


Figure 22: Infrared spectra of PEG4000 A) before and B) after pressure is exerted on the powdered sample.

*3.1.3 Differential Scanning Calorimetry*

On application of heat, PEG4000 was found to melt over the range of 59.23 to 64.37°C, reaching its peak at 62.48°C (Figure 23). Again the white powder turned into a transparent liquid on reaching the melting range and then became a solid transparent mass. Table 2 illustrates all three replicates the author took of PEG4000 and the mean results with the standard error.

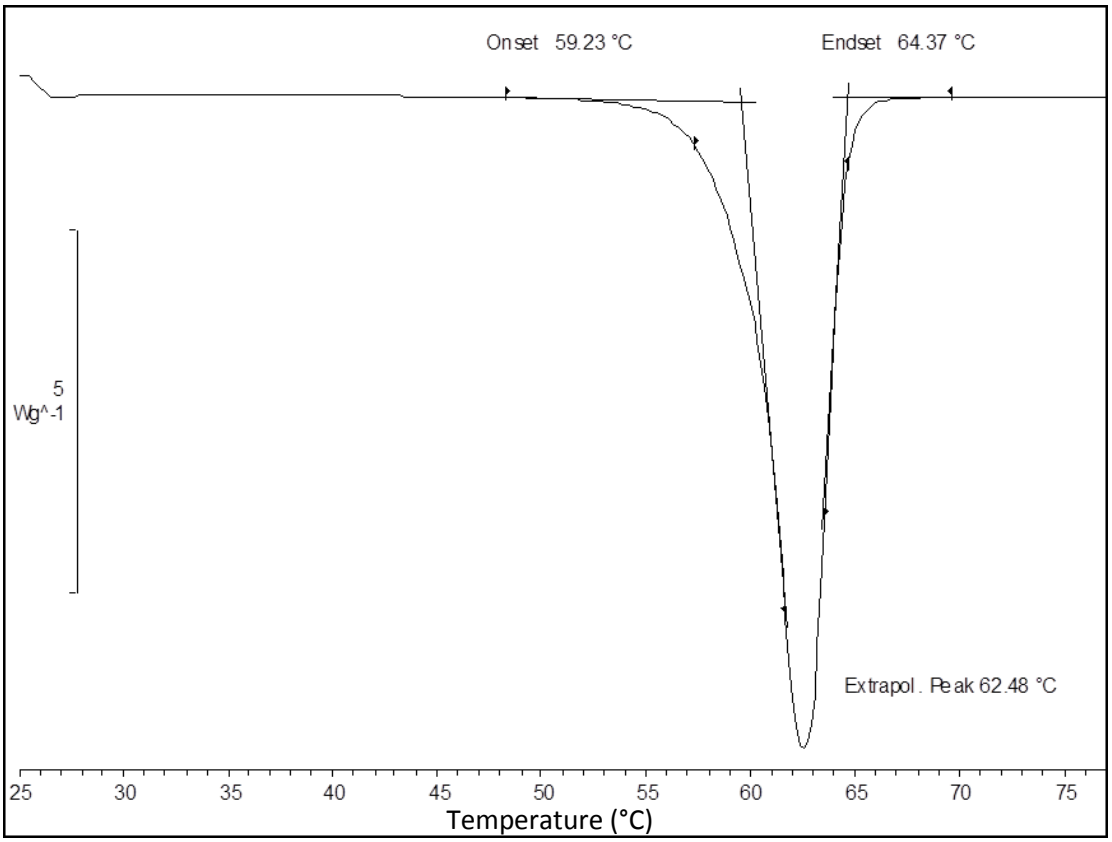


Figure 23: Differential scanning calorimetry spectrum of PEG4000

Table 2: Differential scanning calorimetry from 3 replicates of PEG4000, giving the mean onset, extrapolated peak and endset temperatures.

| Sample | Onset Temperature (°C) | Extrapolated Peak Temperature (°C) | Endset Temperature (°C) |
|---|---|---|---|
| 1 | 59.23 | 62.48 | 64.37 |
| 2 | 57.44 | 60.46 | 61.50 |
| 3 | 59.35 | 62.25 | 64.97 |
| Average | 58.67 | 61.73 | 63.61 |
| S.E. | 0.617639 | 0.638462 | 1.070768 |

In Figure 24, the effect of DSC exposure can be observed. Similar to the infrared spectra of the pressurised sample, the C-O-C peak at 1096 $cm^{-1}$ is observed to drop from 0.66664AU, which is 2.4-fold higher than the CH 841 $cm^{-1}$ peak at 0.27616AU, to 0.2176AU, which is 2-fold higher at than the next highest peak at 0.10745AU. There is also an overall decrease in peaks but again the C-O-C peak is the most marked decrease.

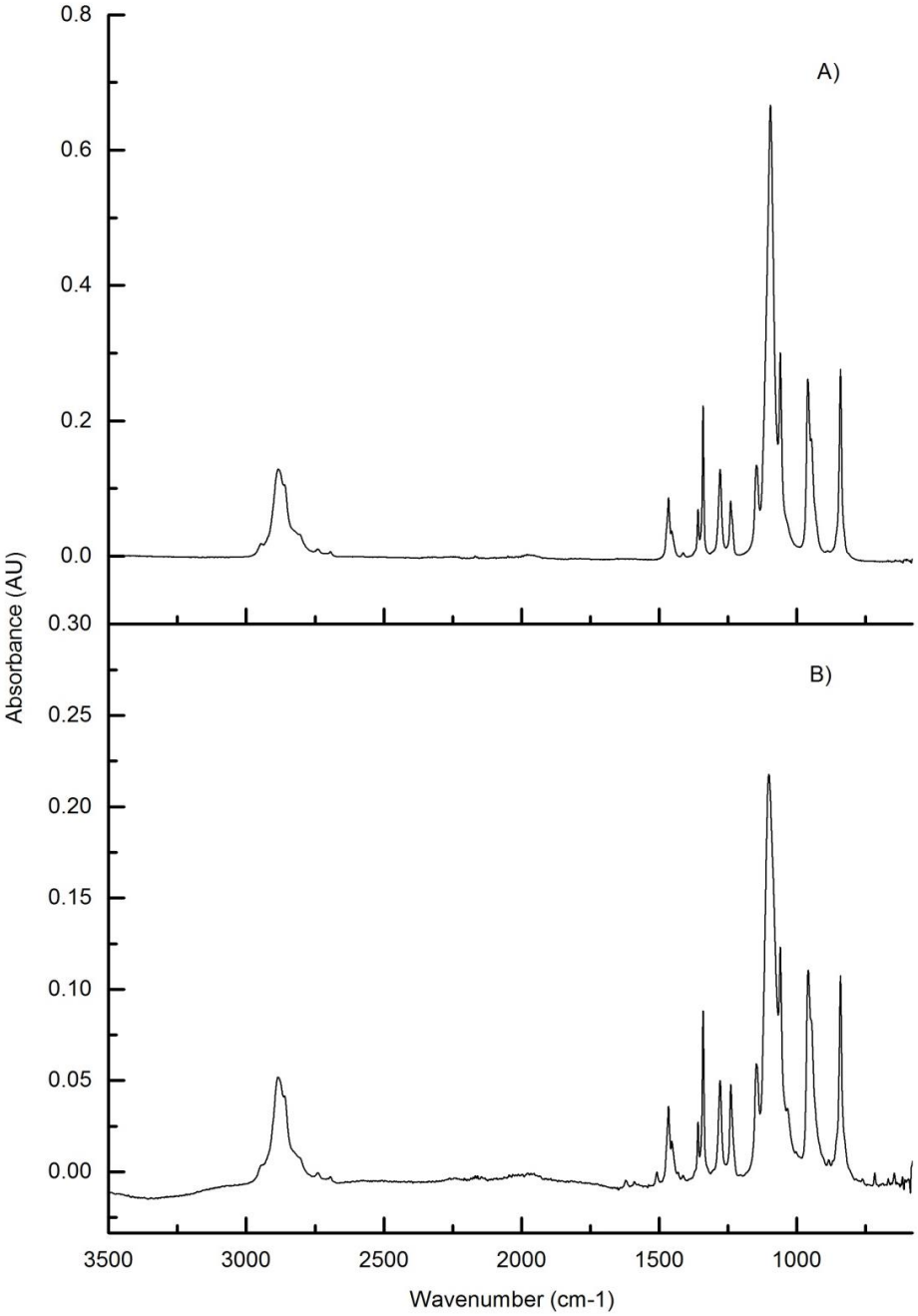


Figure 24: Infrared Spectra of PEG4000 illustrating the effect of DSC treatment on the sample exemplified by A) PEG4000 under ambient conditions and B) After DSC treatment.

*3.1.4 Thermogravimetric Analysis*

On application of high temperatures, PEG4000 was found to almost entirely degrade over a temperature range of approximately 335-450°C (Figure 25). This temperature at which degradation occurs is significantly distinct from the melting range at approximately 57-65°C given by the differential scanning calorimetry results (Figure 23 and Table 2) but this shows that the polymer is stable well beyond its melting temperature. Table 3 gives all three replicates of PEG4000 and a mean and standard error for the temperature ranges and percentage degradation of the thermogravimetric analysis samples. The white powder became blackened and reduced in mass on degradation due to the carbon burning, giving off a strong smell.

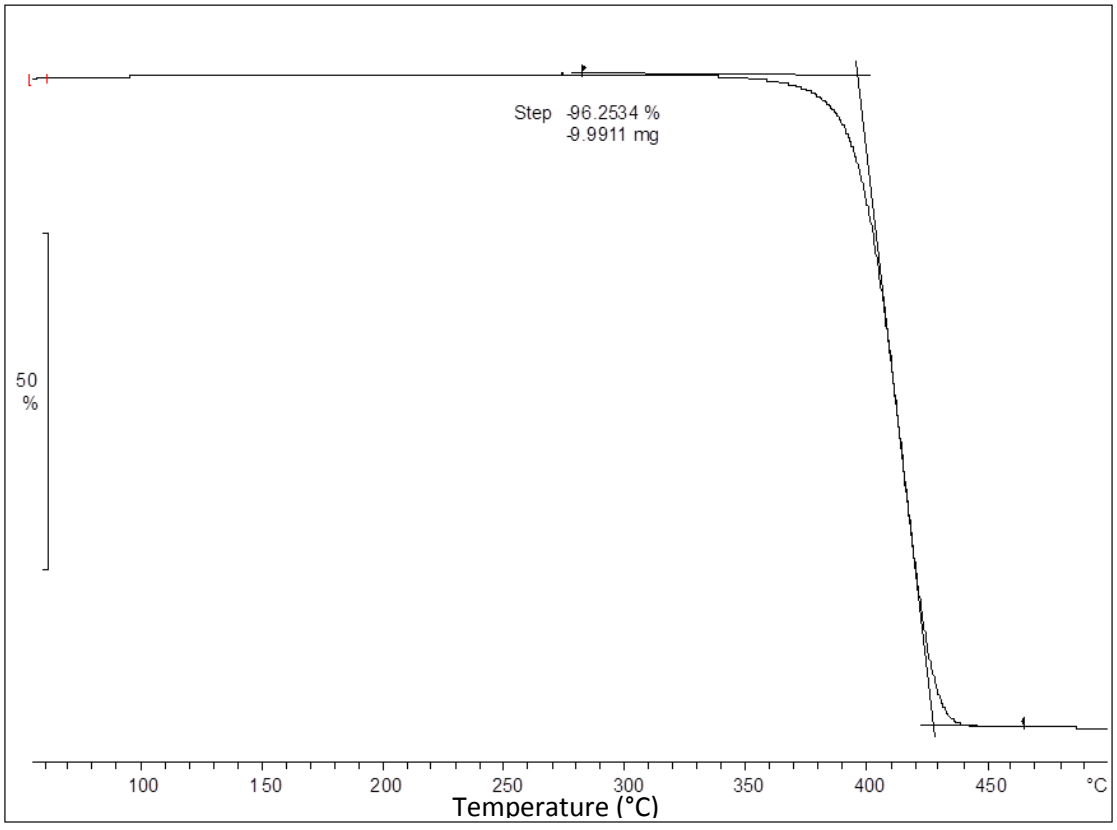


Figure 25: Thermogravimetric analysis of PEG4000

Table 3: Thermogravimetric analysis of 3 replicates of PEG4000 which gives the mean peak degradation.

| Sample | Approximate Temperature Range (°C) | Percentage degradation (%) |
|---|---|---|
| 1 | 335-450 | 96.2534 |
| 2 | 340-440 | 96.665 |
| 3 | 330-445 | 96.6668 |
| Average | 335-445 | 96.5284 |
| S.E. | 2.886751 | 0.137501 |

*3.1.5 Temperature Studies*

To explore the phenomenon of the polymer flowing under pressure the melting temperature of PEG4000 with respect to pressure was probed. Figure 26 illustrates the relationship between temperature and pressure on PEG4000 and shows a linear relationship with temperature being inversely proportional to pressure. The graph provides the basic physicochemical description of PEG4000 with temperature and pressure which would be required for the subsequent studies of drug loading using the large volume press.

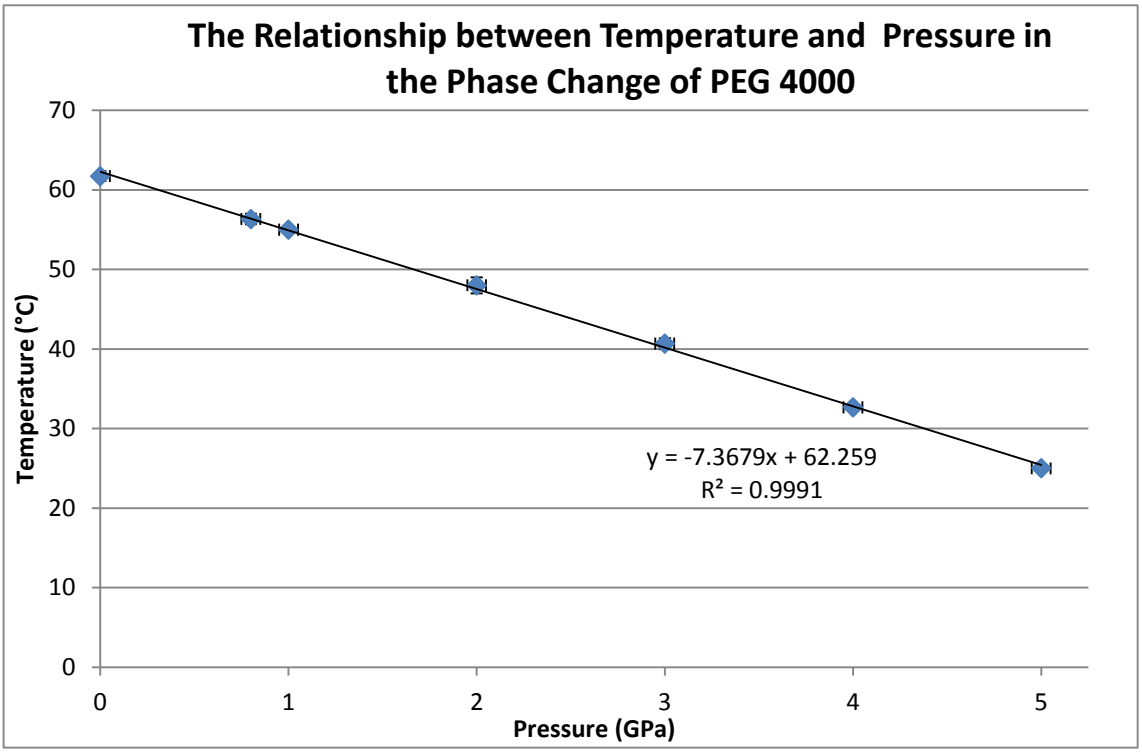


Figure 26: The mean relationship between temperature and pressure in the melting of PEG, where n=3, the vertical error bars from left to right represent SE±0.638462°C, 0.666667°C, 0°C, 1°C, 0.666667°C, 0.333333°C and 0°C respectively. The horizontal error bars represent the 0.05 GPa margin of error generated by the Raman

### *3.2 Hydrocortisone*

#### *3.2.1 Raman*

In Figure 27 a visual representation of the effect of pressure on the hydrocortisone which originates as a white crystalline powder can be observed. Like PEG it loses its colour but unlike PEG it does not fully melt, merely becoming compressed.

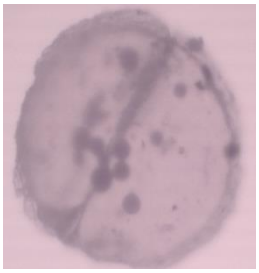

Figure 27: Hydrocortisone after pressurising. It should be noted the dark circles are the rubies used to test the pressure.

In Figure 28 initially at ambient pressure a distinct ridge topped peak can be seen at approximately 2890 $cm^{-1}$ and a distinct double peaked structure can be seen with peaks at approximately 1611 $cm^{-1}$ and 1644 $cm^{-1}$. Like PEG4000, the former falls in the CH region of the spectra and thus could correspond to the aromatic rings found in the structure of hydrocortisone. The 1611 $cm^{-1}$ and 1644 $cm^{-1}$ peaks fall in the C=C region, corresponding to the alkene regions of the steroid backbone. Two of the polymorphs of hydrocortisone require two molecules to describe the whole structure so the peaks at 1611 and 1644 $cm^{-1}$ represent the alkene group on each of these molecules. There are other peaks present in the spectrum, but they do not show distinct changes. On application of pressure the ridges of the CH peak are lost and the peak becomes smooth in a gradual manner, becoming completely smooth by 5GPa. Again the axis breaks are due to the diamond peak being removed from the spectra (~1300 $cm^{-1}$). The peak observed just to the right of the CH peak in some of the spectra is due to a slight influence of the diamond, largely due to the fact that the fluorescence of hydrocortisone makes it slightly more difficult to focus on than PEG alone. In Figure 29, the shift to a higher wavenumber in this region caused by increasing pressure can be observed. There appears to be a fairly linear relationship between pressure and Raman shift, with the shift to a higher wavenumber and thus

increase in Raman shift being directly proportional to the increase in pressure. In Figure 28, with increasing pressure, the alkene peaks are observed to become less defined and eventually merge into a single peak by approximately 4 GPa. Figure 30 illustrates the merging of these two peaks. The merged peak is latterly observed to shift to a higher wavelength suggesting after the merging, the increase in Raman shift seen previously with the CH peak in Figure 29, is replicated in the merged peak. Similarly to PEG4000, on removal of pressure the peaks return to their ambient state as exemplified by Figure 31.

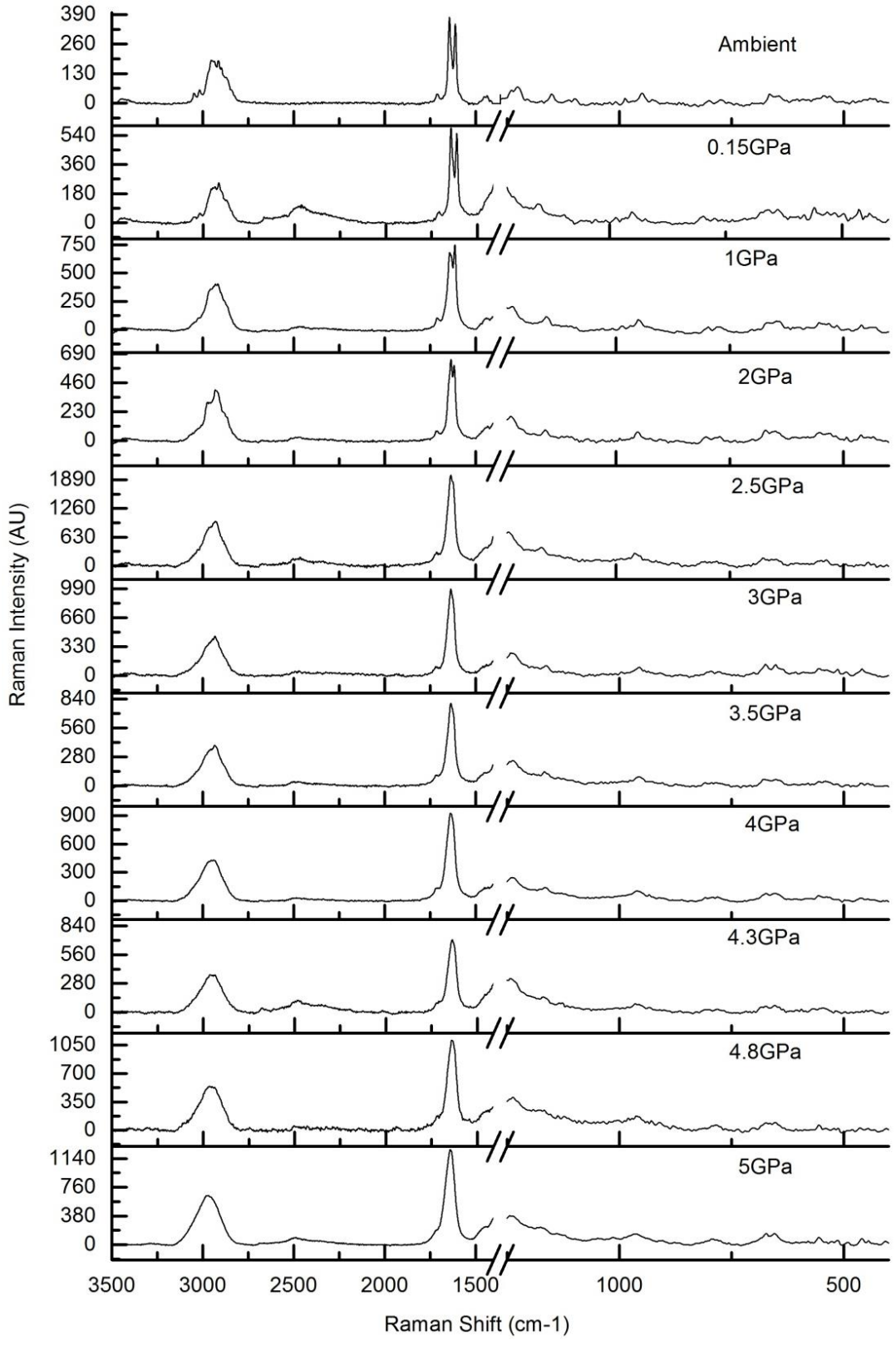


Figure 28: Raman spectra of hydrocortisone illustrating the changes occurring on increasing pressure

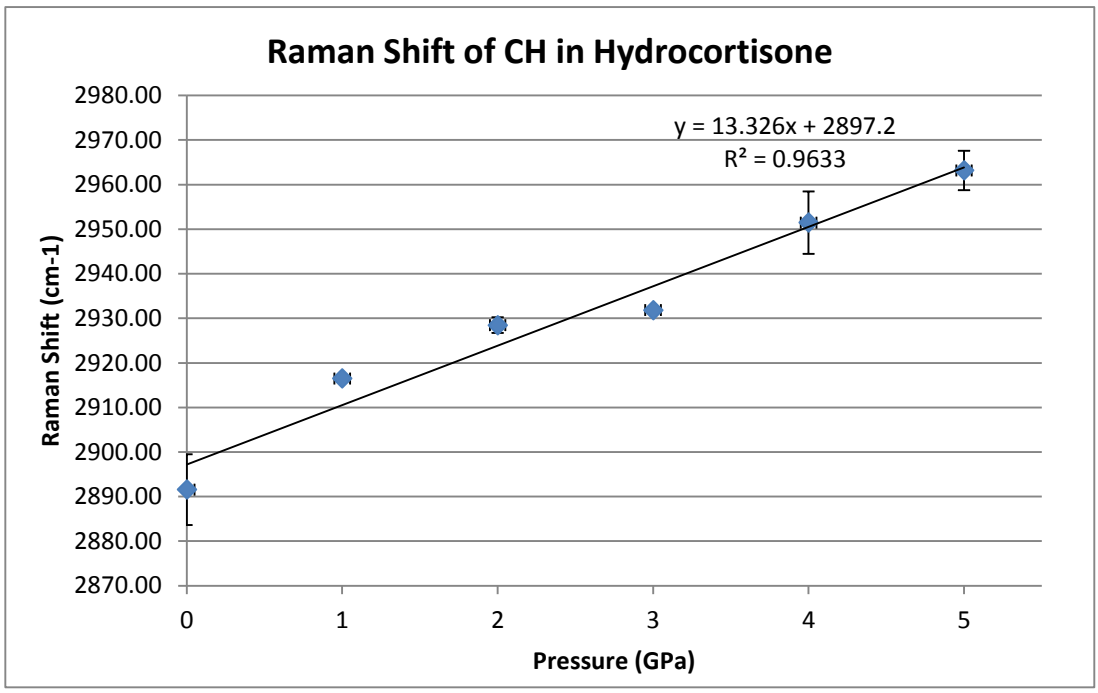


Figure 29: Raman shift of the 2888cm$^{-1}$ CH region of hydrocortisone, in which n=5 and SE±0, 7.65, 6.43, 7.81, 9.41 and 9.96cm$^{-1}$ respectively. The horizontal error bars have the value of 0.05GPa determined by the Raman spectrometer..

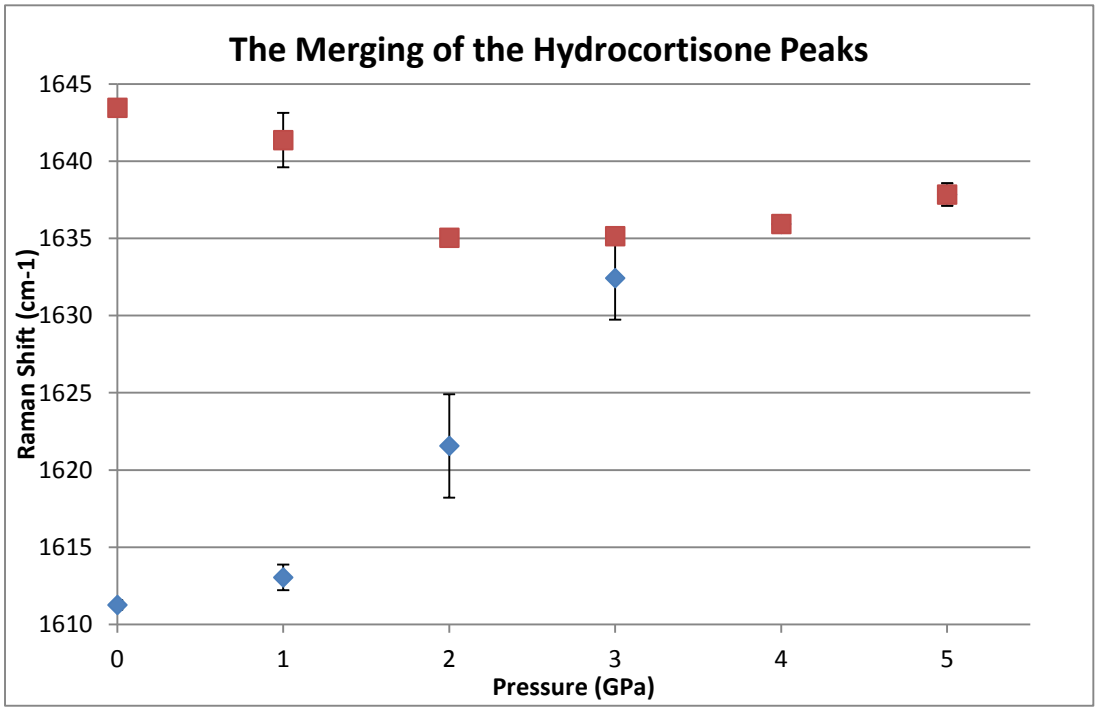


Figure 30: The Raman shift of the 1611cm$^{-1}$ and the 1644cm$^{-1}$ C=C peaks in which n=5 and SE±0.311429, 0.834003, 3.352016, 0.269756, 0.240704 and 0.72436cm$^{-1}$ for the 1611cm$^{-1}$ peak, and 0.198515, 1.765453, 0.3172, 0.269756, 0.240704 and 0.72436cm$^{-1}$ for the 1644cm$^{-1}$ peak respectively. The horizontal error bars have the value of 0.05GPa determined by the Raman spectrometer.

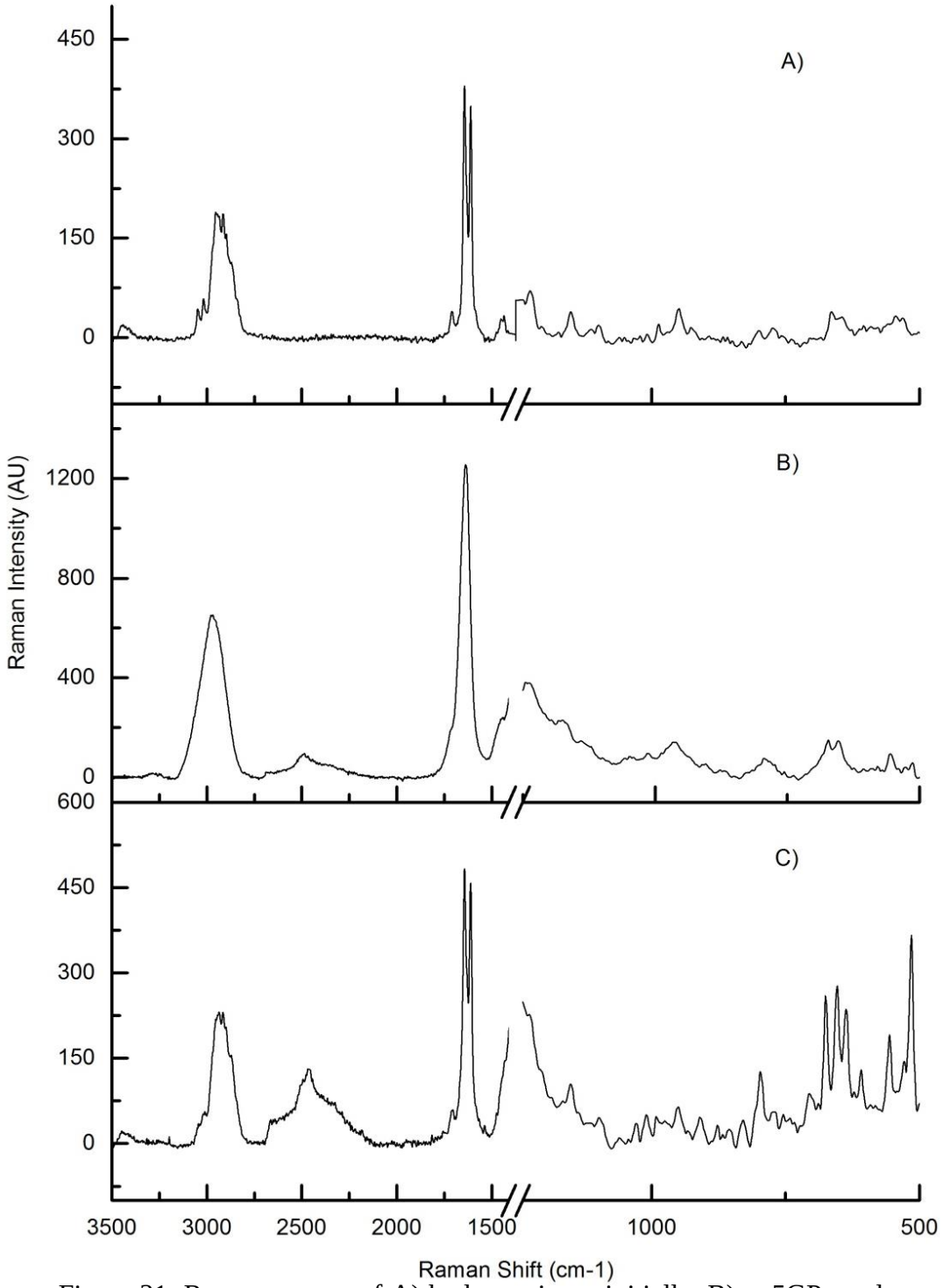

Figure 31: Raman spectra of A) hydrocortisone initially, B) at 5GPa and C) after pressure removal, illustrating return of the original peaks.

*3.2.2 Infrared Spectroscopy*

In Figure 32, the effect of pressure on the functional groups of hydrocortisone as illustrated by infrared spectroscopy can be observed. All the peaks are diminished by pressure by around 9-fold but the greatest change is in the C=C 1642 $cm^{-1}$ as the difference in this peak from the next highest peak at 1046 $cm^{-1}$, representing C-O, is observed to decrease from 1.93-fold at ambient (A) to 1.28-fold after pressure (B), making the change in this particular peak nearly 10-fold, falling from 0.04401 to 0.00466AU, with the next highest peak falling from 0.02284 to 0.00363AU. The latter spectrum (B) is not a particularly good representation but this was consistent with all the samples taken from the diamond anvil cell. This may be, in part, due to the necessarily small samples that we have to use for the pressure experiment.

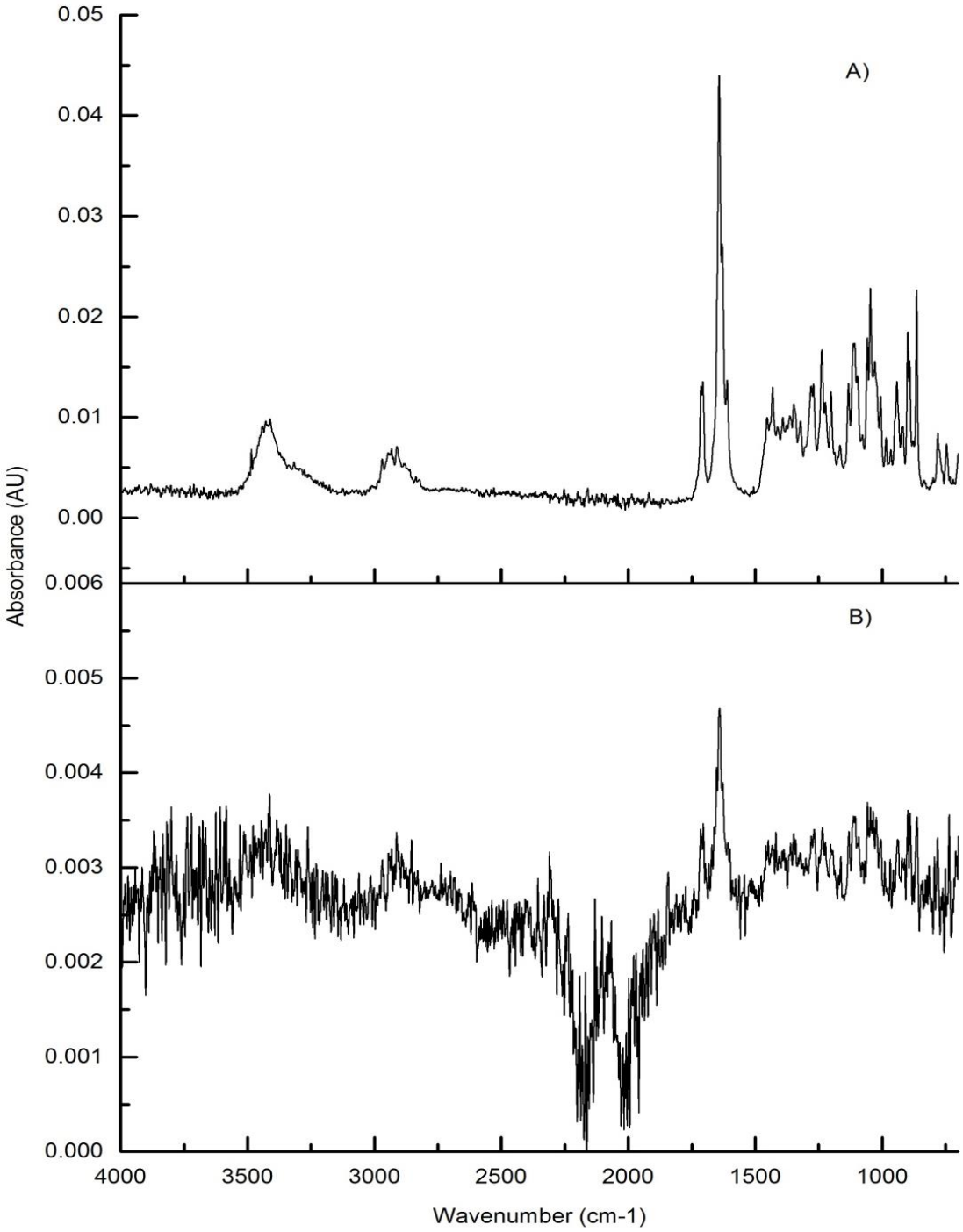


Figure 32: Infrared spectra of hydrocortisone illustrating the changes occurring B) after pressure is applied and removed by comparison to the A) original ambient sample.

*3.2.3 Differential Scanning Calorimetry*

On application of heat, Hydrocortisone was found to melt over the range of 223.61 to 228.06°C, reaching its peak at 226.87°C (Figure 33). Table 4 illustrates all three replicates the author took of hydrocortisone and the mean results with the standard error. Unlike PEG and the pressurised sample, white powder turned into a bright marigold yellow liquid on reaching the melting range and then became a solid shiny yellow mass which is shown in Figure 43. This colour change was suggested to be caused by formation of the degradation product 11β,17α-dihydroxy-3,20-dione-4-pregnene-21-al (Connor, 1974). This colour change is not observed on pressurising the sample suggesting this phase change is not occurring on pressurising.

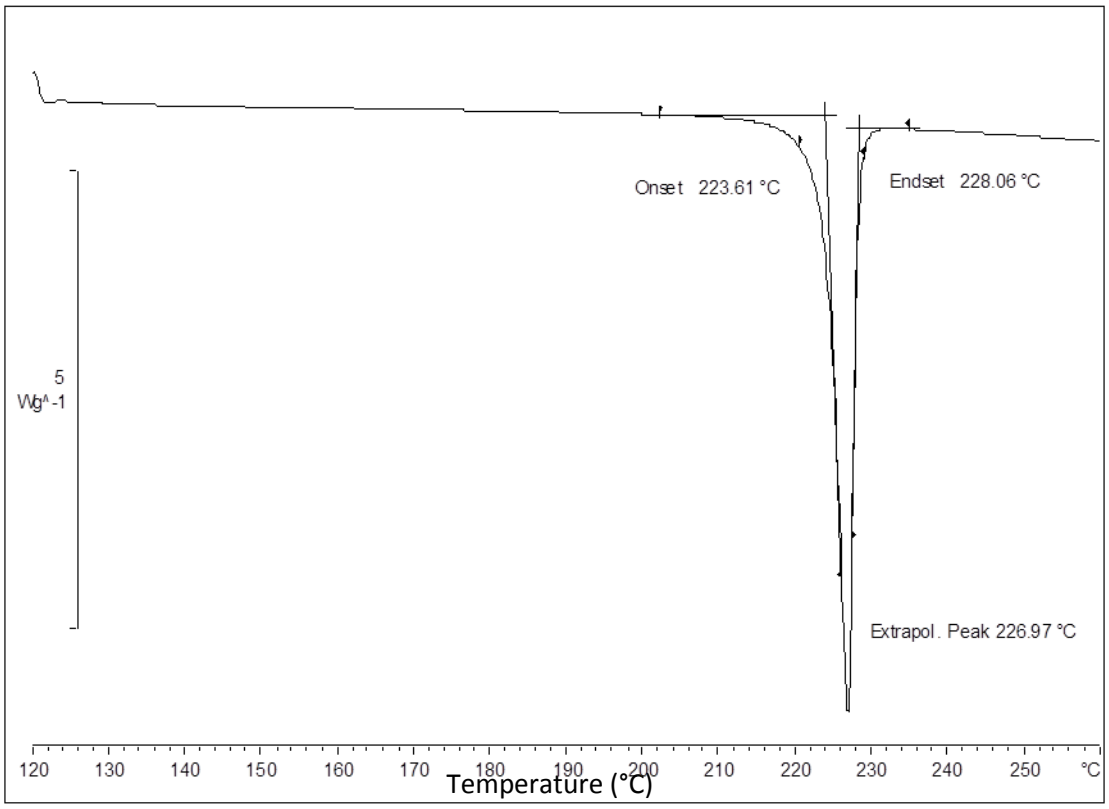


Figure 33: Differential Scanning Calorimetry of hydrocortisone

Table 4: Differential scanning calorimetry of 3 replicates of hydrocortisone, with the mean onset, extrapolated peak and endset temperatures.

| Sample | Onset Temperature (°C) | Extrapolated Peak Temperature (°C) | Endset Temperature (°C) |
|---|---|---|---|
| 1 | 223.50 | 227.13 | 228.46 |
| 2 | 223.61 | 226.97 | 228.06 |
| 3 | 223.35 | 226.68 | 227.93 |
| Average | 223.49 | 226.93 | 228.15 |
| S.E. | 0.075351 | 0.131698 | 0.159478 |

In Figure 34, the effect of DSC exposure on the infrared peaks can be observed. Unlike the pressurised sample, the peaks of the DSC sample (B) actually increase in size relative to the ambient sample (A). The greatest increases are found to be in the CH alkane region at around 2933 $cm^{-1}$, with a 2.75-fold increase from 0.00689 to 0.01892AU, the C=O region at approximately 1706 $cm^{-1}$, with a 2.23-fold increase from 0.01353 to 0.03011AU, the CO region at approximately 1046 $cm^{-1}$, with a 1.96-fold increase from 0.02284 to 0.04488AU, and the C=C region at around 1642 $cm^{-1}$, with a 1.89-fold increase from 0.04401 to 0.08322AU. The OH region at 3428 $cm^{-1}$, does not exhibit as large an increase with only a 1.24-fold increase from 0.00964 to 0.01196AU.

The increase in peak size suggests there is actually a considerable change happening in the molecule on melting which is not occurring on pressurising. This may suggest the formation of an initial degradation product. This is particularly suggested by the fact that the C=O peak increases from a 1.4-fold difference from the smaller OH peak to a 2.52-fold difference. Which may be attributed to the conversion of the alcohol group to an aldehyde group in the formation of 11β,17α-dihydroxy-3,20-dione-4-pregnene-21-al (Connor, 1974). The absence of these changes in the pressurised sample spectra suggest that unlike under high temperature, pressure does not induce degradation.

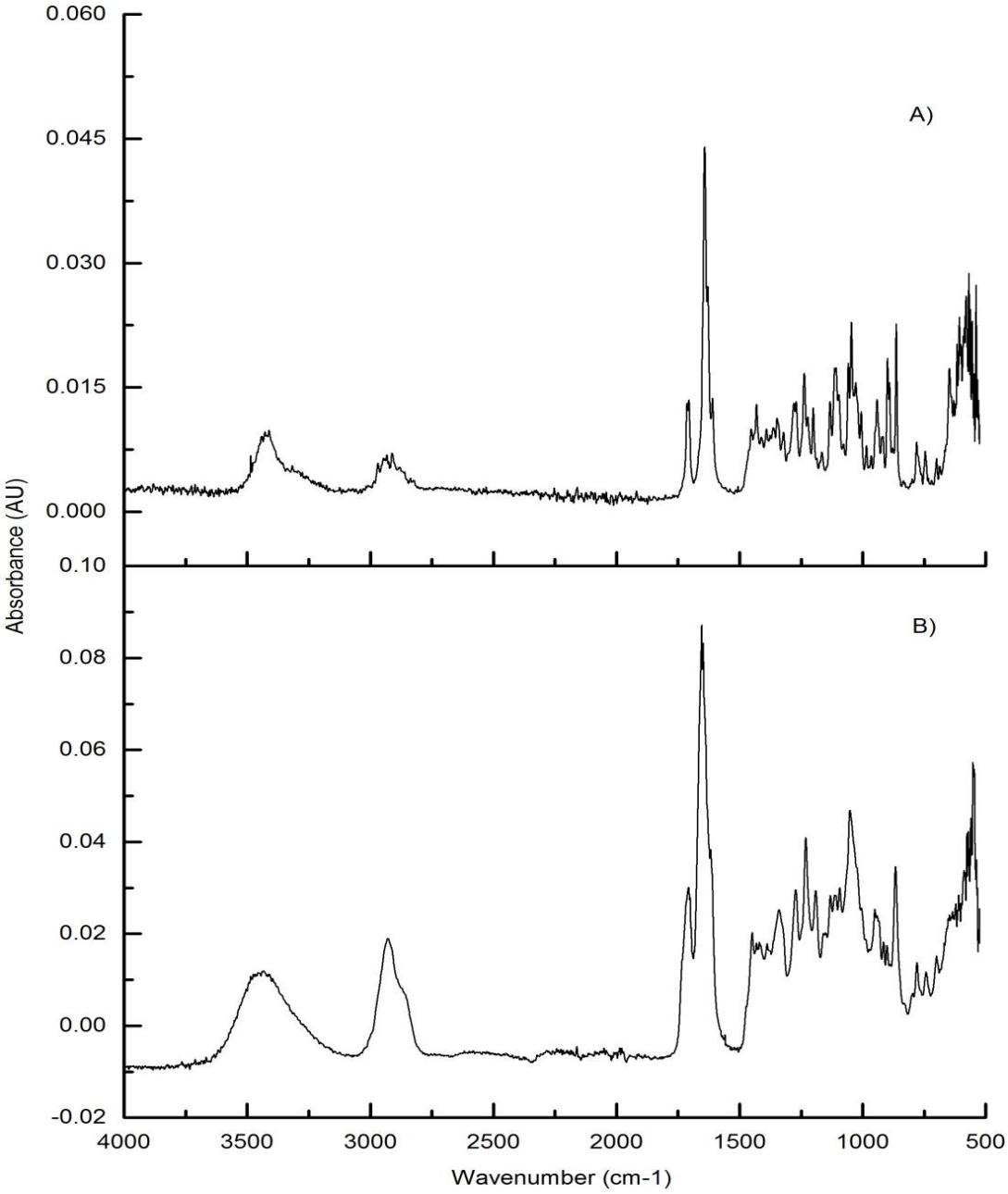


Figure 34: Infrared spectra of hydrocortisone illustrating the effect of DSC treatment on the functional groups, as illustrated by a comparison of the spectra A) before and B) after DSC treatment.

*3.2.4 Thermogravimetric Analysis*

On application of high temperatures, hydrocortisone was found to degrade by around 8% less than PEG4000 over a temperature range of approximately 240-520°C (Figure 35). This temperature at which degradation occurs is distinct from, although still quite close to, the melting range at approximately 223-228.5°C given by the differential scanning calorimetry results (Figure 33 and Table 4). There is an interesting almost double step pattern seen in the degradation. This could suggest the degradation is occurring in steps, perhaps this first step is 11β,17α-dihydroxy-3,20-dione-4-pregnene-21-al formation at around 300ºC (Connor, 1974). Table 5 gives all three replicates of hydrocortisone and a mean and standard error for the temperature ranges and percentage degradation of the thermogravimetric analysis samples. The white powder became blackened and reduced in mass on degradation due to the carbon burning, giving off a strong smell in decomposition.

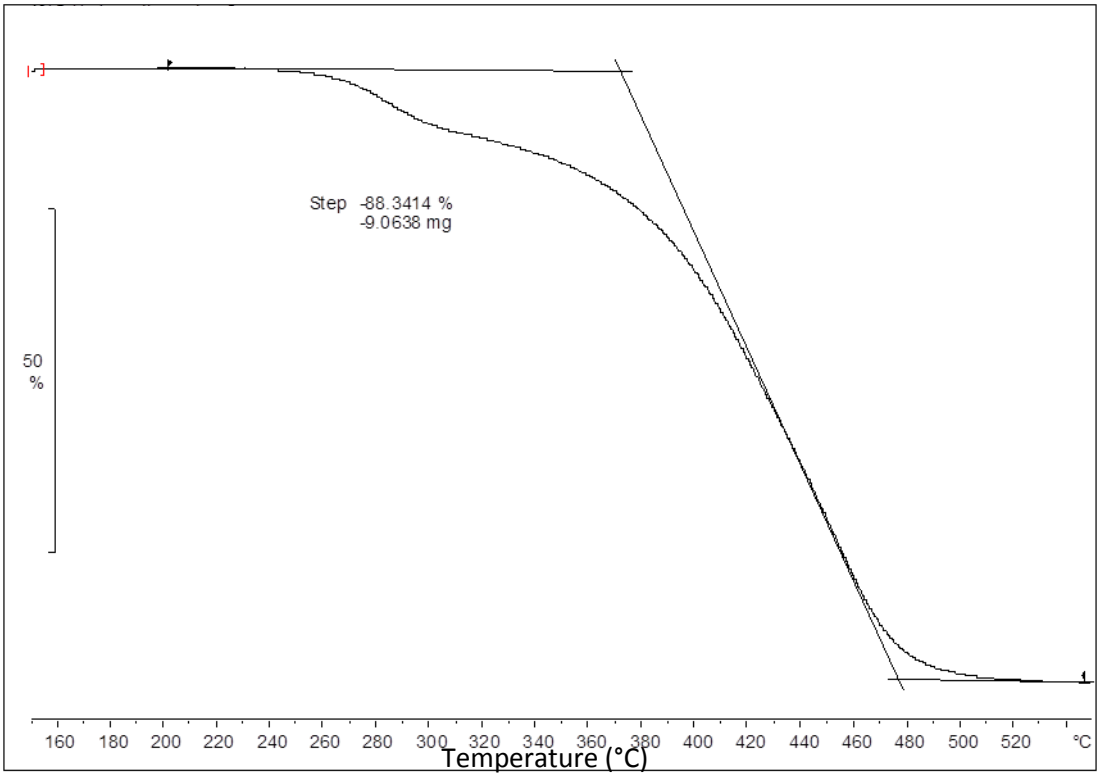


Figure 35: Thermogravimetric analysis of hydrocortisone illustrating the degradation of the drug under high temperatures.

Table 5: Thermogravimetric analysis of 3 hydrocortisone replicates, giving the mean percentage degradation.

| Sample | Approximate Temperature Range (°C) | Percentage degradation (%) |
|---|---|---|
| 1 | 240-515 | 88.3414 |
| 2 | 235-520 | 88.7822 |
| 3 | 240-500 | 88.6812 |
| Average | 238.33-511.67 | 88.6016 |
| S.E. | 6.009252 | 0.133327 |

### *3.3 PEG and Hydrocortisone*

#### *3.3.1 Raman*

In Figure 36 a visual representation of a PEG:Hydrocortisone blend after pressure can be observed, illustrating that again PEG melts and becomes translucent and the hydrocortisone particles can be faintly observed.

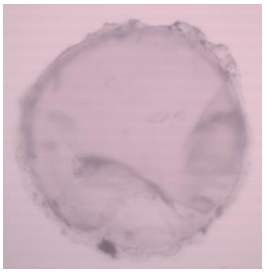

Figure 36: PEG:Hydrocortisone after pressure

Initially the author looked at 90:10 and 80:20 PEG:Hydrocortisone blends, however as the blend taken forward was the 50:50 blend the results of the former can be observed in the appendices and seen to follow a very similar pattern with the only major difference being the size of the hydrocortisone peaks. In Figure 37, at ambient pressure a distinct sizable ridged peak can be seen at approximately 2900 $cm^{-1}$ which is a combination of PEG4000 and hydrocortisone. The distinct double peaked structure of hydrocortisone at 1611 $cm^{-1}$ and 1644 $cm^{-1}$, corresponding to the alkene peaks, can also be observed at a lesser intensity than pure hydrocortisone. The smaller distinct peak with a step like conformation at approximately 844 $cm^{-1}$ C-O-C of PEG can also be observed. The CH region of the spectra corresponds to a combination of the carbons attached to hydrogen atoms found in the main chain of PEG4000 and the aromatic rings of hydrocortisone. On application of pressure the ridges of the CH peak are lost and the peak becomes smooth in a gradual manner, becoming completely smooth by 5GPa. The alkene peaks again merge by 4GPa. Figure 38 is a zoom in to the C-O-C region. It is observed to consist of a step like peak and as the pressure is increased the lower portion of the peak is seen to gradually diminish, completely disappearing by 5GPa. In Figure 39 the smaller step-like feature of the C-O-C region is observed to return on removal of pressure return

as the PEG resolidifies and the distinct double peak of hydrocortisone are also observed to return.

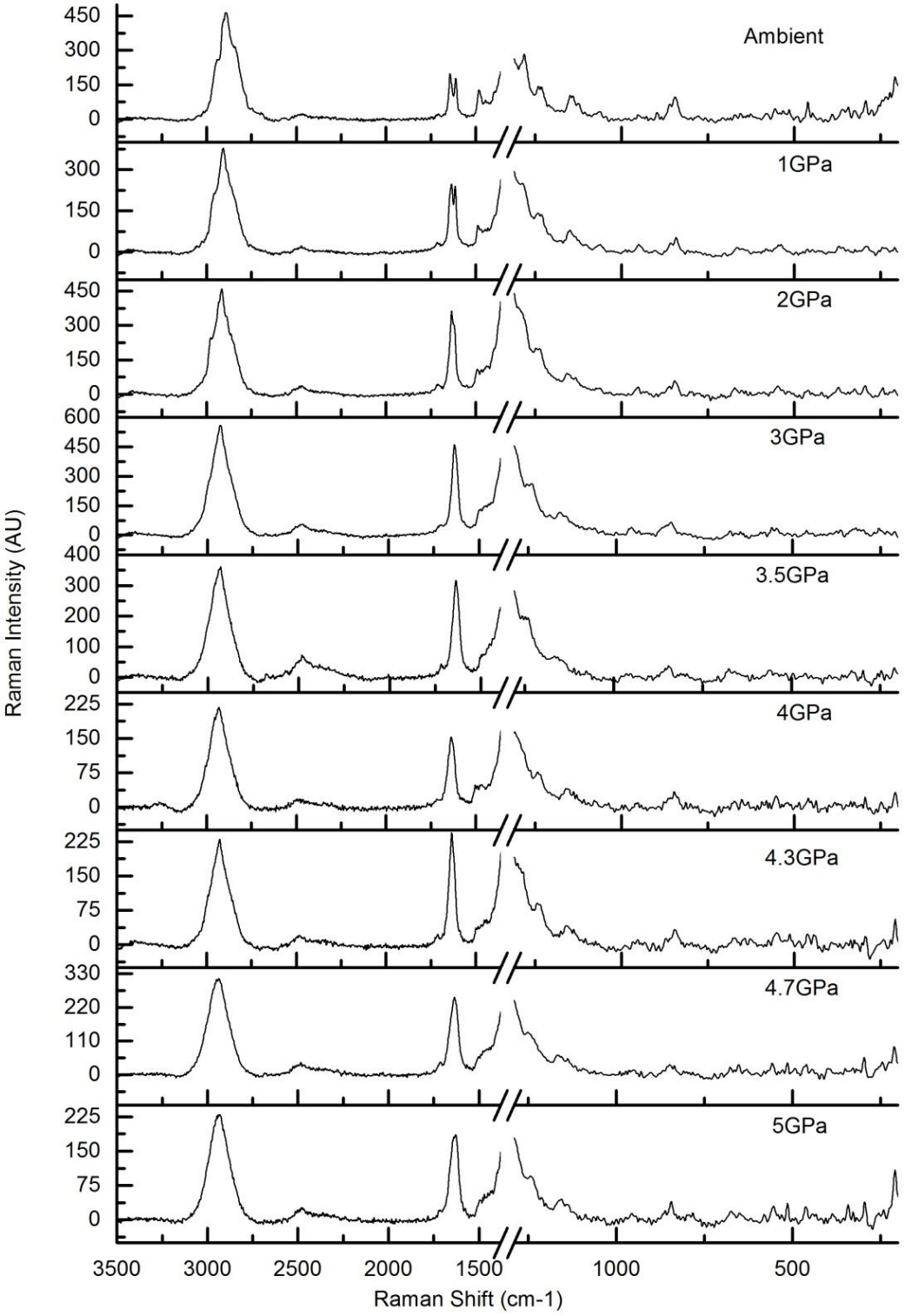


Figure 37: Raman spectra of the 50:50 PEG:hydrocortisone sample, illustrating the effect of increasing pressure on the peaks.

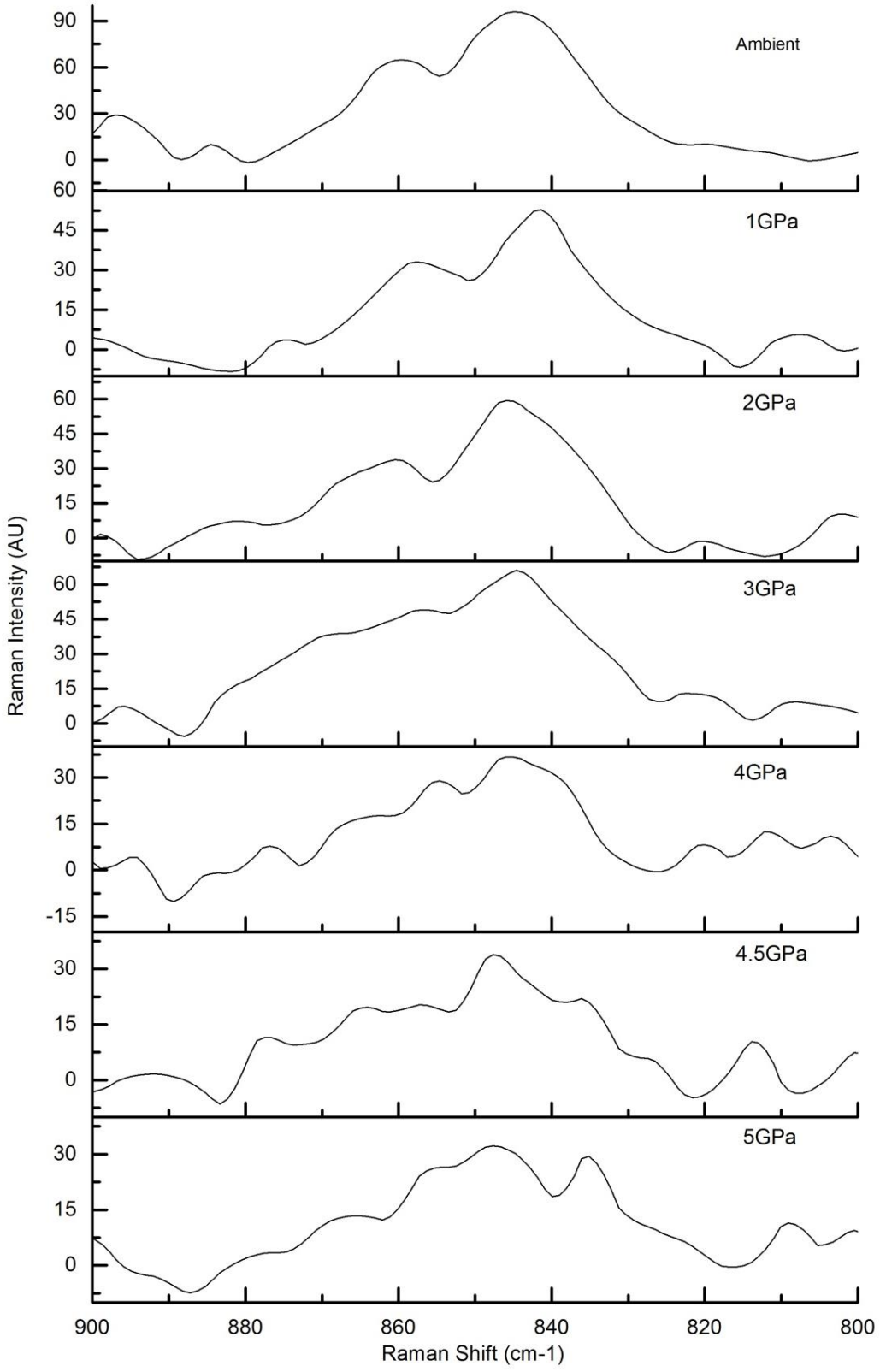


Figure 38: Raman spectra of the 844cm$^{-1}$ C-O-C of the 50:50 PEG:hydrocortisone sample, illustrating the effect of increasing pressure on the peaks.

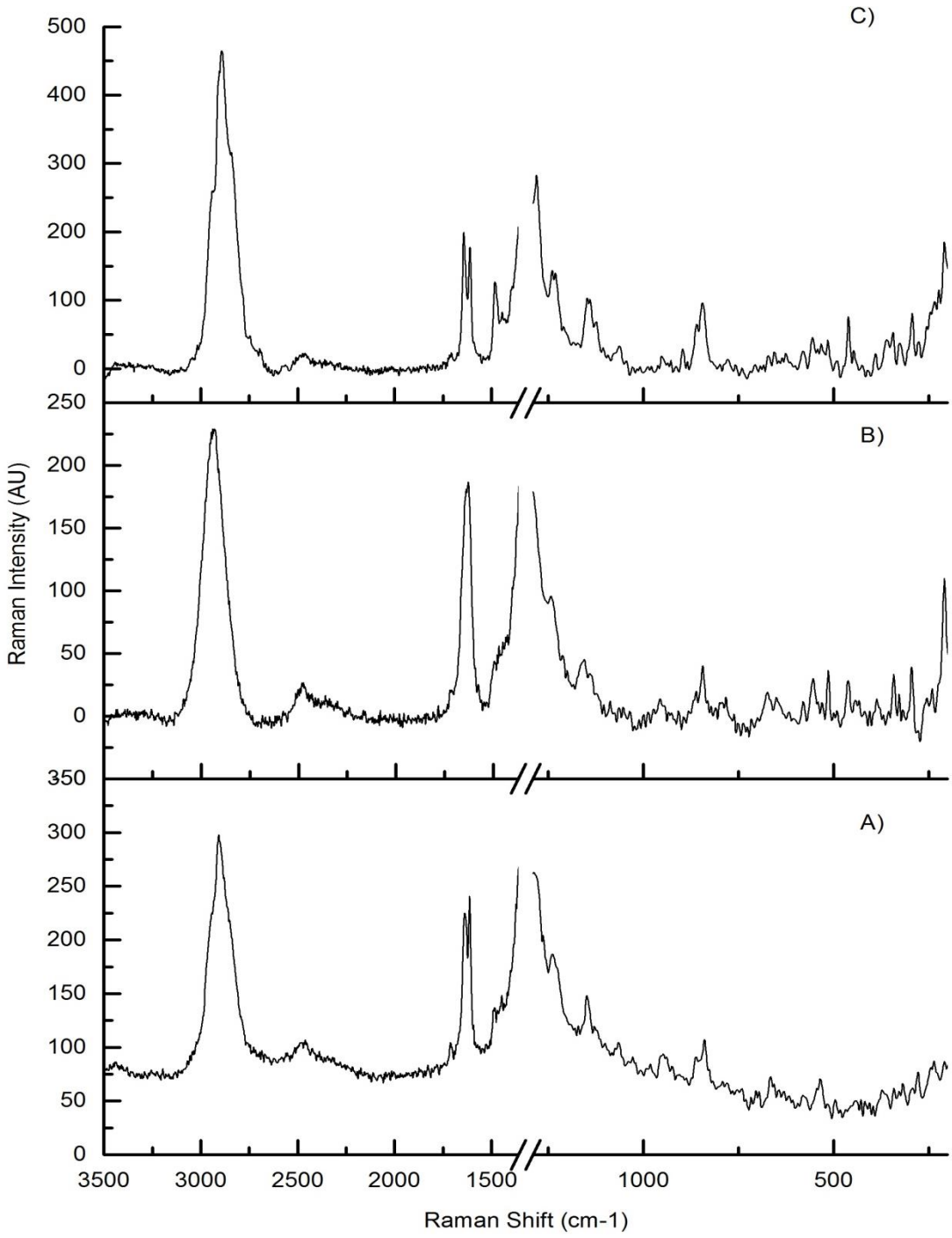


Figure 39: Raman Spectra illustrating the effect of pressure removal by comparison of the 50:50 PEG:hydrocortisone sample (A) at ambient pressure, (B) at 5GPa and (C) after pressure removal.

*3.3.2 Infrared Spectroscopy*

Again the data for the 90:10 and 80:20 PEG:Hydrocortisone blends can be found in the appendices and the only difference to the 50:50 blend is the fact that the hydrocortisone peaks are less prominent. In Figure 40 all the peaks are diminished by pressure but as with pure PEG the greatest decrease is seen in the 1096 $cm^{-1}$ region corresponding to the C-O-C region. In the ambient sample spectra (A) this peak, at 0.64335AU is 3.24-fold higher than the next highest peak at 842 $cm^{-1}$, with an absorbance of 0.19883AU. Whereas, after pressure (B), although all the peaks decrease in height, this peak, at 0.09451AU, is only 2.58-fold higher than the 842 $cm^{-1}$ peak, at an absorbance of 0.03661AU. The change in this particular region supports the changes in C-O-C Raman peaks. Hydrocortisone peaks can be seen at the OH region at 3429 $cm^{-1}$, the C=O region at 1706 $cm^{-1}$ and the aromatic C=C region at 1630 $cm^{-1}$, and their size is directly proportional to the percentage of hydrocortisone present at ambient. The hydrocortisone peaks are seen to fall after pressure with the OH region falling from 0.02412AU to an absorbance less than zero, the C=O region falling from 0.03158 to 0.00607AU and the C=C region falling from 0.07021 to 0.00531AU. This is undoubtedly due to experimental error during the collection of the background and subsequent sample readings.

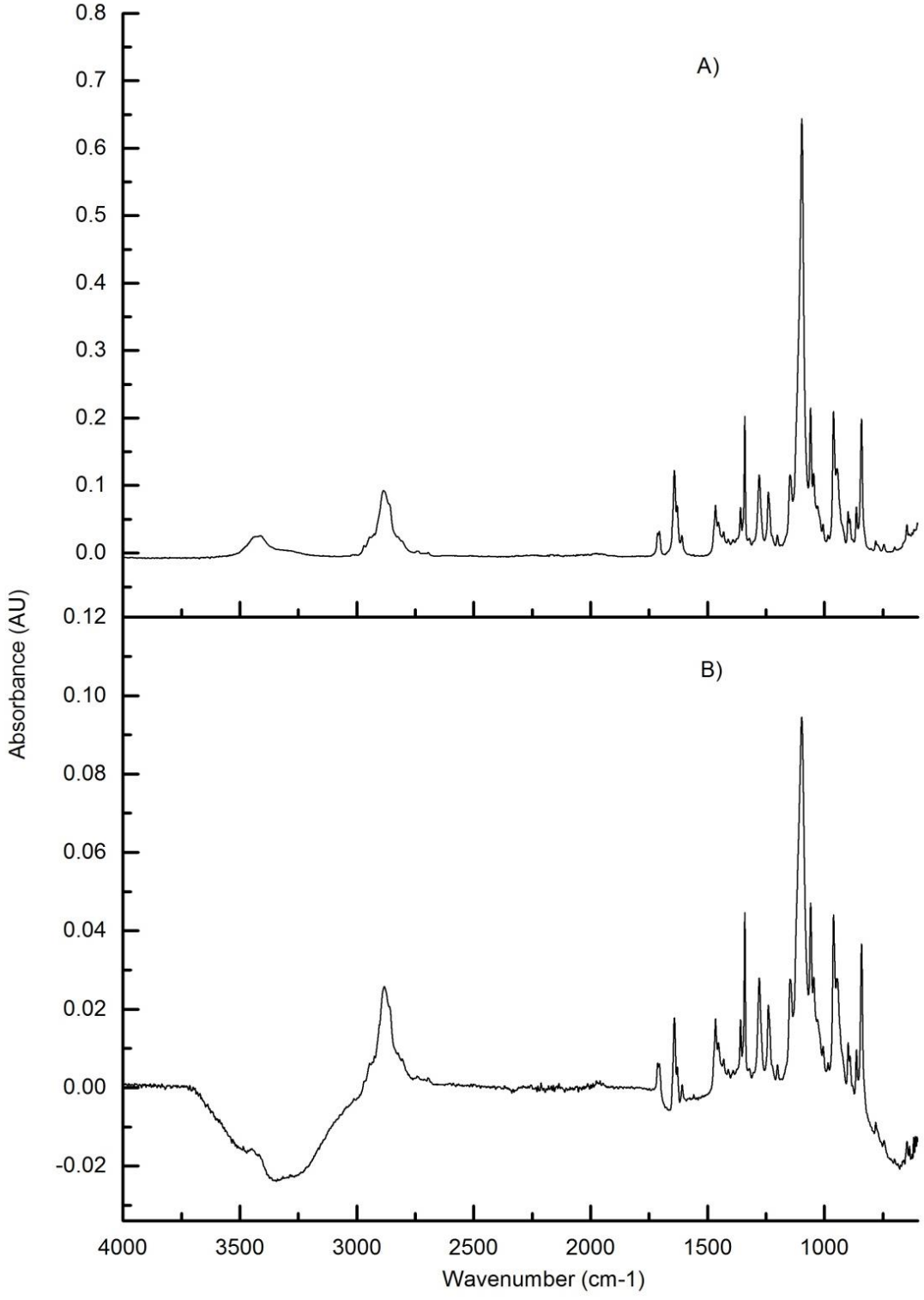


Figure 40: Infrared spectra of the 50:50 PEG:hydrocortisone sample, illustrating the effect of pressure on the functional groups.

*3.3.3 Differential Scanning Calorimetry*

Again the data for the 90:10 and 80:20 PEG:hydrocortisone blends is shown in the appendices. In Figure 41, the 50:50 blend showed a PEG melting range of 57.72 to 63.46°C, reaching its peak at 61.01°C, and a hydrocortisone melting range of 186.91 to 208°C, reaching its peak at 203.04°C. Table 8 illustrates all three replicates the author took of hydrocortisone and the mean results with the standard error. In Figure 42, the effect of DSC exposure on the infrared spectrum can be observed. As the PEG4000 peaks decrease as before, the hydrocortisone CH influence becomes more prominent. The 3.24-fold difference in the 1096 $cm^{-1}$ PEG peak, at 0.64346AU, relative to the next highest peak, at 0.19883AU, at ambient drops to a 2.77-fold difference, comparing the 841 $cm^{-1}$ peak at 0.16436AU with the 1096 $cm^{-1}$ peak at 0.45464AU, after pressure has been applied and removed confirming the same reaction still occurs in the presence of hydrocortisone. Figure 43 shows the DSC pans which have been reopened after heating, hydrocortisone and PEG are both observed to have undergone colour changes with the former undergoing a white to yellow colour change and the latter undergoing a white to colourless change, both of which are believed to have occurred on melting.

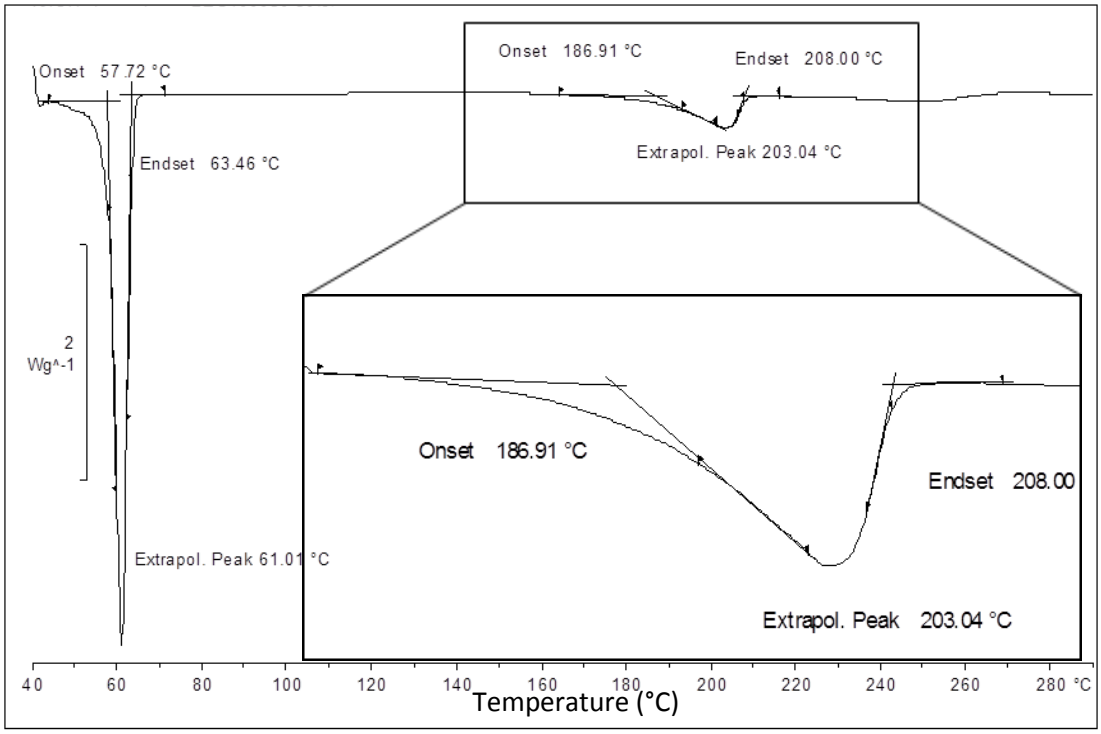


Figure 41: Differential scanning calorimetry of the 50:50 PEG:hydrocortisone sample, showing the melting points for PEG and hydrocortisone.

Table 8: Differential scanning calorimetry of 3 replicates of 50:50 PEG:hydrocortisone, with the mean onset, extrapolated peak and endset temperatures.

| | PEG | | | Hydrocortisone | | |
|---|---|---|---|---|---|---|
| Sample | Onset (°C) | Extrapolated Peak (°C) | Endset (°C) | Onset (°C) | Extrapolated Peak (°C) | Endset (°C) |
| 1 | 57.88 | 60.76 | 64.10 | 187.24 | 204.56 | 209.04 |
| 2 | 58.18 | 61.53 | 63.50 | 187.85 | 204.14 | 208.50 |
| 3 | 57.72 | 61.01 | 63.46 | 186.91 | 203.04 | 208.00 |
| Average | 57.93 | 61.1 | 191.06 | 187.33 | 203.91 | 208.51 |
| S.E. | 0.13483 | 0.22679 | 0.20699 | 0.27534 | 0.45319 | 0.30030 |

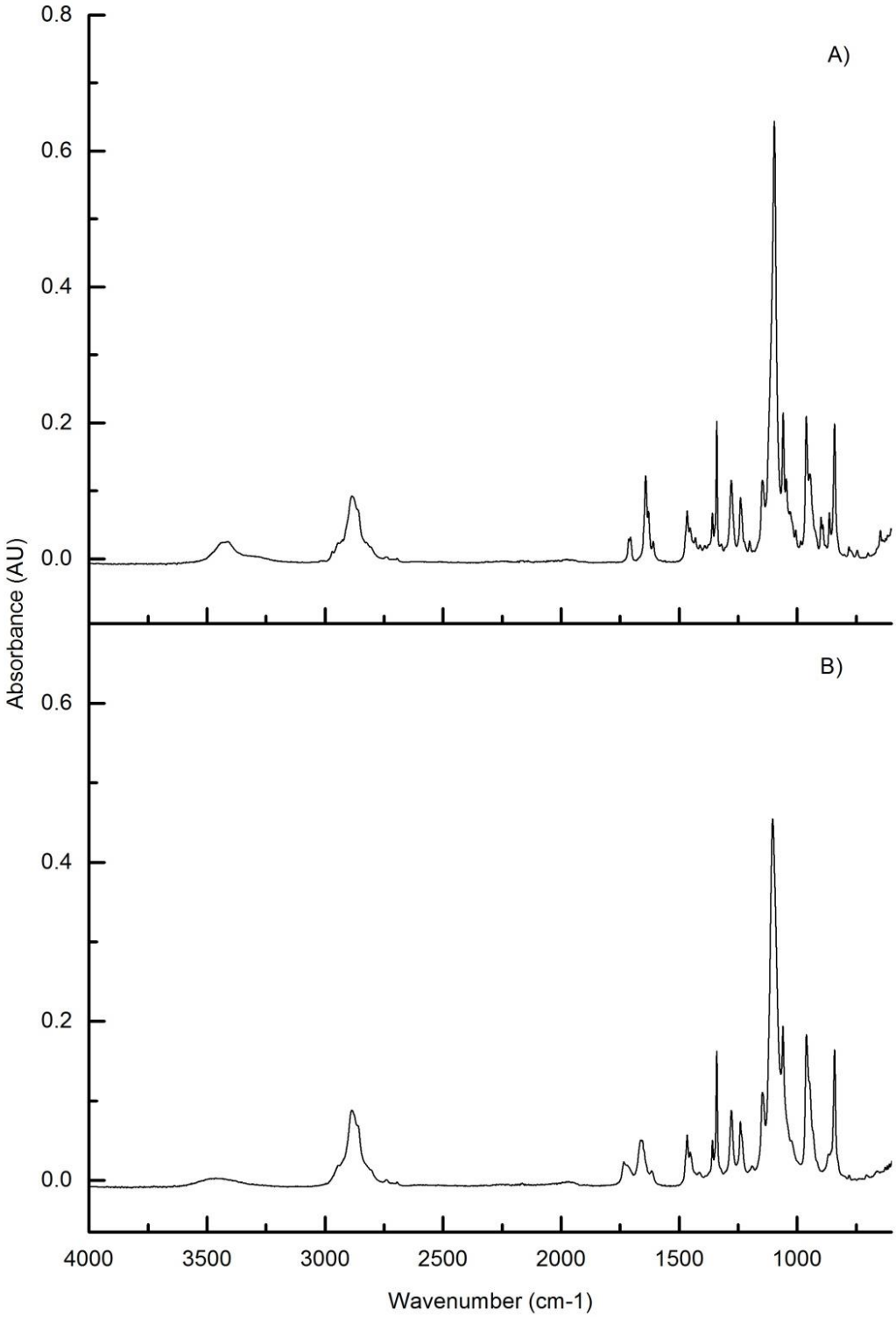


Figure 42: Infrared spectra of the 50:50 PEG:hydrocortisone sample, illustrating the effect of DSC treatment on the functional groups.

Figure 43: DSC pans containing hydrocortisone (left) and PEG4000 (right) after exposure to over 210°C and 60°C respectively

*3.3.4 Thermogravimetric Analysis*

Again the data for the 90:10 and 80:20 PEG:hydrocortisone samples is shown in the appendices. On application of high temperatures, the 50:50 PEG:hydrocortisone blend was found to almost entirely degrade over a temperature range of approximately 215-475°C (Figure 44). The percentage degradation is about around 7% less and the temperature range starts about 120°C lower and 30°C higher than PEG alone. The step formation of hydrocortisone can also be faintly observed. This temperature at which degradation occurs is significantly distinct from the melting ranges at approximately 57-65°C for PEG and 160-210°C for hydrocortisone given by the differential scanning calorimetry results (Figure 24 and Table 2). Table 11 gives all three replicates and a mean and standard error for the temperature ranges and percentage degradation of the thermogravimetric analysis samples. Again the white powder became blackened and reduced in mass on degradation due to the carbon burning, giving off a strong smell.

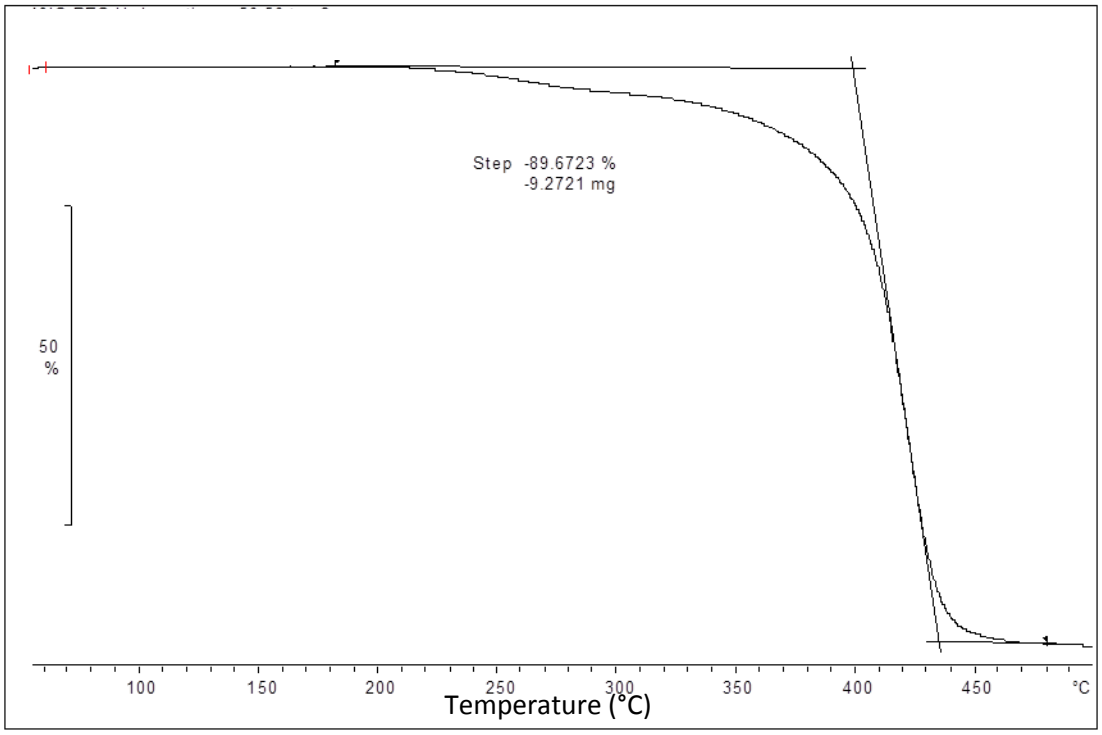


Figure 44: Thermogravimetric of the 50:50 PEG:hydrocortisone sample, showing the percentage degradation occurring.

Table 11: Thermogravimetric analysis of 3 replicates of 50:50 PEG:hydrocortisone, giving the mean percentage degradation.

| Sample | Approximate Temperature Range (°C) | Percentage degradation (%) |
|---|---|---|
| 1 | 215-475 | 89.0733 |
| 2 | 220-480 | 89.4071 |
| 3 | 210-470 | 89.6723 |
| Average | 215-475 | 89.38 |
| S.E. | 2.886751 | 0.173294 |

*3.3.5 Drug Release Studies*

50:50 Samples were selected to take forward in the current study due to them being the most comparable to previous formulations. Initially a drug release study was carried out in pH7.4 PBS analysing the drug release using UV spectrometry. For the PBS study there was only one replicate due to major issues with the nanoUV spectrometer in latter studies (absorbance was showing as negative figures in latter studies even on the standard solutions). This was attributed to the self cleaning function of the spectrometer occurring simultaneously to the absorbance reading causing the spectrometer to effectively read air instead of the sample. The samples were not suitable for use with a normal UV as the extracted samples were too small to be read in a cuvette. This was also not repeated as the simulated intestinal and gastric fluid media were more comparable to gastrointestinal fluids and thus with limited time were considered to be of more value to the study. However, the author chose to still include this as the curve in Figure 45 exhibited the same immediate release, sustained release, immediate release pattern as the later drug release studies (Figures 46, 51 and 52). Figure 45 shows both release over 6 hours and over the full 24 hours. Initially there is a rapid increase in drug release from the diamond anvil cell samples over the first 30 minutes of the study, with 10.67% being released by this point. There is then a period of sustained release of 2 and a half hours, with 13% release by the end of this, before another rapid increase in drug release over the next 2 hours, up to 77.49%. 115.58% has released by 24 hours. This is slightly over the total mass expected to be present. One of the limitations of the study is that the sample inserted into the diamond cell was necessarily small and so despite ensuring a well-mix sample using the ball mill we could not ensure a evenly distributed sample in the cell. For this reason 5 sample disks generated by the diamond anvil cell were used in the drug release but there are still failings in this study.

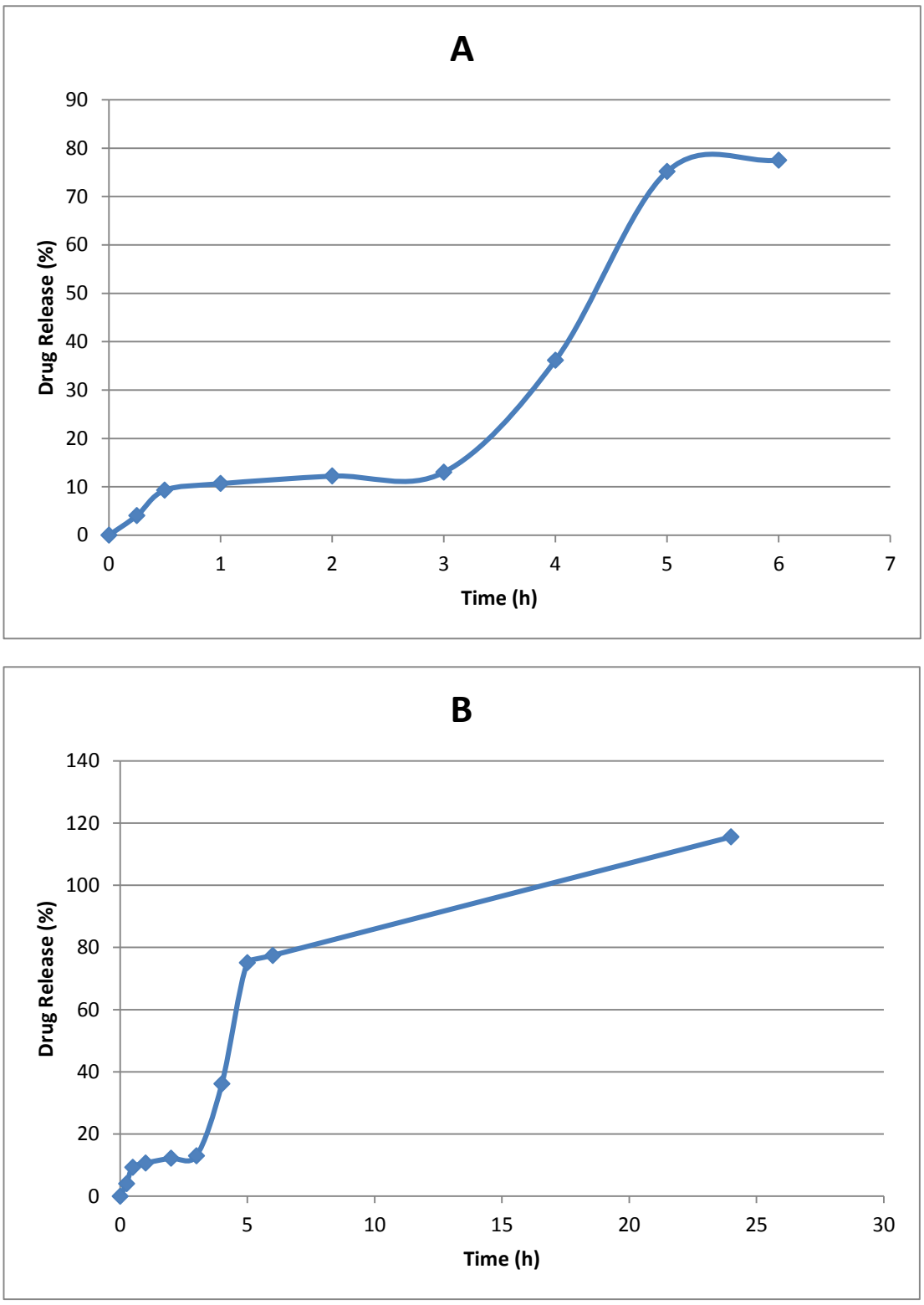


Figure 45: Drug release from DAC samples in pH7.4 PBS using nanoUV analysis, where n=1 (due to issues with the nanoUV replicates could not be taken). The top pane (A) illustrates the first 6 hours and the bottom pane (B) illustrates the full 24 hours

Latterly the drug release from the 50:50 PEG4000:hydrocortisone diamond anvil cell samples was studied in simulated intestinal and gastric fluids. The analysis method was switched to HPLC which in fact gives more information about what happens to the drug. Figure 46 illustrates the drug release in simulated intestinal and gastric fluids. HPLC revealed that hydrocortisone was degrading in aqueous solutions, as once the drug release was analysed additional area under the curve peaks were found to be present close to the main drug peak. From the literature, these peaks were found to be hydrocortisone derivatives (Walters and Dunbar, 1982). As such Figure 46 illustrates the drug release looking at the pure drug present alone and the drug release taking into account the derivatives which have formed in the stagnant drug release media. Similar to Figure 45, drug release was found to occur in a step-like manner.

Looking at the drug and derivative samples first, initially an immediate release burst can be observed in both simulated intestinal and gastric fluids. In the former this takes the form of an average release of 55.89% over 30 minutes and in the latter this takes the form of 54.02% over 1 hour. This is then followed by a sustained release period of 5 and a half hours for the simulated intestinal fluid sample, by which point a total average release of 72.77% had occurred. For the simulated gastric fluid, the initial burst is again followed by a sustained release period, this time of 5 hours, by which a total average release of 62.25% had been achieved. For both the simulated intestinal and gastric fluid samples the sustained release period was followed by another immediate release burst over 2 hours to the 8 hour time point. By 8 hours, an average of 111.4% had been released in simulated intestinal fluid and an average of 107.88% had been released in simulated gastric fluid. For both sets of samples, drug release was shown to have levelled off by a final 24 hour time point. Surprisingly this time point was at 97.87% and 89.57% in simulated intestinal and gastric fluids respectively. This may be attributed to greater degradation. As 8 hours was found to be the peak of the curve unpaired T-tests were carried out in OriginPro comparing the mean maximum release of the pure and derivative containing samples. The P-value was found to be less than 0.05, at a value of 0.024, and thus the difference between the two maximums is significant.

Observing the pure drug samples, initially again an immediate release burst can be observed. However this only reached an average of 12.24% drug release at 30 minutes in simulated intestinal fluid and 11.38% at 1 hour in simulated gastric fluid. Again there was a period of sustained release lasting 5 and a half hours in simulated intestinal fluid, during which the average drug release reached was 19.06%. This is then followed by another immediate release burst of 2 hours, reaching the 8 hour time point at 41.84%. Again this drops by the 24 hour time point, which may be due to increased degradation, reaching an average of 24.15% release. Likewise in the simulated gastric fluid there is a sustained release period starting after the initial burst of release, however, unlike in simulated intestinal fluid, this prevails until the 24 hour time point at 28.54% release. Thus there is only 18.70% release by the 8 hour time point. It should be noted all of the samples have quite big error bars, even though they correspond to standard error rather than standard deviation, the largest of which are found with the samples consisting of both hydrocortisone and its derivatives. The standard error values are detailed in A3.1 of Appendix 3. Unpaired T-tests were once again carried out in OriginPro comparing the mean maximum release of the pure and derivative containing samples. The P-value was found to be less than 0.05, at a value of 0.00439, and thus the difference between the two maximums is significant. In addition to this unpaired T-tests were carried out comparing the samples in different media. Both the pure and derivative containing samples were found to have maximum release values not significantly different from each other in different media as both had P-values over 0.05 at 0.38628 and 0.80281 for the pure and derivative samples respectively.

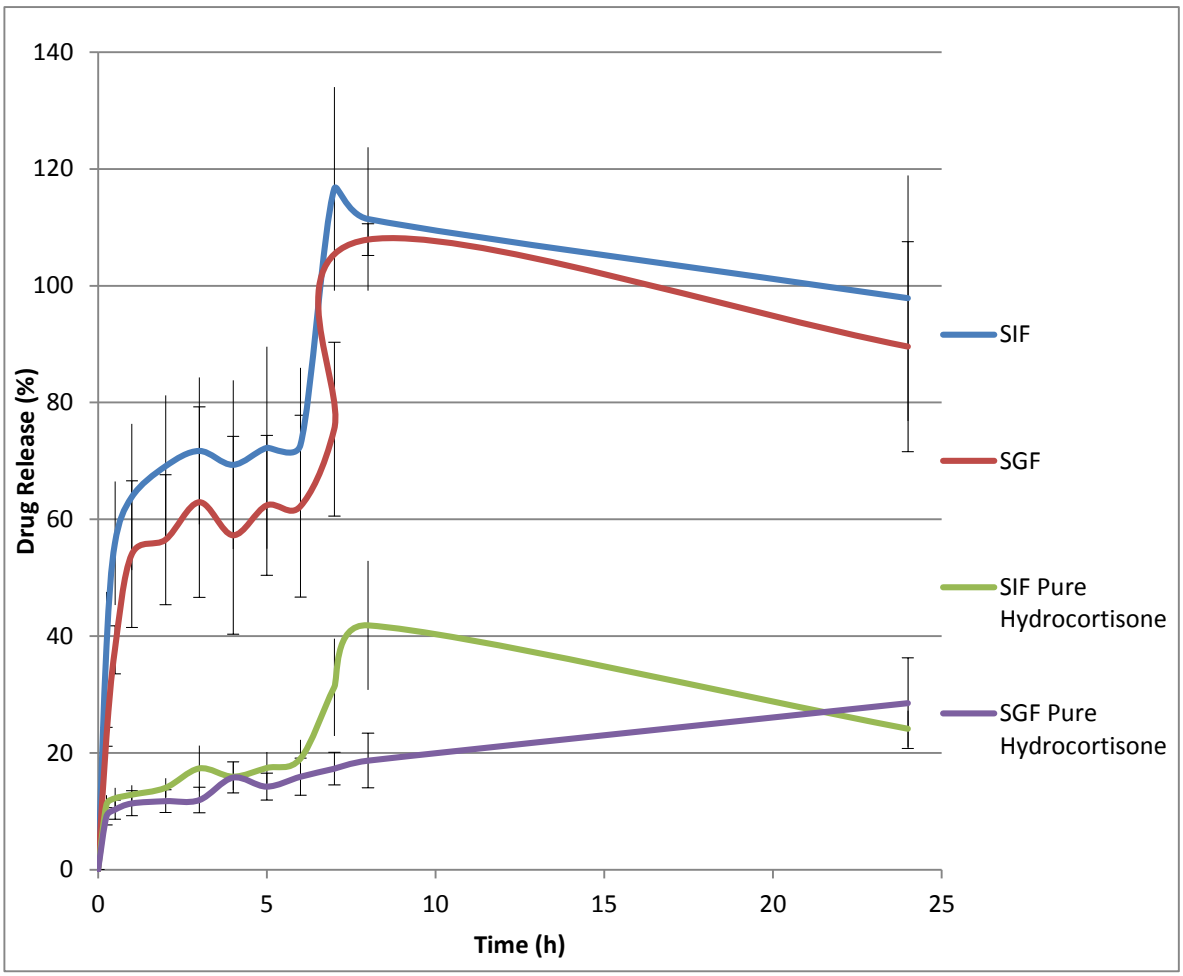


Figure 46: Drug release from 50:50 PEG:hydrocortisone DAC samples in pH6.8 simulated intestinal fluids (SIF) and simulated gastric fluids (SGF). The pure samples and those with the degradation derivatives are both shown. For each sample n=3 S.E.± values detailed in Appendix 3. For the difference between pure and derivative containing samples $P<0.05$, but for comparison of the samples different media $P>0.05$.

### *3.4 High Pressure Scale Up*

#### *3.4.1 Raman*

On scale up, once again the author looked at a 50:50 PEG:hydrocortisone blend. In Figure 47, the sample generated using water as a pressure transmitting medium is compared with hydrocortisone alone, PEG alone and also an ambient sample. The 2900 $cm^{-1}$ peak is thought to be a combination of PEG4000 and hydrocortisone due to the peak being very like the hydrocortisone CH peak but has the height of the PEG one and also an additional ridge at the top of the peak. However the rest of the Raman spectra appears to mirror the hydrocortisone spectrum with a very prominent double peaked structure of at 1611 $cm^{-1}$ and 1644 $cm^{-1}$, corresponding to the alkene groups, and lesser peaks at lower wavenumbers which also seem to be more like those of hydrocortisone than PEG.

In Figure 48, the 50:50 PEG:hydrocortisone sample generated using petroleum ether as a pressure transmitting medium is compared with hydrocortisone alone, PEG alone and an ambient 50:50 PEG:hydrocortisone sample. The physical characterisation of this spectrum is much more comparable to the diamond anvil cell samples (Figure 37) as there is a much more even distribution of PEG and hydrocortisone.

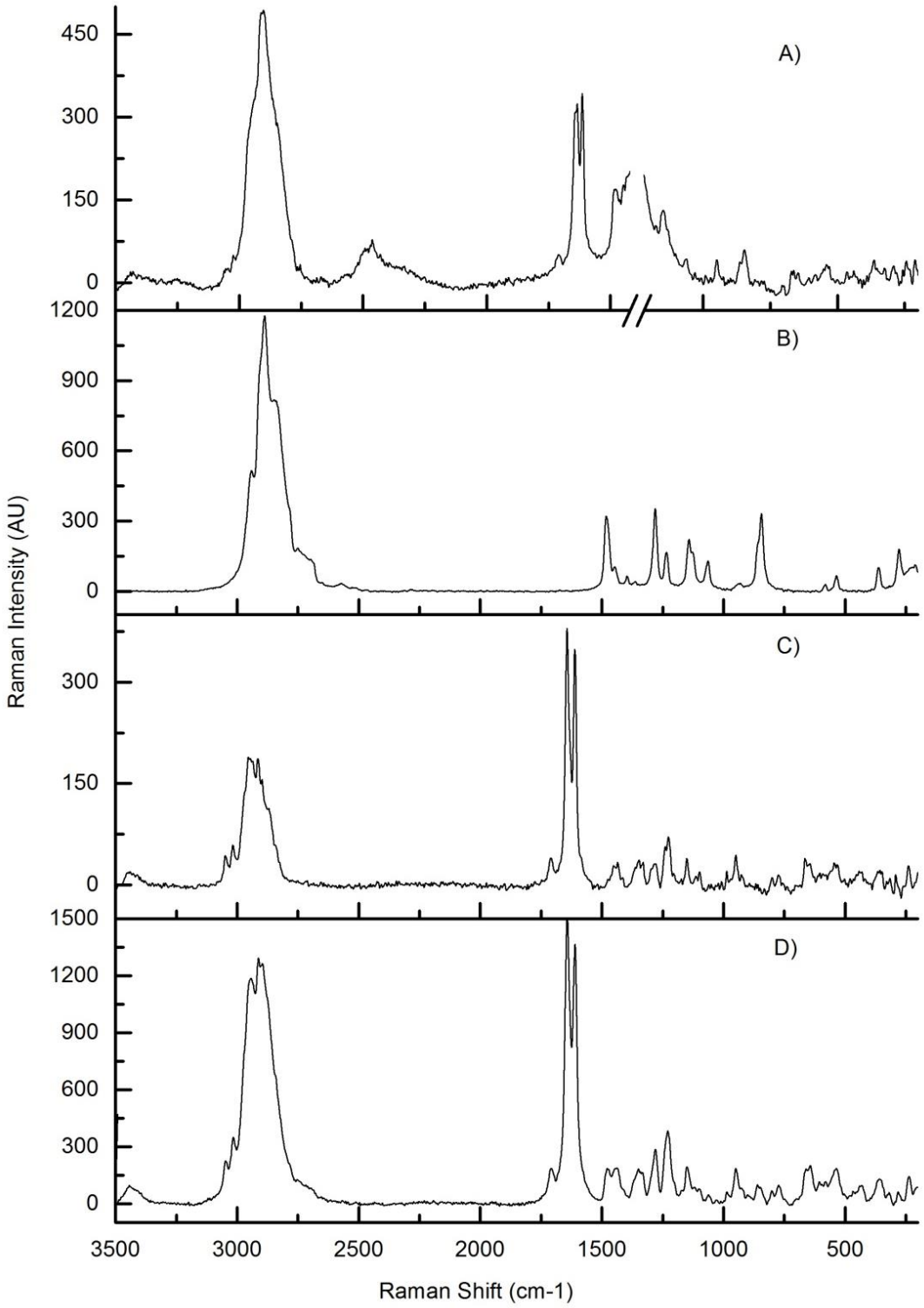


Figure 47: Raman spectra comparing the functional groups of the D) 50:50 PEG:hydrocortisone large volume sample made using water as a pressure transmitting medium with that of the A) unpressurised sample, B) PEG4000 and C) hydrocortisone.

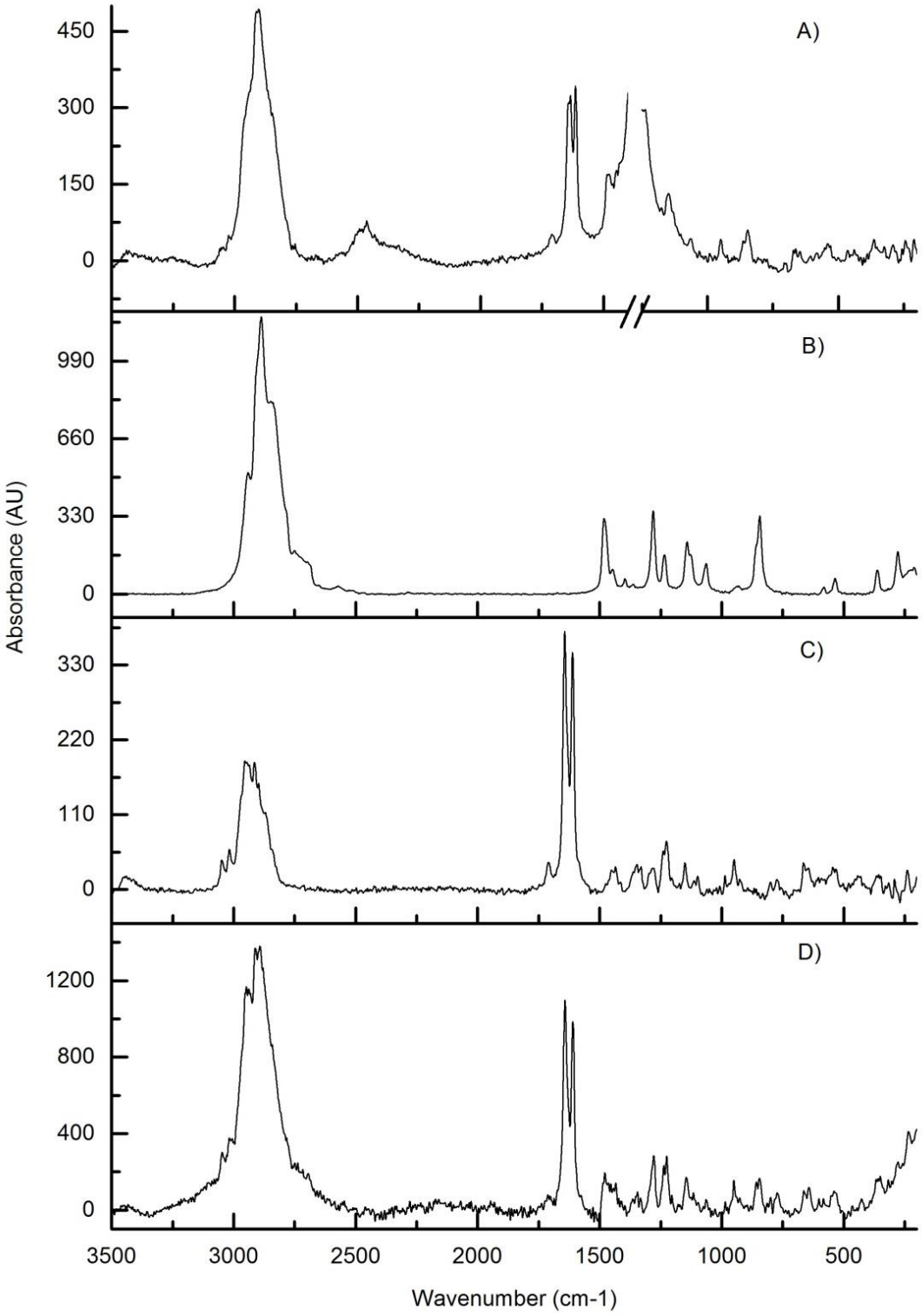


Figure 48: Raman spectra comparing the functional groups of the D) 50:50 PEG:hydrocortisone large volume sample made using petroleum ether as a pressure transmitting medium with that of the A) unpressurised sample, B) PEG4000 and C) hydrocortisone.

*3.4.2 Infrared Spectroscopy*

Figure 49 illustrates the infrared spectrum of the 50:50 PEG:hydrocortisone sample prepared using water as a pressure transmitting medium compared to PEG alone, hydrocortisone alone, the ambient 50:50 PEG:hydrocortisone ambient ballmilled sample and the water extracted from the pressure cell by ultra filtration. The spectrum of the pressurised sample is observed to be very similar to that of hydrocortisone, with the only difference being the presence of a 1096 $cm^{-1}$ C-O-C peak. On investigation of the water solute sample, which was too fluorescent to undergo Raman spectroscopy, a prominent C-O-C peak was detected as well as the CH regions of 1457 and 1349 $cm^{-1}$, and CO regions of 1252 and 1298 $cm^{-1}$ present in PEG.

Figure 50 illustrates the infrared spectrum of the 50:50 PEG:hydrocortisone sample prepared using petroleum ether as a pressure transmitting medium compared to PEG alone, hydrocortisone alone and the ambient 50:50 PEG:hydrocortisone ambient ballmilled sample. As the petroleum ether largely evaporates off there is no solute sample for this spectra. The pressurised sample spectrum is observed to be very similar to that of the ballmilled ambient sample, featuring both hydrocortisone and PEG regions. The large volume spectrum supports the Raman spectrum of this blend in that again it is much more comparable to the diamond anvil cell sample (Figure 40) due to its more even ratio of PEG to hydrocortisone peaks.

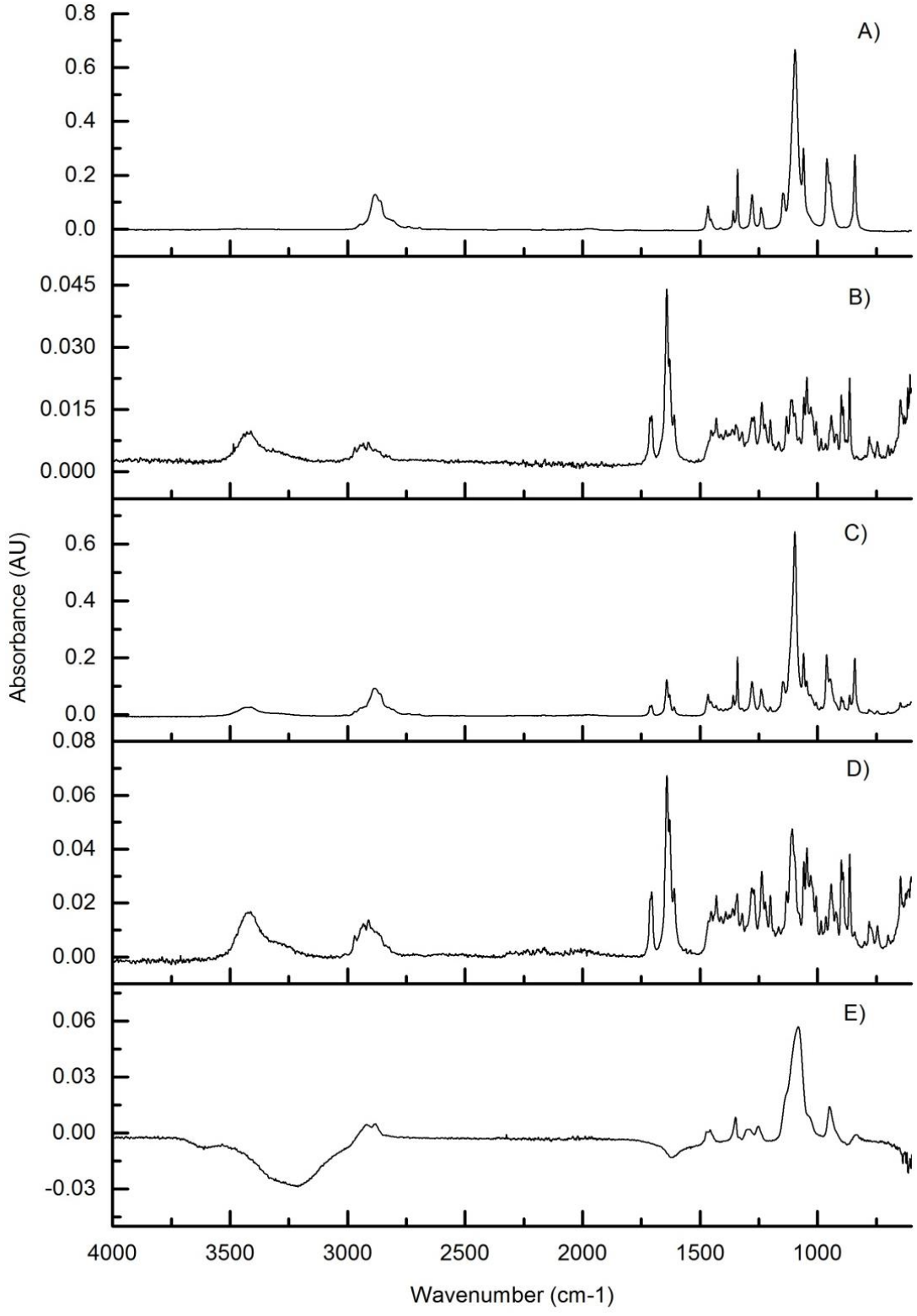


Figure 49: Infrared spectra comparing the functional groups of the D) 50:50 PEG:hydrocortisone large volume sample made using water as a pressure transmitting medium with that of the A) PEG, B) hydrocortisone, C) unpressurised sample and E) the water solute extracted from the pressurised sample.

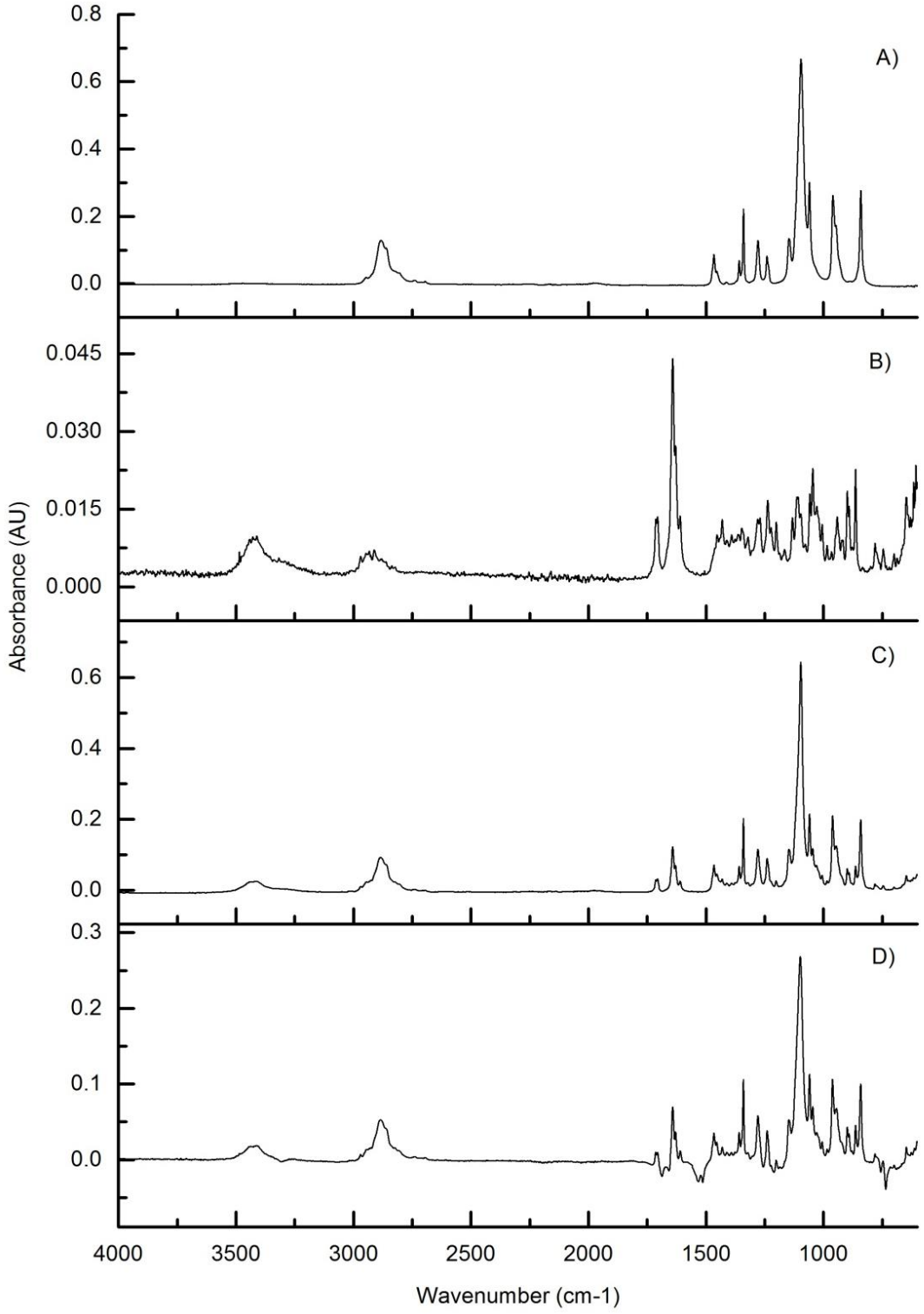


Figure 50: Infrared spectra comparing the functional groups of the D) 50:50 PEG:hydrocortisone large volume sample made using petroleum ether as a pressure transmitting medium with that of the A) PEG, B) hydrocortisone and C) unpressurised sample.

*3.4.3 Drug Release Studies*

The advantage of scale up is unlike the needle loading method used for the diamond anvil cell, a more precise measurement of the drug added to the large scale cell can be made as the whole volume of the 50:50 PEG:hydrocortisone ballmilled sample can be added to the cell prior to pressure being applied. As the particle size achieved is greater it is also more forgiving in terms of distribution than the small scale diamond cell samples. The larger quantity of material also allows the removal and replacement of the whole 1ml of media at each time point reducing the time spent by the drug in stagnant media, reducing the risk of degradation of the drug.

Drug release was carried out on large volume samples containing around 500μg of hydrocortisone in 1ml of simulated intestinal (Figure 51) or gastric fluids (Figure 52). Initially looking at the samples in simulated intestinal fluids, a similar shape of drug release curve as Figure 46 can be observed, albeit with more of a sustained release character. Looking at the sample containing hydrocortisone derivatives in addition to the pure drug, in the first 8 hours release is relatively rapid with an average of 16% drug release being achieved. After this there is a period of sustained release until the 7 day mark with an average of around 7% drug release each day. On reaching the 7 day mark, an average of 62.52% drug release had been achieved. Over the following 3 days there is another immediate release burst, whereby an average of 104.48% drug release is achieved. With hindsight the experiment may have needed an additional time point as the drug release curve is not entirely flat by 10 days. In the pure drug sample a similar pattern is observed, although the overall drug release is lower. The immediate release burst is observed to occur over 6 hours releasing 8.94% and again there is a sustained release period until the 7 day mark but only 40.96% is released by this point, with an average of 5.85% release per day. This is then followed by another immediate release burst which takes the release up to an average of 80.30%. It should be noted the error bars are slightly smaller than that of the diamond anvil cell samples. The standard error values are detailed in A3.2 of Appendix 3. The difference between the maximum release values were compared using an unpaired T-test, and were found not to be significant with a P-value of over 0.05, at 0.18.

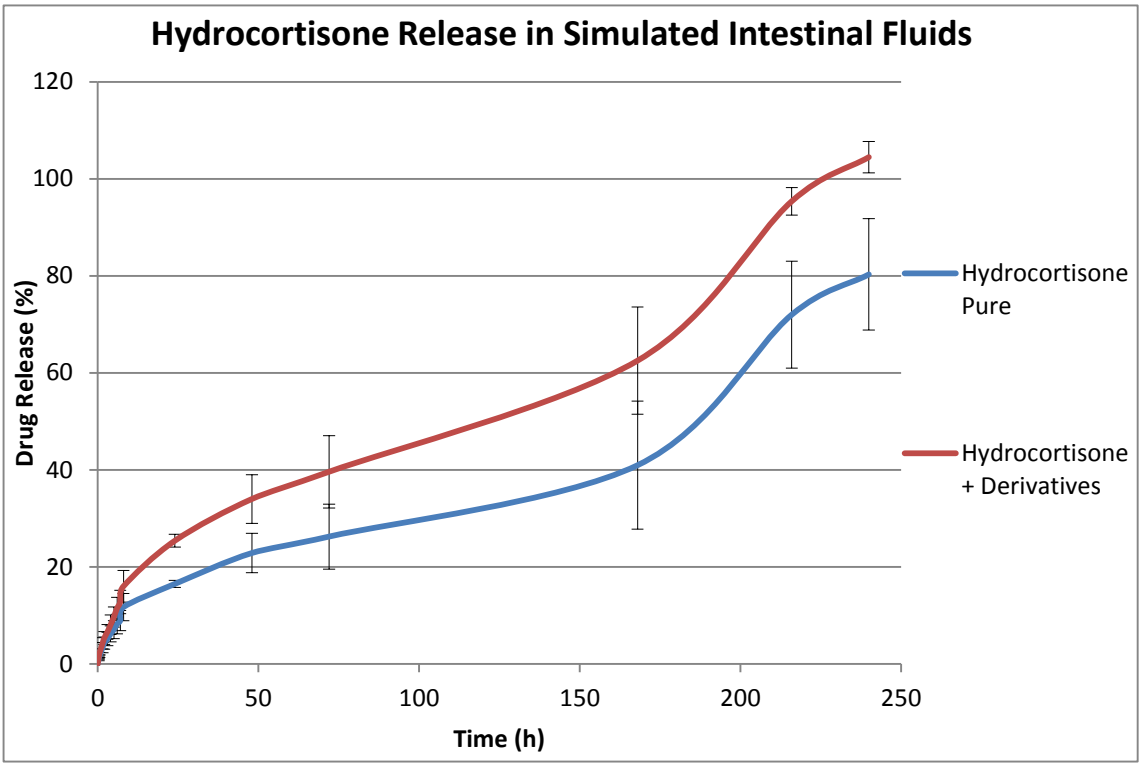


Figure 51: Drug release from 50:50 PEG:hydrocortisone large volume pressurised samples in simulated intestinal fluid, where n=3 for each and SE± the values given in A3.2 of Appendix 3. P>0.05 for the maximum release comparison of pure and derivative containing samples.

Investigating the samples in simulated gastric fluid (Figure 52) a slightly different pattern is observed, with an additional step like feature in the curve. Initially, looking at the derivative containing sample, in the first 24 hours there is an immediate release burst in which an average of 32.37% drug release is achieved. Following this there is a delay in release of 24 hours where only 36.74% release is reached. There is then another burst of immediate release over the next 24 hours where release reaches an average of 62.64%. There is a sustained release period of 4 days after which 86.20% release is reached, with an average of 5.89% release per day. There is then a final immediate release burst reaching 116.47% drug release by the 10 day mark. Again an additional data point may have been required to fully level the curve off. Examining the pure sample, the pattern of a matching curve at lower percentage drug releases seen in the simulated intestinal fluid samples is mirrored in the simulated gastric fluid samples. Initially there is a burst of immediate release over the first 6 hours reaching 7.89% release, followed by a brief sustained release period culminating in the curve nearly levelling off, reaching 17.46% release by 48 hours. This is followed by another burst of immediate release over the next 24 hours reaching 39.32% drug release by 72 hours. There is then a sustained release period which continues until the 10 day point is reached at 79.53% release. The maximum values were compared via unpaired T-tests using OriginPro. There is not a significant difference between the samples as demonstrated by a P-value over 0.05, at 0.356. Again comparing the simulated intestinal fluid samples with the simulated gastric fluid samples, neither the pure samples nor the samples with derivatives were found to be significantly different with P-values of 0.982 and 0.577 respectively. The standard error values are detailed in A3.3 of Appendix 3.

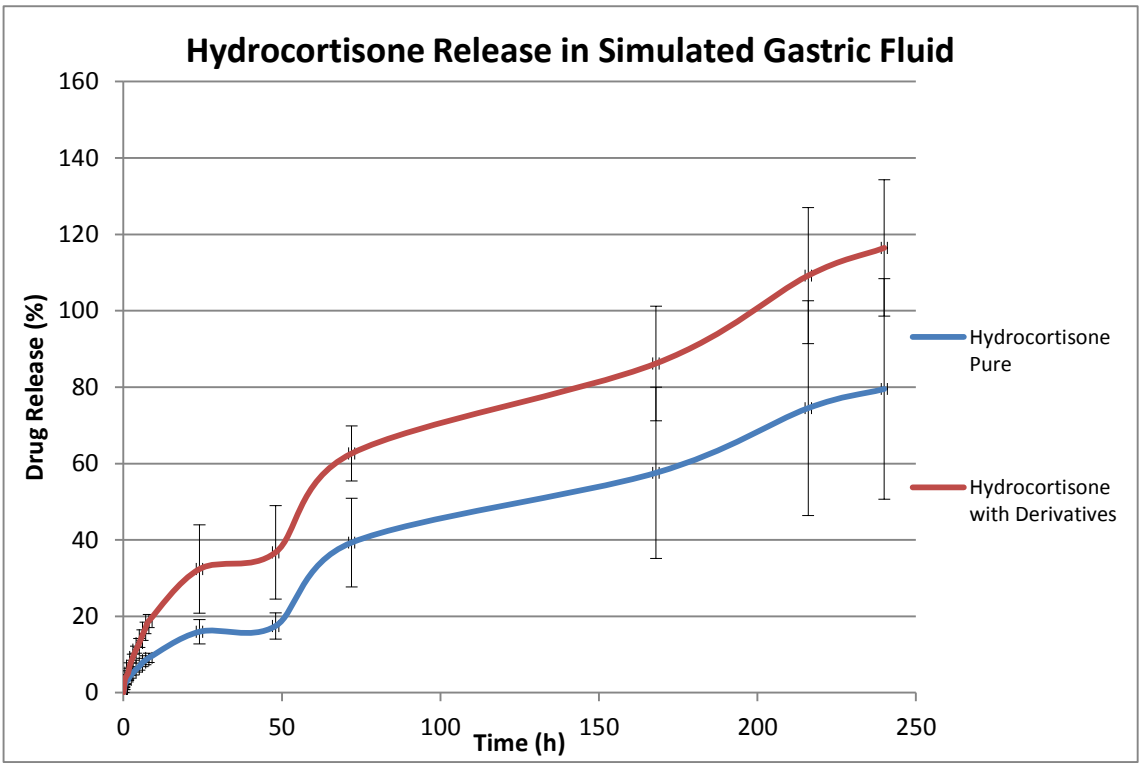


Figure 52: Drug release from 50:50 PEG:hydrocortisone large volume pressurised samples in simulated gastric fluid, where n=3 for each and SE± the values given in A3.3 of Appendix 3. P>0.05 for the comparison of the maximum release of pure and derivative containing samples.

# Chapter 4: Discussion

The aim of this study was to investigate the effect of pressure on polyethyelene glycol to create an effective drug delivery system for poorly water soluble drugs, with a view to increase their bioavailability.

## *4.1 PEG*

PEG was found to melt under high pressure conditions as marked by the flowing of the substance observed accompanied by the colour change from white to colourless by 5GPa. On removal of pressure the transparency is retained as the powder becomes a solid disk. This melting action is believed to be due to loss of the C-O-C second peak and the smoothing of the CH peak present in the Raman spectra, both of which could be attributed to the reduction in the population of the bond energies of PEG4000 on becoming molten. This change is then reversed on removal of the pressure, suggesting a return of the rigidity on solidifying. These changes are mirrored in the infrared spectroscopy with the greatest change being observed in the C-O-C peak as it is significantly diminished after pressure.

Differential scanning calorimetry illustrated that PEG4000 melts over an average range of 58.67 to 63.61°C, with an average peak temperature of 61.73°C. Like the pressure treated samples, the infrared spectra taken of these samples showed a decrease in the size all the peaks compared to an ambient sample with the most considerable change occurring in the C-O-C peak, confirming that the same type of melt transition is generated by pressure as by the normal temperature method. Thermogravimetric analysis demonstrated that, on average, PEG degrades by 96.53% between 335 and 445°C. The distinct temperature difference in PEG's melting range relative to the point at which it degrades is highly useful as it indicates it is stable at its melting point and does not degrade. Which due to the other similarities observed may suggest the similar reaction under high pressure is also not causing degradation.

Due to the pressure being observed to induce a solid to liquid phase change at 5GPa at room temperature and the temperature range 58.67 to 63.61°C at which PEG melts and is stable, as proven by differential scanning calorimetry and thermogravimetric analysis, it was hypothesised pressure could be used to reduce the temperature required to melt PEG. This was proven via temperature versus pressure studies, which showed the two variables to be inversely proportional. There have been a number of studies carried out paring pressure and temperature using the diamond anvil cell techniques largely on crystals, but little has been studied on powders previously in this apparatus in combination with temperature (Shinoda and Noguchi, 2008, Hazen and Finger, 1981). High pressure has been shown a means of melting polymers before, however previously work has been in polymers which tend to increase in melting point such as ethylene vinyl acetate copolymers, rather than reducing it (Seeger et al., 2004). As such this study is fairly novel.

### *4.2 Hydrocortisone*

On application of pressure, the Raman spectra of hydrocortisone exhibit a smoothing and shift to a higher wavenumber of the peak of the aromatic CH functional group at 2890 $cm^{-1}$ as well as a merging of the 1611 $cm^{-1}$ and 1644 $cm^{-1}$ alkene peaks. These peaks correspond to the two C=C bonds present in two of the three polymorphs of hydrocortisone. Forms I and II require two molecules to describe the crystal structure and therefore there are two C=C functional groups per polymorph, where as form III only consists of one molecule and thus only one C=C functional group (Suitchmezian et al., 2007). Therefore the hydrocortisone polymorph present in this study must be either form I or II. The alkene bond present in each molecule should have a similar energy but the packing effects exerted by the crystal structure causes the stretching frequencies to change in wavenumber slightly, as can be observed in Figure 30. As the pressure is applied to the crystalline structure the molecules receive different forces and therefore move at different rates. The change in the C=C region is supported by the infrared spectra. Due to the return of these peaks on return to ambient it is suggested that the changes in these peaks are not resulting in permanent

changes to the molecule, which can be confirmed by the differential scanning calorimetry results.

The differential scanning calorimetry results suggest hydrocortisone on average melts over the temperature range of 223.49 and 228.15°C, with an extrapolated peak of 226.93°C. Hydrocortisone can exist in three polymorphic forms. As this is a single endothermic peak, rather than two as exhibited by the Form III polymorph, it is suggested this batch of hydrocortisone is in fact Form I or Form II (Suitchmezian et al., 2007). The higher melting point does suggest it is Form I as a previous study showed an onset temperature for this to be 222ºC and an extrapolated peak temperature to be 225ºC, compared with an onset temperature of 220ºC and an extrapolated peak temperature of 222ºC for Form II, although due to changing conditions this cannot be said for certain (Suitchmezian et al., 2007). Thermogravimetric analysis reveals the melting range is very close to the degradation range, the start of which is exhibited by the presence of the colour change to yellow on formation of 11β,17α-dihydroxy-3,20-dione-4-pregnene-21-al. This results in a major increase in the size of the C=O and the CH infrared peaks. This is not observed in the pressurised samples and thus this degradation step is avoided.

### *4.3 PEG + Drug*

The 50:50 PEG:hydrocortisone blend was investigated by Raman spectroscopy. PEG and hydrocortisone behave in the same manner as they did alone and PEG effectively entaps hydrocortisone. Differential scanning calorimetry revealed the melting point of PEG was unchanged by combination with hydrocortisone but PEG did have a shielding effect on hydrocortisone, lowering its melting point slightly. Thus it could be suggested due to the inversely proportional relationship of temperature and pressure that PEG still flows in the same manner in the presence of hydrocortisone as it does alone. The white to yellow colour change is still observed in the hydrocortisone in the DSC samples but not the pressurised samples further supporting the theory that hydrocortisone does not reach the level of degradation

under pressure as it does at the higher range of its relatively unstable temperature induced molten state, which is indicated by the thermogravimetric analysis.

The 50:50 blend was chosen to take forward to drug release testing as this blend was thought to be most useful formulations have a high ratio of drug but due to the poor solubility of hydrocortisone this drug needs to be balanced with a sufficient level of PEG. Initially a drug release study on the diamond anvil cell particles was carried out in pH7.4 PBS with analysis by UV spectroscopy. Although this was not repeated due to issues with the UV equipment and also simulated fluids being deemed to have a better in vitro/in vivo correlation, Figure 45 shows the same pattern of drug release which was observed in later studies, with a period of immediate release followed by a period of sustained release and then another period of immediate release. 115.58% was released by 24 hours, which is slightly over the expected drug release, which may suggest there is an uneven distribution of drug in the sample. This can be attributed to there being such a small amount, mere micrograms, added to the pressure cell using a needle and no real way of being certain of the amount of each substance on that needle.

After consideration of the studies, the diamond anvil cell samples were then studied in simulated intestinal and gastric fluids. The mass of drug expected to release in the 1ml of fluid was 25μg as this was comparable to the standard dose of 25mg per day which in standard USP testing would be in 1L. So as such the 25μg/ml is directly comparable. The analysis method was changed from UV spectroscopy to HPLC due to issues with the equipment. HPLC was actually found to be more useful overall as, unlike UV analysis alone, it was able to reveal the substantial instability of hydrocortisone in aqueous solution. HPLC revealed that hydrocortisone was degrading in aqueous solutions, as once the drug release was analysed additional area under the curve peaks were found to be present close to the main drug peak. From the literature, these peaks were found to be hydrocortisone derivatives (Walters and Dunbar, 1982). This formation of derivatives via degradation is supported by a number of previous studies.

Hydrocortisone has been shown previously to degrade under aqueous conditions. In a previous study looking at hydrocortisone in aqueous solutions, it was noted that an oxidative degradation resulting in the generation of 21-dehydrohydrocortisone which latterly broke down into a 17-carboxylic acid and a 17,20 dihydroxy-21-carboxylic acid derivative, and a non-oxidative reaction giving a 17-oxo, 17-deoxy-21-aldehyde and 17-deoxy-20-hydroxy-21-carboxylic acid derivative. Breakdown was almost entirely caused by reactions of the $C_{17}$-dihydroxyacetone side chain. In 0.1M acetate buffer at pH5.07 the greatest degradation appears to be non-oxidation resulting in 17-deoxy-21-dehydrohydrocortisone at 35% at its peak at 142 hours, although there is also some oxidative degradation of the aldehyde group resulting in 21-dehydrohydrocortisone formation at 10% at its peak of 113 hours. There is a drop in this to 5% at 142 hours. In 0.1M phosphate buffer at pH6.19 the opposite is observed with greater non-oxidative degradation, reaching 55% at 25 hours, and less oxidative degradation, reaching 10% at 25 hours (Hansen and Bundgaard, 1980). However this degradation can be decreased by addition of stabilising agents such as fructose (Bansal et al, 1983) or disodium edentate. The latter can be used to reduce oxidative degradation as it can prevent generation of 21-dehydro degradation products. The non-oxidative reaction seems to be triggered by highly acidic conditions as the non-oxidative 17-deoxy steroid-glycox degradation products are formed in the presence of acidic conditions. Thus the use of enteric coatings to protect against the acidic gastric environment could be incorporated into a formulation to prevent this degradation (Hansen and Bundgaaard, 1980). This previous evidence supports the observed degradation and may suggest which products are being formed although further analysis of the media would be required to confirm this in the current sample.

Taking into account these derivatives, in the first 30 minute immediate release burst, an average of 55.89% of the sample was released in simulated intestinal fluid. In the first 1 hour immediate release burst, an average of 54.02% of the sample was released in simulated gastric fluid. The sustained release period resulted in 72.77% and 62.25% release by 6 hours in simulated intestinal and gastric fluids respectively. An average of 111.4% and 107.88% release occurred by 8 hours in simulated intestinal and simulated gastric fluids respectively. Again this is over 100% which

does suggest, as in Figure 45, that there is an uneven distribution of drug in the samples which again can be attributed to the sample size and method of production. This can be supported by the size of the error bars. Although both sets of drug release have levelled off after 8 hours, the drug release is found at 24 hours to be in fact 97.87% and 89.57% in simulated intestinal and gastric fluids respectively. This could be attributed to greater degradation of the hydrocortisone to a level which cannot be read by the HPLC. Although this may be due to problems with the HPLC method. The lack of disparity between the two pH values at their maxiumum does however suggest there is some level of pH independence to the system.

Looking at the pure samples, the release in simulated intestinal fluid shows a similar pattern of release to the overall sample including derivatives, however only 12.24% release is achieved in the first immediate release burst and 41.84% after the second. Again after by the 24 hour time point there is a considerable drop in the release to 24.15%, which may be attributed to further degradation. By 8 hours and 24 hours 69.58% and 73.72% of the hydrocortisone released was lost to degradation respectively. Likewise the release in simulated gastric fluid there is considerably less release observed without taking the derivatives into account. After the first immediate release burst, only 11.38% release had been achieved and unlike the simulated intestinal fluid sample sustained release continues until 24 hours, with ultimately 28.54% release overall. Thus there is only 18.70% release by 8 hours, which may suggest the acidity of the simulated gastric fluid causes greater degradation of hydrocortisone in the crucial first 8 hours than the less acidic simulated intestinal fluid. This is supported by the fact that by 8 hours and 24 hours 89.18% and 61.03% of the hydrocortisone released was lost to degradation respectively. The uneven distribution can also be observed in these samples in the form of the error bars.

The pattern of release observed in most of samples is quite comparable to standard oral dose regimens of hydrocortisone (Abad-Santos et al., 2002, Simon et al., 2010), but due to it being from a single administration it is possibly more comparable to a pulsatile system (Tangri and Khurana, 2011). The pulsatile nature of the system is

believed to stem from the fact the centre of the high pressure particles receives the greatest level of pressure from the combination of the diamonds and powder mass working together and thus may create a region which is less easily degraded relative to the more loosely pressurised periphery. This drug release pattern is quite significant as it actually mirrors conventional oral cortisol replacement regimens without the need for multiple dosing. This could be applicable to cortisol replacement therapy in paediatric and geriatric care, as these two groups tend to be more difficult to treat due to refusal of medication or forgetfulness (Gröschl et al., 2002 and Nikolaus et al., 1996). The reduction of multiple dosing is also highly significant as multiple dosing often can result in overdosing or underdosing. The former can lead to toxic side effects and the latter can lead to break through symptoms (Nikolaus et al., 1996).

Chan and Debono (2010) suggested a number of sustained and immediate release combinations which support the theory that the formulation could be adapted follow the circadian rhythm. However unlike the current formulation they suggest the addition of a delayed release period, which would mean adding an purely excipient layer outside the formulation as it stands to allow the patient self administer before sleeping and have a burst of hydrocortisone before waking. Johannsson et al. (2009) also suggest the use of an immediate release burst but they then employ a prolonged period of sustained release which may suggest a future modification to the current system.

### *4.4 High Pressure Scale Up*

The 50:50 PEG:hydrocortisone blend was pressurised using a large volume press to investigate the capacity of this high pressure study for scale up. Due to the large volume press not being able to reach as high a pressure as the diamond anvil cell, temperature was employed to compensate, drawing on the previous evidence of the inversely proportional relationship between pressure and temperature. Due to the larger volume of substance the powder density could not be used to transmit the exerted pressure alone and as such a pressure transmitting medium was required.

Initially water was employed for this purpose. The Raman and infrared spectra (Figures 48 and 50) for the high pressure sample generated in this way illustrated an abnormally high content of hydrocortisone, which was not comparable to the spectra of the diamond anvil cell generated samples (Figures 38 and 41). The only influence of PEG which can be observed is that of the height seen in the CH region of the Raman (Figure 47) and the C-O-C region present in the infrared spectrum (Figure 49). The rest of both spectra were nearly identical to the hydrocortisone spectra. The infrared spectrum was taken of the water filtered off the sample (Figure 49). Due to the high fluorescence of the solute sample, conferred by the hydrocortisone, the Raman spectrum could not be taken of this but as infrared is not affected by fluorescence, the infrared spectrum could be taken. The very prominent PEG C-O-C peak, CH peaks and CO peaks were observed in the spectrum of the water, suggesting that most of the PEG present in the sample originally had leached into the water due to its high aqueous solubility.

Latterly the 50:50 PEG:hydrocortisone was pressurised utilising petroleum ether as a pressure transmitting medium, as this largely evaporates off after the pressure is removed (Figures 49 and 51). A more even distribution of PEG to hydrocortisone was observed with the CH region exhibiting a combination of the hydrocortisone and PEG ridges observed on the peak. The alkene peaks are also less prominent than they were in the water pressurised sample. PEG also has more of a role in the $CH_2$ region. In the infrared, a more even distribution is also observed with both substances boasting a similar number of peaks each and neither substance overshadowing the other with OH, C=O, CH, C-O and =CH regions present for hydrocortisone and CH, C-O and C-O-C regions present for PEG4000. These factors in combination suggest the blend remains intact in this sample once the petroleum ether has evaporated off.

Drug release was carried out on approximately 500μg of hydrocortisone, entapped within 50:50 PEG:hydrocortisone large volume press particles, in 1ml samples of simulated intestinal and gastric fluids (Figures 52 and 53). A different method of sample extraction was adopted for scale up as the concentration present in the solution was high enough that the removal and replacement of the 1ml whole

solution and calculation of the cumulative observed concentrations was feasible. It also reduced the time period that the drug was present in a stagnant aqueous solution prior to HPLC analysis in the hope less degradation would occur.

Looking initially at the samples in simulated intestinal fluid, a similar immediate release, sustained release, immediate release pattern as that observed in Figure 46 can be observed, although it does exhibit more of a sustained release character. An average of 16% release is achieved from the immediate release burst over the first 8 hours, with an average of 8.94% of this burst being made up of pure hydrocortisone. An average of 62.52% release is achieved by the 7 day mark, following a period of sustained release, with an average of 40.96% being made up of pure hydrocortisone. The second immediate release burst allows a maximum mean release of 104.48%, with an average of 80.30% of this being made up of pure hydrocortisone. As there is only 24.18% lost to degradation by this final time point, compared to 73.72% lost by the final time point of the diamond anvil cell sample, the hypothesis that less degradation occurred on removal and replacement of the full 1ml of media was proven to be correct. Although the overall release is still over 100% the error bars are smaller than the ones corresponding to the diamond anvil cell samples, suggesting there is a more even distribution of drug in the large volume samples. With hindsight the author should have continued the study for another 24 hours to allow the curve to completely level off but this was not possible due to time constraints.

Looking at the samples in simulated gastric fluid, there is a similar pattern again, but unlike previously there is a split in the initial immediate release burst, at 24 hours for the overall sample and 6 hours for the pure sample, where there is a delay in release until the 48 hour time point before the burst resumes tailing into the sustained release period at 72 hours, which culminates in another much more muted immediate release burst at the 7 day point, reaching its maximum at 10 days. For the overall sample, consisting of both pure hydrocortisone and its degradation products, there is an average of 116.47% release, which is slightly over 100% again, however the error bars are not as large as that of the diamond anvil cell samples so distribution is still slightly better. There is only 79.53% pure drug observed, which suggests 36.94% is

lost to degradation. This is slightly higher than the simulated intestinal fluid samples, which does suggest again the high acidity is resulting in greater degradation. However this is not as high a level as the diamond anvil cell samples and so again the removal and replacement of the full 1ml of media each time is reducing the period of exposure of the drug to the stagnant aqueous solution and thus reducing degradation. With hindsight the author should have continued the study for another 24 hours to allow the curve to completely level off but this was not possible due to time constraints. The difference in the SGF curves in comparison to the SIF curves, which are more comparable to both sets of diamond anvil cell samples, could be attributed to hydrocortisone's adhesive sticky nature as the sample tended to stick to the eppendorf wall.

Overall the high volume studies were found to be relatively comparable to the diamond anvil cell studies in terms of the drug release pattern being independent of pH and the same immediate release, sustained release, immediate release pattern. However the large volume sample drug release released at a much slower rate. Two considerations to make are a) the effect that the pressure-transmitting medium had on the large volume samples and b) the effect of hydrostatic versus non-hydrostatic medium. Both of these questions require further work to be carried out on this system giving thought to the requirement of having pressure transmitting medium for the large volume experiments.

## *4.4 Future*

### *4.4.1 Formulation Changes*

Looking towards the future, the formulation could be modified for more efficient drug release and delivery. Different concentrations of drug could be explored more, for example taking forward the 80:20 PEG:hydrocortisone blend. Due to the greater mass of the large volume samples release occurs over a much longer time period. This method of production, however, is more feasible on an industrial scale, as such the dose would need to be modified to a level which would give an overall release of 25mg/L, possibly by altering the ratio of drug to polymer, although this would have

to be done with extreme care as there is a chance of making the system too soluble. Taking forward the 80:20 blend also may allow tailoring of the dose to the patient. Personalised medicine is a growing field and as previous evidence has shown cortisol is released at different levels in each individual, based on factors such as genetics or stress levels, this may be a potential area for exploration (Abad-Santos et al., 2001).

The formulation also could be modified to include stabilising agents such as disodium edentate to withstand oxidative degradation or encased in an enteric coating to protect the drug against the acidic effects of the gastric fluid, which would normally generate non-oxidative degradation of hydrocortisone to allow the drug to reach the site of absorption intact (Hansen and Bundgaard, 1980, Tangri and Khurana, 2011).

*4.4.2 Applications*

The formulation could also be applied to a number of different functions as the pulsatile nature of the release pattern can be highly useful. Pulsatile systems are defined as drug delivery formulations with the capacity to release the drug at a specific area of the body and/or time via use of a combination of delayed release periods and immediate release periods, and they are usually formulated to fit a specific circadian rhythm (Rao et al., 2013).

Pulsatile systems have been widely used previously for delivery of drugs such as peptic and duodenal ulceration, cardiovascular conditions, arthritis, asthma, diabetes, neurological conditions, cancer and hypercholesterolemia, as it is well documented as a method of targeting release and timing it to fit circadian rhythms (Tangri and Khurana, 2011). Diabetes mellitus can be treated orally using pulsatile systems be targeting the increase in glucose level in the fed state with sulfonylurea and biguanides such as metformin. Arthritis can be treated orally by targeting the circadian rhythm of the greatest pain on waking using pulsatile release of NSAIDs (Rao et al., 2013). Zolpidem has been shown to benefit from formulation with PEG4000 before and due to its purpose as an insomnia treatment it could be adapted in the current system for a pulsatile release by allowing a burst to allow the patient to

fall asleep and a further burst to keep the patient asleep, as many insomnia suffers tend to wake in the middle of the night (Trapani et al., 1999). As such the current system may be applied to some of these drugs.

Pulsatile release is particularly useful for early morning or night time dosing and also for mimicking natural body functions which follow circadian rhythms such as release of hormones. As such in the case of the current study it could be tailored to release the drug at times mimicking cortisol release for patients with adrenal insufficiency (Tangri and Khurana, 2011, Simon et al. 2010, Johannsson et al.,2007, Chan and Debono, 2010).

The advantage in the case of highly unstable drugs such as hydrocortisone it can be tailored to release near the drug's absorption site, minimising the time in the gastrointestinal fluid (Rao et al., 2013). A delayed release period can also be highly effective in preventing breakdown of drugs in the gastric acid of the stomach and are required to reach the intestine before absorption can occur. Equally so this delayed release period can reduce the effects of first pass metabolism (Tangri and Khurana, 2011). The ability to target the drug also increases bioavailability, reduces the risk of overdosing through dose dumping and minimises toxicity and adverse effects (Rao et al., 2013). However, for the current study to progress the delivery system may need to be tested with other poorly soluble drugs.

*4.4.3 Other Drugs*

If the current study was to be taken forward the drug would have to be changed for another poorly soluble drug as the instability of hydrocortisone renders the system of little use in vivo. If the drug was replaced with a more stable agent the drug release would be more comparable to a suitable drug delivery system in vivo. The drug could be replaced with drugs such as the anti-arthritis agents prednisone and naproxen, or the bronchodilator and anti-inflammatory agent theophylline used in asthmatic patients (Barnes, 2010, Kirwan and Buttgereit, 2012). The pulsatile nature of the system may prove useful for these drugs as arthritis and asthma both operate under a circadian rhythm with these conditions being at their worst on waking

(Burioka et al., 2010, Kirwan and Buttgereit, 2012). Thus these drugs could be administered at night, releasing a burst of drug release prior to waking. A pulse prior to sleeping may also allow the patient to fall asleep without discomfort. Theophylline use within a pulsatile system has been previously documented as part of a swellable dosage form (Dashevsky and Mohamad, 2006). It is hoped with the use of a different drug, a better, smoother drug release profile could be achieved, potentially with less margin of error between samples and thus greater reliability due to the drug staying intact under aqueous conditions. This in turn may allow greater comparability to previous work.

*4.4.4 Other Polymers*

Although polyethylene glycol is one of the most commonly used polymers for drug delivery, it is by no means perfect. The increasing use of this polymer has revealed a number of problems. Hypersensitivity is a problem which occurs due to interactions between the polymer and the immune system. As early as the 1950s, polyethylene glycol was associated with embolisms due to severe blood clotting. Anaphylactic shock can also be triggered due to complement activation, for example through the negative effects of histamine and proinflammatory cytokine expression. There can also be gastrointestinal disturbances on oral administration. Cutaneous topical administration can cause skin allergies such as contact dermatitis (Knop et al., 2010). There is also evidence that it can potentially result in a worsening effect on the adverse effects of alcohol, as shown in rats in vivo (Cho et al., 1992). Changes in pharmacokinetic behaviour are another issue associated with polyethylene glycol. PEGylated liposomes and polyethylene glycol based micelles have been associated with enhanced blood clearance and thus potentially decreased bioavailability (Knop et al., 2010).

Non-biodegradablility of polyethylene glycol is further problem which potentially could be overcome. Potentially using lower molecular weight polyethylene glycols could overcome this problem but below 400Da toxicity is exhibited by the polymers, due to its breakdown into diacid and hydroxyl acid metabolites (Veronese and Pasut, 2005, Knop et al., 2010). Conversely, degradation under stress is another issue with

polyethylene glycol. This can result during various procedures including simple flow of solutions, stirring or ultrasound treatment (Knop et al., 2010).

There is also evidence it may potentially cause pancreatitis as seen in a 75 year old woman (Franga and Harris, 2000). Toxicity of side-products is also of great concern. The main bi-product of polyethylene glycol production is the cyclic dimer of ethylene glycol, 1,4-dioxane. This is of concern as it has been suggested to have carcinogenic effects, limiting the amount which can be present in a formulation to 10ppm. Studies in mice have not shown this effect and as such it is still under debate in America. The polymer can also include ethylene glycol monomers which have not fully polymerized. This also has been associated with cancer (Knop et al., 2010). Excretion of polyethylene glycol can also cause problems. Like other polymers, it is normally removed from the body in the urine or faeces but high molecular weight polyethylene glycols can build up in the liver, resulting in macromolecular syndrome. The molecular weight can be reduced by decreasing the chain length via enzyme degradation by cytochrome P450 or alcohol dehydrogenase in the body. Toxic effects can occur if this does not happen (Veronese and Pasut, 2005).

As a result of all these problems, there may be a need for alternative polymers. In the current study it is hoped further investigation can be carried out using chitosan, which is a polysaccharide consisting of linear β (1-4)-linked monosaccharides. It is made up of β (1-4)-2-acetamido-D-glucose and β (1-4)-2-amino-D-glucose joined with glycosidic bonds (Wang et al., 2011). The primary peptide groups give chitosan characteristics, such as being a cation and possessing mucoadhesive properties, which can be utilised in drug delivery. Chitosan is acquired from the formation of a peptide group from an acetamide group in chitin. Chitin is a chemically inactive polysaccharide found in the shells of marine crustaceans such as lobsters, shrimp and crabs. Formation of chitosan is achieved by exposure of chitin to alkaline conditions causing deacetylation. As it is derived from a substance isolated from a living creature it possesses a good level of biocompatibility which is highly advantageous in a drug delivery system. It is also cheap to produce as its origin is naturally occurring and relatively abundant. Chitosan is fairly reactive and utilised at

molecular weights from 3800 to 20,000Da. It can be utilised in powder, paste, film, fibre and other states (Agnihotri et al., 2004). Chitosan can exist in a number of forms, as the number of primary peptide groups in the polymer main chain and the molecular weight of this polymer can vary considerably. This variation primarily arises from the reaction circumstances involved in the production of chitosan from chitin. A typical batch of chitosan on the market has about 66-95% primary amine groups in the polymer main chain (Sonia and Sharma, 2011). As such chitosan polymorphism could prove an interesting area of research.

The advantage of chitosan over polyethylene glycol is that it degrades into glycosylated amines, which the body can absorb and treat like peptides and sugars obtained from food. As such the risk of toxicity and thus adverse effects is significantly less (Agnihotri et al., 2004). One disadvantage chitosan has is in many cases it only dissolves in more acidic conditions and thus release from a chitosan based oral delivery system would either occur in the stomach or would require additional disintegrants (Agnihotri et al., 2003). This means chitosan has a number of applications in gastroretention, examples of which are detailed below. However there are some instances in which solubility is improved to give a better range of oral drug delivery applications. The degree of deacetylation chitosan undergoes in its production from chitin can have an impact as those with 40% deacetylation or less are capable of dissolution in substances up to pH 9, however those with 85% deacetylation or more fail to dissolve over pH6.5. This solubility effect is due to salt formation at lower degrees of deacetylation (Hejazi and Amiji, 2003). This would allow release to occur in the intestines, giving a broader range of drugs which may be used with chitosan. To allow dissolution at a neutral pH N-trimethylated and N-triethylated oligosaccharide forms of the polymer have also been generated. Thus although it is primarily used for mucoadhesive and gastroretentive applications, it is becoming easier to use it in other oral formulations (Agnihotri et al., 2004).

Chitosan has previously been shown to be effective in enhancing the solubility of poorly soluble drugs. For example griseofulvin can be effectively emulsified in chitosan microparticles (Agnihotri et al., 2004). Low molecular weight chitosan can

increase water solubility of oral formulations such as that of docetaxel, insulin and paclitaxel (Markovsky et al., 2012). Chitosan paclitacel conjugates have also been effectively formulated using a biodegradable succinate linker. Cyclosporin A was encapsulated in chitosan nanoparticles for use in eyedrops (Hu et al., 2013). For poorly soluble acidic agents, including indomethecin, the anionic nature of the drug can interact with the cationic nature of the polymer to form a gel, allowing controlled release to occur. More rapid release of the drug can occur in the colon due to the increase in pH enhancing the gelling effect which is initially evoked in the acidic environment of the stomach (Illum, 1998). Chitosan has been effectively used for a gastroretentive drug formulation using the poorly soluble drug verapamil, using both mucoadhesive properties and the ability to float on the gastric fluid (Sonia and Sharma, 2011).

### *4.7 Conclusions*

Ultimately, PEG4000 was shown to effectively melt at high pressure transitioning fully from a solid to a liquid state at 5GPa. Hydrocortisone does not melt under pressure or physically change and thus could be effectively encapsulated in the PEG at high pressure. Drug release was observed to occur from the diamond anvil cell samples in simulated intestinal and gastric fluids over 8 hours in a pulsatile fashion, mimicking traditional cortisol replacement therapy but with one administration rather than multiple administrations daily. The establishment of the inversely proportional relationship of temperature and pressure for the solid to liquid phase transition of PEG allowed the investigation of scale up. Due to the greater mass of drug utilised drug release occurred over 10 days in a similar pulsatile fashion to the small volume study. Unfortunately due to the highly unstable nature of hydrocortisone in aqueous solutions future work would have to consider the use of stabilisers such as fructose or disodium edentate, or carry out studies on a different drug as the pulsatile character of the system could be applied to a number of drugs for conditions exhibiting a circadian rhythm. Overall PEG does increase the solubility of poorly soluble drugs but further work could be carried out in terms of formulation.

## Acknowledgements

The author would like to thank her supervisor Iain Oswald, Dimitrios Lamprou, Amit Delori, Ian Hutchison, Philipp Seib, Anne Goudie and Ibrahim Khadra for all their help, patience and support over the course of this project.

## References


1. Abad-Santos F., Zapater P., Novalabos J., Gallego-Sandín S., Gálvez-Múgica M.A., Priego J. and García A.G., 2002, Survey of Oral Hydrocortisone Utilization in Madrid (Spain), Pharmacological Research, 45(1):15-20

2. Agnihotri S.A., Mallikarjuna N.N. and Aminabhavi T.M., 2004, Recent Advances on Chitosan-based Micro- and Nanoparticles in Drug Delivery, Journal of Controlled Release, 100:5-28

3. Asker A.F. and Whitworth C.W., 1975, Dissolution of Acetylsalicyclic Acid from Acetylsalicyclic Acid-Polyethylene Glycol 6000 Coprecipitates, Die Pharmazie, 30(8):530-531

4. Bansal N.P., Holleran E.M. and Jarowski C.I., 1983, Stabilizing Effect of Fructose on Aqueous Solutions of Hydrocortisone, Journal of Pharmaceutical Sciences, 72(9):1079-1082

5. Barnes P.J., 2010, Theophylline, Pharmaceuticals, 3:725-747

6. Blagden N., De Matas M., Gavan P.T. and York P., 2007, Crystal Engineering of Active Pharmaceutical Ingredients to Improve Solubility and Dissolution Rates, Advanced Drug Delivery Reviews, 59:617-630

7. British Pharmacopoeia Commission Secretariat of the Medicines and Healthcare Products Regulatory Agency, 2014, British Pharmacopoeia, London, U.K., Volume V, Appendix XII B

8. Brooks N.J., Gauthe B.L.L.E., Terrill N.J., Rogers S.E., Templer R.H., Ces O. and Seddon J.M., 2010, Automated High Pressure Cell for Pressure Jump X-ray Diffraction, Review of Scientific Instruments, 81,064103:1-10

9. Burioka N., Fukuoka Y., Koyanagi S., Miyata M., Takata M., Chikumi H., Takane H., Watanabe M., Endo M., Sako T., Suyama H., Ohdo S. and Shimizu E., 2010, Asthma: Chronopharmacotherapy and the Molecular Clock, Advanced Drug Delivery Reviews, 62(9-10):946-955

10. Ceppatelli M., Frediani M. and Bini R., 2011, High-pressure Reactivity of L,L-Lactide, The Journal of Physical Chemistry, 115:2173-2184

11. Chan S. and Debono M., 2010, Replication of Cortisol Circadian Rhythm: New Advances in Hydrocortisone Replacement Therapy, Therapeutic Advances in Endocrinology and Metabolism, 1(3):129-138

12. Chiou W.L. and Riegelman S., 1999, Preparation and Dissolution Characteristics of Several Fast-release Solid Dispersions of Griseofulvin, Journal of Pharmaceutical Sciences, 58:1505-1510

13. Cho C.H., Hui W.M., Liao N.X., Liu X.G., Lam S.K. and Ogle C.W., 1992, Polyethylene Glycol: It's Adverse Gastric Effects in Rats, Journal of Pharmacy and Pharmacology, 44(6):518-520

14. Cho K., Wang X., Nie S., Chen Z.G. and Shin D.M., 2008, Therapeutic Nanoparticles for Drug Delivery in Cancer, Clinical Cancer Research, 14:1310-1316

15. Connor P., 1974, Catalytic Degradation of Hydrocortisone Disodium Phosphate Solutions by Copper(I1) Ions, Science Communications, Journal of Pharmacy and Pharmacology, 26 (Supplement), 69P

16. Daneshvar M., Kim S. and Gulari E., 1990, High-Pressure Phase Equilibria of Poly(ethylene glycol)-Carbon Dioxide Systems, Journal of Physical chemistry, 94:2124-2128

17. Dashevsky A. and Mohamad A., 2006, Development of Pulsatile Multiparticulate Drug Delivery System Coated with Aqueous Dispersion Aquacoat® ECD, International Journal of Pharmaceutics, 318(1-2):124-131

18. Fabbiani F.P.A., Allan D.R., Parsons S. and Pulham C.R, 2005, An Exploration of the Polymorphism of Piracetam using High Pressure, CrystEngComm, 7(29):179-186

19. Fabbiani F.P.A. and Pulham C.R., 2006, High-pressure Studies of Pharmaceutical Compounds and Energetic Materials, Chemical Society Reviews, 35:932-942

20. Fang J. and Kiran E., 2006, Crystallization and Gelation of Isotactic Poly(4-methyl-1-pentene) in *N*-pentane and in *N*-pentane and $CO_2$ at High pressures, Journal of Supercritical Fluids, 38:132-145

21. Fang J. and Kiran E., 2009, Gelation, Crystallization and Morphological Transformations of Syndiotactic Polystyrene in Acetophenone and Acetophenone + Carbon Dioxide Mixtures at High Pressures, Journal of Supercritical Fluids, 49:93-102

22. Feng B., Zarechnyy O.M. and Levitas V.I., 2013, Strain-induced Phase Transformations Under Compression, Unloading, and Reloading in a Diamond Anvil Cell, Journal of Applied Physics, 113, 173514:1-9

23. Fleckenstein B.S., Sterr J. and Langowski H., 2013, The Effect of High Pressure Processing on the Integrity of Polymeric Packaging – Analysis and Categorization of Occurring Defects, Packaging Technology and Science, Online Publication DOI:10.1002/pts.2018:1-21

24. Foroutan and Watson, 1999, The *In Vitro* Evaluation of Polyethylene Glycol Esters of Hydrocortisone 21-succinate as Ocular Prodrugs, International Journal of Pharmaceutics, 182(1):79-92

25. Fox M.E., Szoka F.C. and Fréchet J.M.J., 2009, Soluble Polymer Carriers for the Treatment of Cancer: The Importance of Molecular Architecture, Accounts of Chemical Research, 42(8):1141-1151

26. Franga D.L. and Harris J.A., 2000, Polyethylene Glycol-induced Pancreatitis, Gastrointestinal Endoscopy, 52(6):789-791

27. Funnell N.P., Marshall W.G. and Parsons S., 2011, Alanine at 13.6 GPa and its pressure-induced amorphisation at 15 GPa, CrystEngComm, 13:5841-5848

28. Gillies E.R. and Fréchet J.M.J., 2005, Dendrimers and Dedritic Polymers in Drug Delivery, Drug Delivery Today, 10(1):35-43

29. Gröschl M., Rauh M. and Dörr H.G., 2002, Cortisol and 17-Hydroxyprogesterone Kinetics in Saliva after Oral Administration of Hydrocortisone in Children and Young Adolescents with Congenital Adrenal Hyperplasia due to 21-Hydroxylase Deficiency, Journal of Clinical Endocrinology & Metabolism, 87(3):1200-1204

30. Guo Y., Wang X., Shu X., Shen Z. and Sun R., 2012, Self-Assembly and Paclitaxel Loading Capacity of Cellulose-graft-poly(lactide) Nanomicelles, Journal of Agricultural and Food Chemistry, 60:3900-3908

31. Hansen J. and Bundgaard H., 1980, Studies on the Stability of Corticosteroids V. The Degradation Pattern of Hydrocortisone in Aqueous Solution, International Journal of Pharmaceutics, 6:307-319

32. Hazen R.M. and Finger L.W., 1981, High-temperature Diamond-anvil Pressure Cell for Single-crystal Studies, Review of Scientific Instruments, 52:75-79

33. Hejazi R. and Amiji M., 2003, Chitosan-based Gastrointestinal Delivery Systems, Journal of Controlled Release, 89:151-165

34. Hu L., Sun Y. and Wu Y., 2013, Advances in Chitosan-based Drug Delivery Vehicles, Nanoscale, 5:3103-3111

35. Huh K.M., Lee S.C., Cho Y.W., Lee J., Jeong J.H. and Park K., 2005, Hydrotropic Polymer Micelle System for Delivery of Paclitaxel, Journal of Controlled Release, 101(1-3):59-68

36. Illum L., 1998, Chitosan and Its Use as a Pharmaceutical Excipient, Pharmaceutical Reseach, 15(9):1326-1331

37. Janssens S. and Van Den Mooter G., 2009, Review: Physical Chemistry of Solid Dispersions, The Journal of Pharmacy and Pharmacology, 61(12):1571-1586

38. Jenkins A.D., Kratochvíl P., Stepto R.F.T. and Suter U.W., 1996, International Union of Pure and Applied Chemistry: Glossary of Basic Terms in Polymer Science, Pure and Applied Chemistry, 68(12):2287-2311

39. Johannsson G., Bergthorsdottir R., Nilsson A.G., Lennernas H., Hedner T. and Skrtic S., 2009, Improving Glucocorticoid Replacement Therapy Using a Novel Modified-release Hydrocortisone Tablet: a Pharmacokinetic Study, European Journal of Endocrinology, 161:119-130

40. Johannsson G., Filipsson H., Bergthorsdottir R., Lennernäs H. and Skrtic S., 2007, Long-Acting Hydrocortisone for Glucocorticoid Replacement Therapy, Hormone Research, 68(Supplement 5):182-188

41. Johnston B.F., Marshall W.G., Parsons S., Urquhart A.J. and Oswald I.D.H., 2014, Investigation of Acrylic Acid at High Pressure Using Neutron Diffraction, Journal of Physical Chemistry B, 118(14):4044-4051

42. Joshi H.N., Tejwani R.W., Davidovich M., Sahasrabudhe V.P., Jemal M., Bathala M.S., Varia S.A. and Serajuddin A.T.M., 2004, Bioavailabilty Enhancement of a Poorly Water-soluble Drug by Solid Dispersion in Polyethylene Glycol-polysorbate 80 Mixture, International Journal of Pharmaceutics, 269:251-258

43. Kawabata Y., Wada K., Nakatani M., Yamada S. and Onoue S., 2011, Formulation Design for Poorly Water-soluble Drugs Based on Biopharmaceutics Classification System: Basic Approaches and Practical Applications, International Journal of Pharmaceutics, 420:1-10

44. Kawakami K., 2012, Modification of Physicochemical Characteristics of Active Pharmaceutical Ingredients and Application of Supersaturatable Dosag Forms for Improving Bioavailability of Poorly Absorbed Drugs, Advanced Drug Delivery Reviews, 64:480-495

45. Kim J.Y., Kim S., Pinal R. and Park K., 2011, Hydrotropic Polymer Micelles as Versatile Vehicles for Delivery of Poorly Water-soluble Drugs, Journal of Controlled Release, 152:13-20

46. Kim S., Kim J., Jeon O., Kwon I.C. and Park K., 2009, Engineered Polymers for Advanced Drug Delivery, European Journal of Pharmaceutics and Biopharmaceutics, 71:420-430

47. Kirkorian K., Ellis A. and Twyman L.J., 2012, Catalytic Hyperbranched Polymers as Enzyme Mimics; Exploiting the Principles of Encapsulation and Supramolecular Chemistry, Chemical Society Reviews, 41:6138-6159

48. Kirwan J.R. and Buttgereit F., 2012, Symptom Control with Low-dose Glucocorticoid Therapy for Rheumatoid Arthritis, Rheumatology, 51(4):14-20

49. Knop K., Hoogenboom R., Fischer D. and Schubert U.S., 2010, Poly(ethylene glycol) in Drug Delivery: Pros and Cons as well as Potential Alternatives, Angewandte Chemie International Edition, 49:6288-6308

50. Kolhe P., Khandare J., Pillai O., Kannan S., Lieh-Lai M. and Kannan R., 2004, Hyperbranched Polymer-Drug Conjugates with High Drug Payload for Enhanced Cellular Delivery, Pharmaceutical Research, 21(12):2185-2195

51. Ku M.S. and Dulin W., 2012, A Biopharmaceutical Classification-based Right-First-Time Formulation Approach to Reduce Human Pharmacokinetic Variability and Project Cycle time from First-In-Human to Clinical Proof-Of-Concept, Pharmaceutical Development and Technology, 17(3):285-302

52. Kumar B.P., Chandiran I.S., Bhavya B. and Sindhuri M., 2011, Micoparticulate Drug Delivery System: A Review, Indian Journal of Pharmaceutical Science and Research, 1(1):19-37

53. Lee M.K., Kim S., Ahn C. and Lee J., 2010, Hydrophilic and Hydrophobic Amino Acid Copolymers for Nano-comminution of Poorly Soluble Drugs, International Journal of Pharmaceutics, 384:173-180

54. Leuner C. and Dressman J., 2000, Improving Drug Solubility for Oral Delivery Using Solid Dispersions, European Journal of Pharmaceutics and Biopharmaceutics, 50:47-60

55. Li Q., Xiao X., Zhang X. and Zhang W., 2013, Controlled Synthesis of Graft Polymer Through the Coupling Reaction Between the Appending β-keto Ester and the Terminal Amine, Polymer, 54:3230-3237

56. Li X. and Jasti B.R., 2005, Design of Controlled Release Drug Delivery Systems, McGraw-Hill Professional, New York, pages 34, 166 and 348

57. Madhav N.V.S. and Kala S., 2011, Review on Microparticulate Drug Delivery System, International Journal of PharmTech Research, 3(3):1242-1254

58. Markovsky E., Baabur-Cohen H., Eldar-Boock A., Omer L., Tiram G., Ferber S., Ofek P., Polyak D., Scomparin A. and Satchi-Fainaro R., 2012, Administration, Distribution, Metabolism and Elimination of Polymer Therapeutics, Journal of Controlled Release, 161:446-460

59. McConnell E.M., Bell P.M., Ennis C., Hadden D.R., McCance D.R., Sheridan B. and Atkinson A. B., 2002, Effects of Low-dose Oral Hydrocortisone Replacement Versus Short-term Reproduction of Physiological Serum Cortisol Concentrations on Insulin Action in Adult-onset Hypopituitarism, Clinical Endocrinology, 56:195-201

60. Merrill L. and Bassett W.A., 1974, Miniature Diamond Anvil Pressure Cell for Single Crystal Xray Diffraction Studies, Review of Scientific Instruments, 45:290-294

61. Narang A.S. and Varia S., 2011, Role of Tumor Vascular Architecture in Drug Delivery, Advanced Drug Delivery Reviews, 63:640-658

62. Nikolaus T., Kruse W., Bach M. and Specht-Leible N., 1996, Elderly Patients' Problems with Medication, European Journal of Clinical Pharmacology, 49:255-259

63. Ooya T., Lee J. and Park K., 2003, Effects of Ethylene Glycol-based Graft, Star-shaped, and Dendritic Polymers on Solubilization and Controlled Release of Paclitaxel, Journal of Controlled Release, 93:121-127

64. Pouton C.W., 2006, Formulation of Poorly Water-soluble Drugs for Oral Administration: Physicochemical and Physiological Issues and the Lipid Formulation Classification System, European Journal of Pharmaceutical Sciences, 29:278-287

65. Price J.C., Wade A. and Weller P.J., 1994, Handbook of Pharmaceutical Excipients, American Pharmaceutical Association/ The Pharmaceutical Press, Washington D.C. and London, pages 355-361

66. Pühse M., Keerl M., Scherzinger C., Richtering W. and Winter R., 2010, Influence of Pressure on the State of Poly(*N*-isopropylacrylamide) and Poly(*N*,*N*-diethylacrylamide) Derived Polymers in Aqueous Solution as Probed by FTIR-Spectroscopy, Polymer, 51:3653-3659

67. Qui L.Y. and Bae Y.H., 2006, Polymer Architecture and Drug Delivery, Pharmaceutical Research, 23(1):1-30

68. Ranade V.V. and Hollinger M.A., 2004, Drug Delivery Systems, MyiLibrary. 2nd ed., CRC Press, Boca Ranton, Florida, pages 63-114

69. Rao N.G.R., Soumya P., Revathi K. and Nayak B.S., 2013, A Review on Pulsatile Drug Delivery System, International Research Journal of Pharmacy, 4(3):31-44

70. Roberts A.D. and Zhang H., 2013, Poorly Water-soluble Drug Nanoparticles via Solvent Evaporation in Water-soluble Porous Polymers, International Journal of Pharmaceutics, 447:241-250

71. Sant V.P., Smith D. and Leroux J., 2004, Novel pH-sensitive Supramolecular Assemblies for Oral Delivery of Poorly Water Soluble Drugs: Preparation and Characterization, Journal of Controlled Release, 97:301-312

72. Seeger A., Freitag D., Freidel F. and Luft G., 2004, Melting Point of Polymers Under High Pressure Part I: Influence of the Polymer Properties, Thermochimica Acta, 424:175-181

73. Serpe M.J. and Craig S.L., 2007, Physical Organic Chemistry of Supramolecular Polymers, Langmuir, 23:1626-1634

74. Shinoda K. and Noguchi N., 2008, An Induction Heating Diamond Anvil Cell for High Pressure and Temperature Micro-Raman Spectroscopic Measurements, Review of Scientific Instruments, 79(015101):1-4

75. Simon N., Castinetti F., Ouliac F., Lesavre N., Brue T. and Oliver C., 2010, Pharmacokinetic Evidence for Suboptimal Treatment of Adrenal Insufficiency with Currently Available Hydrocortisone Tablets, Clinical Pharmacokinetics, 49(7):455-463

76. Sonia T.A. and Sharma C.P., 2011, Chitosan and Its Derivatives for Drug Delivery Perspective, Advanced Polymer Science, 243:23-54

77. Soppimath K.S., Aminabhavi T.M., Kulkarni A.R. and Rudzinski W.E., 2001, Biodegradable Polymeric Nanoparticles as Drug Delivery Devices, Journal of Controlled Release, 70:1-20

78. Stevenson C.L., Santini J.T. Jr. and Langer R., 2012, Reservoir-Based Drug Delivery Systems Utilizing Microtechnology, Advanced Drug Delivery Reviews, 64:1590-1602

79. Suitchmezian V., Jeβ and Näther C., 2007, Structural, Thermodynamic, and Kinetic Aspects of the Trimorphism of Hydrocortisone, Journal of Pharmaceutical Sciences, 97(10):4516-4527

80. Suttiruengwong S., Rolker J., Smirnova I., Arlt W., Seiler M., Lüderitz L., Pérez de Diego Y. and Jansens P.J., 2006, Hyperbranched Polymers as Drug Carriers: Microencapsulation Kinetics, Pharmaceutical Development and Technology, 11:55-70

81. Tahara K., Yamamoto K. and Nishihata T., 1996, Application of Model-independent and Model Analysis for the Investigation of Effect of Drug Solubility on its Release Rate from Hydroxypropyl Methylcellulose Sustained Release Tablets, The International Journal of Pharmaceutics, 133:17-27

82. Takale A.A., Banerjee S.K., Gadhave M.V. and Gaikwad D.D., 2012, Microparticles in Drug Delivery System: A Review, International Journal of Institutional Pharmacy and Life Sciences, 2(2):349-359

83. Tangri P. and Khurana S., 2011, Pulsatile Drug Delivery Systems: Methods and Advances, International Journal of Drug Formulation and Research, 2(3):100-102

84. Threlfall T.L., 1995, Analysis of Organic Polymorphs, Analyst, 120:2435-2460

85. Toothaker R.D., Sundaresan G.M., Hunt J.P., Goehl T.J., Rotenberg K.S., Prasad V.K., Craig W.A. and Welling P.G.

86. Torchilin V.P., 2004, Targeted Polymeric Micelles for Delivery of Poorly Soluble Drugs, 61:2549-2559

87. Trapani G., Franco M., Latrofa A., Pantaleo M.R., Provenzano M.R., Sanna E., Maciocco E. and Liso G., 1999, Physicochemical Characterization and In Vivo Properties of Zolpidem in Solid Dispersions with Polyethylene Glycol 4000 and 6000, International Journal of Pharmaceutics, 184:121–130

88. Ussher M., Aveyard P., Reid F., West R., Evans P., Clow A., Hucklebridge F., Fuller J., Ibison J. and Steptoe A., 2011, A Randomised Placebo-controlled Trial of Oral Hydrocortisone for Treating Tobacco Withdrawal Symptoms, Psychopharmacology, 216:43-51

89. Vasconcelos T., Sarmento B. and Costa P., 2007, Solid Dispersions as Strategy to Improve Oral Bioavailability of Poor Water Soluble Drugs, Drug Discovery Today, 12(23/24):1068-1075

90. Veronese F.M. and Pasut G., 2005, PEGylation, Successful Approach to Drug Delivery, Drug Delivery Today, 10:1451-1458

91. Walters M.J. and Dunbar W.E., 1982, High-Performance Liquid Chromatographic Analysis of Hydrocortisone Drug Substance, Tablets, and Enema, Journal of Pharmaceutical Sciences, 71(4):446-451

92. Wang J.J., Zeng Z.W., Xiao R.Z., Xie T., Zhou G.L., Zhan X.R. and Wang S.L., 2011, Recent Advances of Chitosan Nanoparticles as Drug Carriers, International Journal of Nanomedicine, 6:765-774

93. Xiong Y. and Kiran E., 1998, High-pressure Light Scattering Apparatus to Study Pressure-induced Phase Separation in Polymer Solutions, Review of Scientific Instruments, 69:1463-1471

94. Yang W. and Pierstorff E., 2012, Reservoir-Based Polymer Drug Delivery Systems, Journal of Laboratory Automation, 17(1):50-58

95. Zarechnyy O.M., Levitas V.I. and Ma Y., 2012, Coupled Plastic Flow and Phase Transformation Under Compression of Materials in a Diamond Anvil Cell: Effects of Transformation Kinetics and Yield Strength, Journal of Applied Physics, 111, 023518:1-5

# Appendices

## *Appendix 1: 90:10 PEG:Hydrocortisone Pressure Studies*

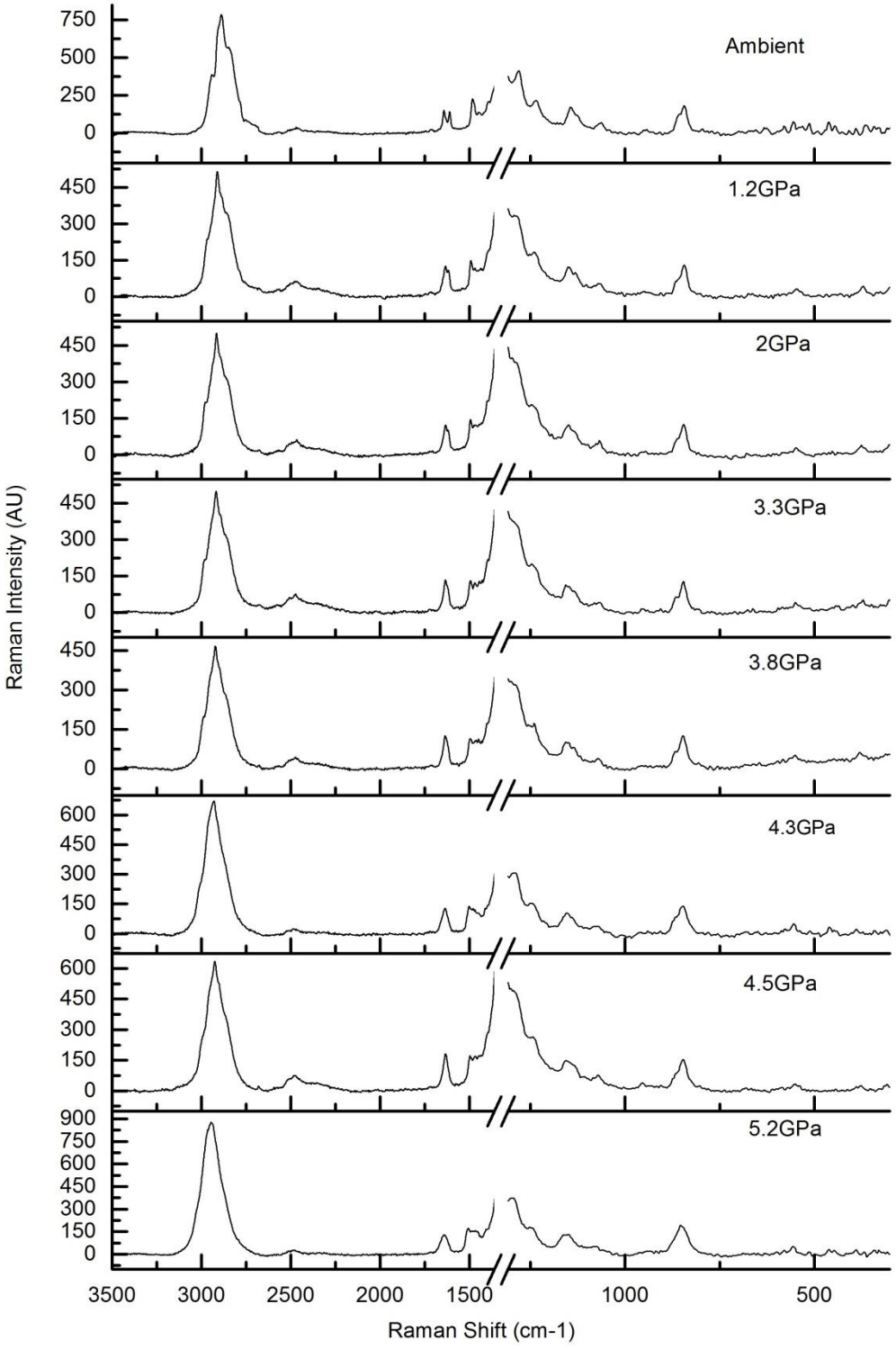


A1.1: Raman spectra of the 90:10 PEG:hydrocortisone blend illustrating the effect of increasing pressure.

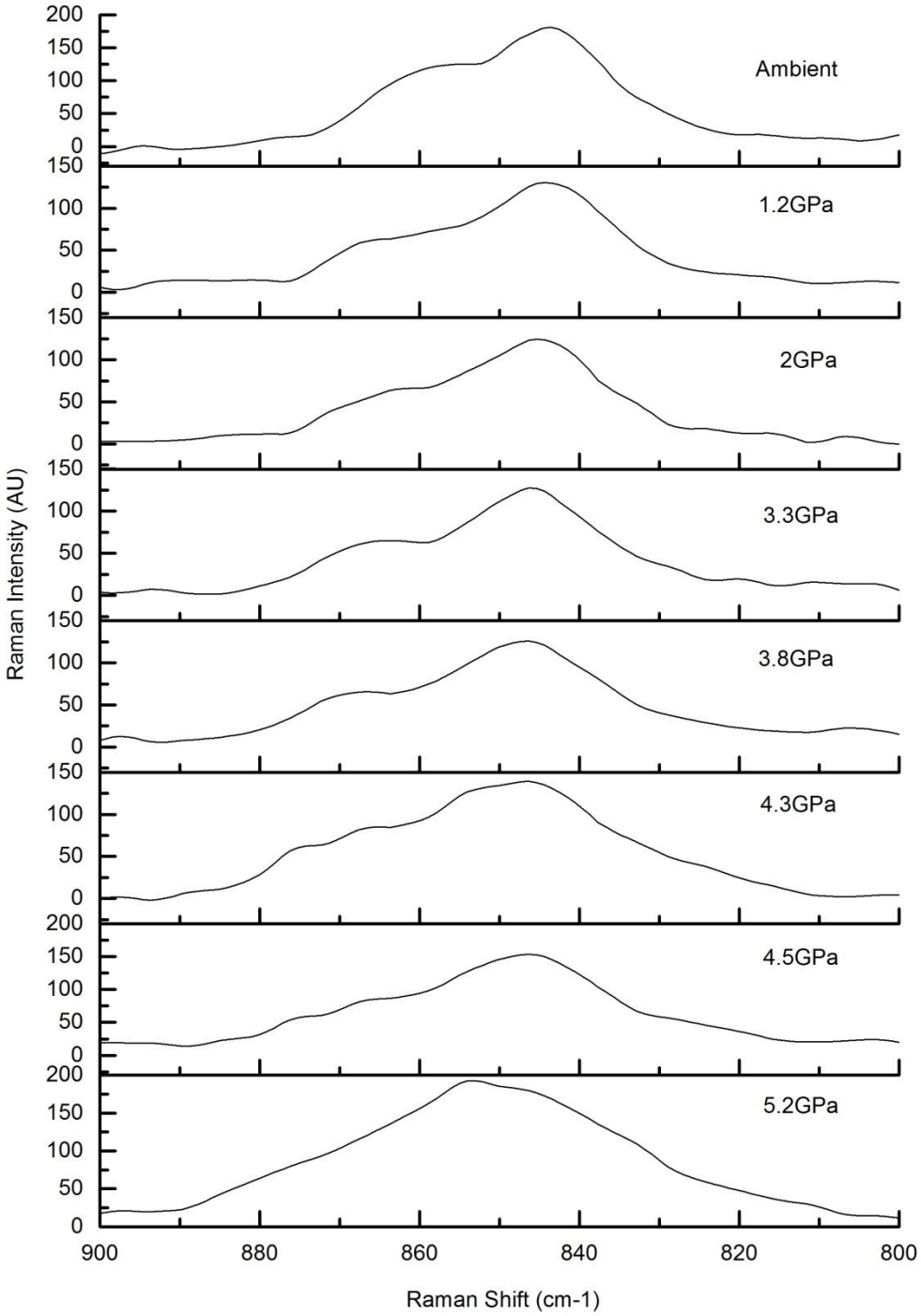


A1.2: Raman spectra of the C-O-C region of the 90:10 PEG:hydrocortisone blend illustrating the effect of increasing pressure.

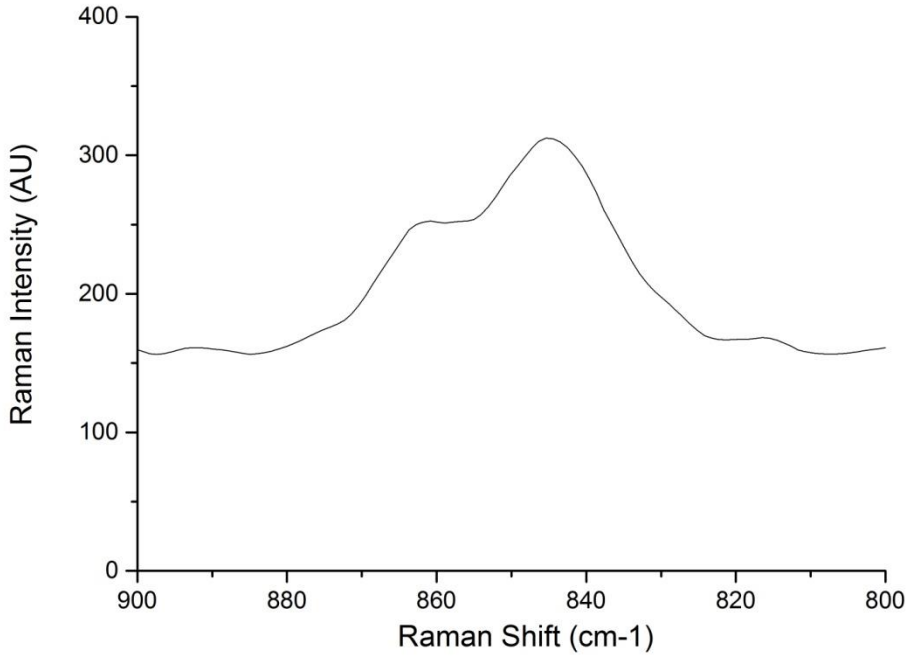


A1.3: Raman spectrum of the 90:10 PEG:hydrocortisone blend C-O-C region after pressure removal.

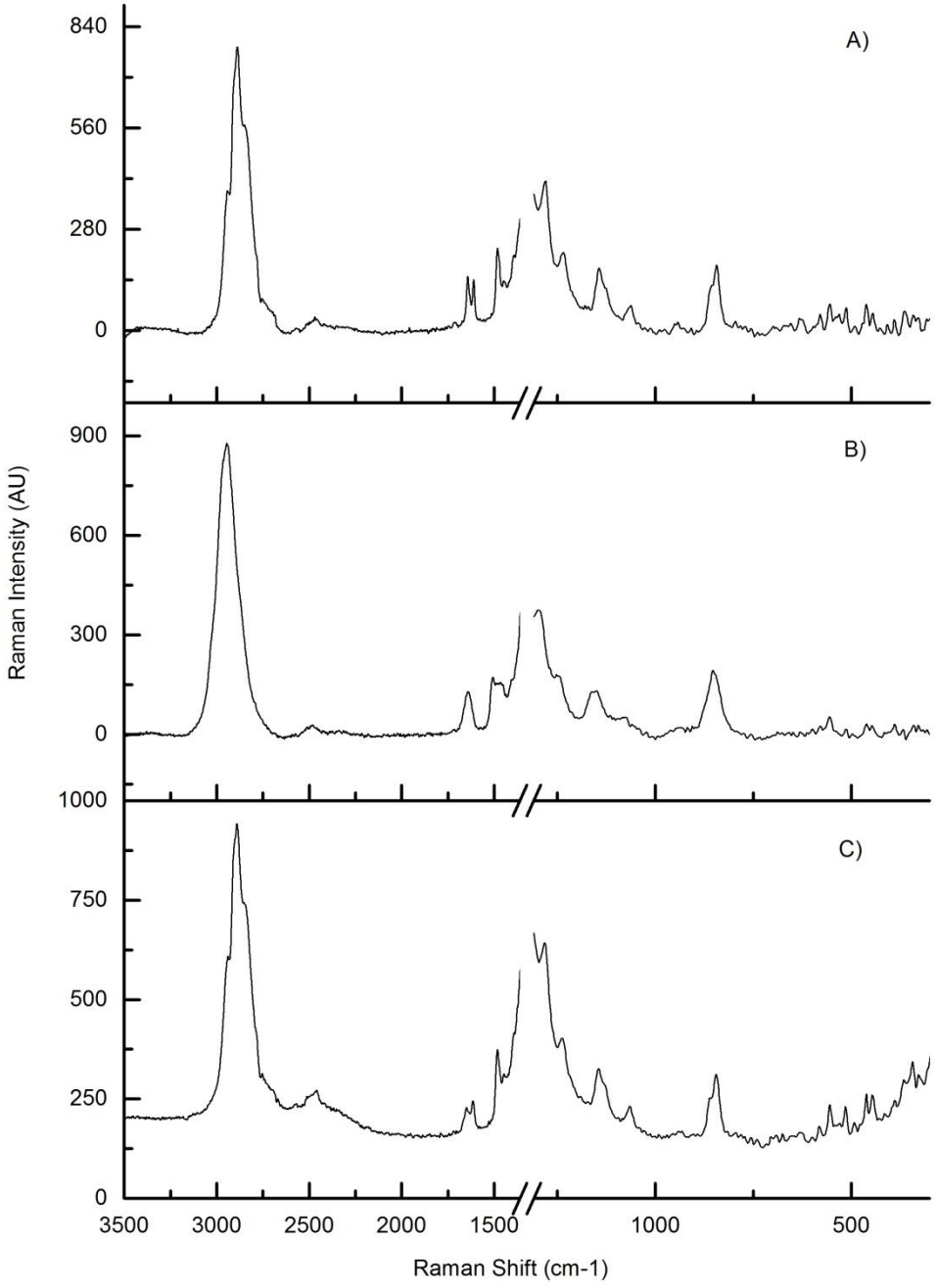


A1.4: Raman spectra showing the effect of pressure removal on the 90:10 PEG:hydrocortisone blend, illustrating A) the blend at ambient pressure, B) at 5GPa and C) after pressure removal.

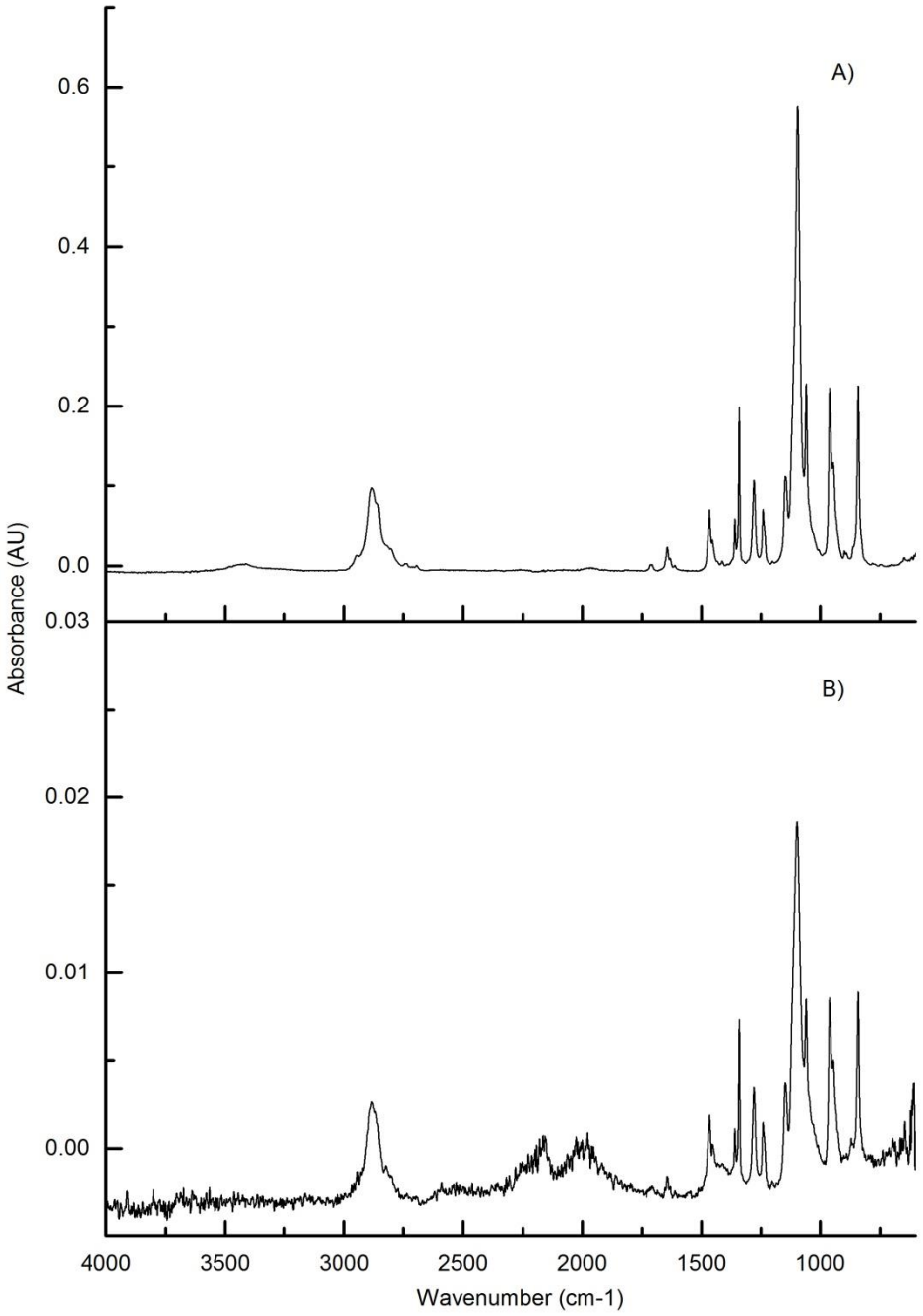


A1.5: Infrared spectra of the 90:10 PEG:hydrocortisone blend illustrating the effect of pressure by comparison of the sample A) under ambient conditions and B) after pressure.

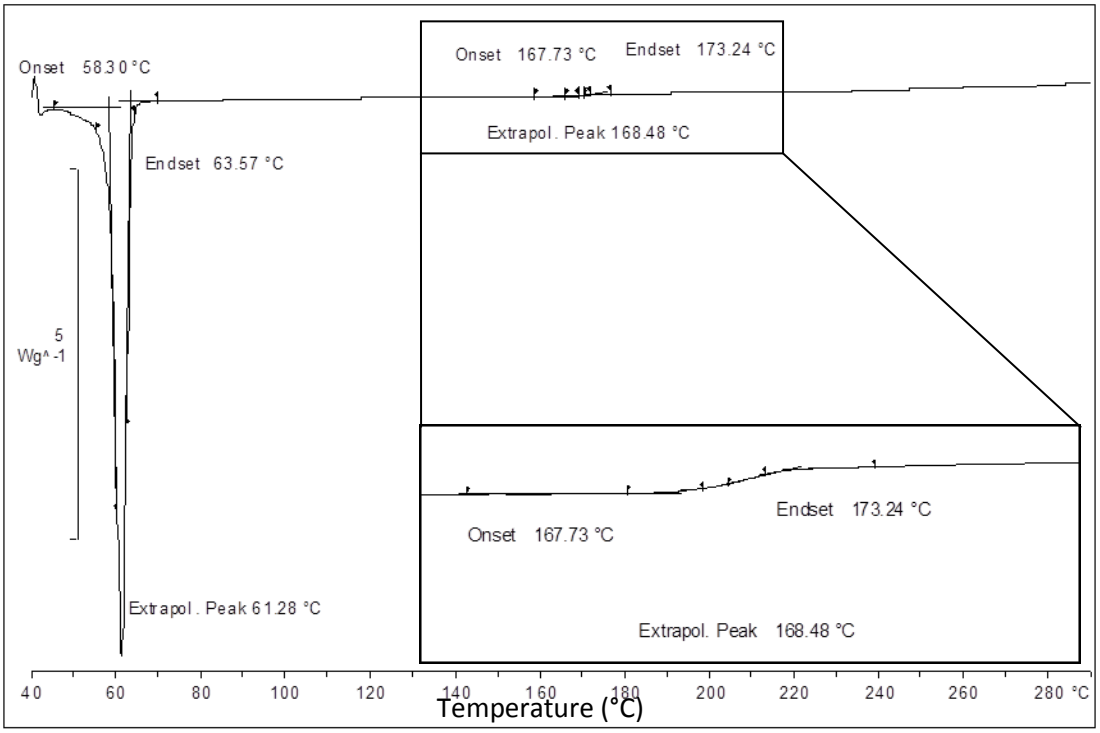


A1.6: Differential scanning calorimetry of the 90:10 PEG:hydrocortisone sample, showing the melting points for PEG and hydrocortisone.

A1.7: Differential scanning calorimetry of 3 replicates of 90:10 PEG:hydrocortisone, with the mean onset, extrapolated peak and endset temperatures.

| | PEG | | | Hydrocortisone | | |
|---|---|---|---|---|---|---|
| Sample | Onset (°C) | Extrapolated peak (°C) | Endset (°C) | Onset (°C) | Extrapolated Peak (°C) | Endset (°C) |
| 1 | 58.30 | 61.28 | 63.57 | 167.73 | 168.48 | 173.24 |
| 2 | 58.08 | 61.31 | 62.81 | 168.49 | 168.83 | 173.01 |
| 3 | 58.03 | 61.69 | 63.30 | 166.80 | 169.20 | 172.95 |
| Average | 58.14 | 61.43 | 63.23 | 167.67 | 168.84 | 173.07 |
| S.E. | 0.082932 | 0.131951 | 0.222436 | 0.488683 | 0.207873 | 0.08838 |

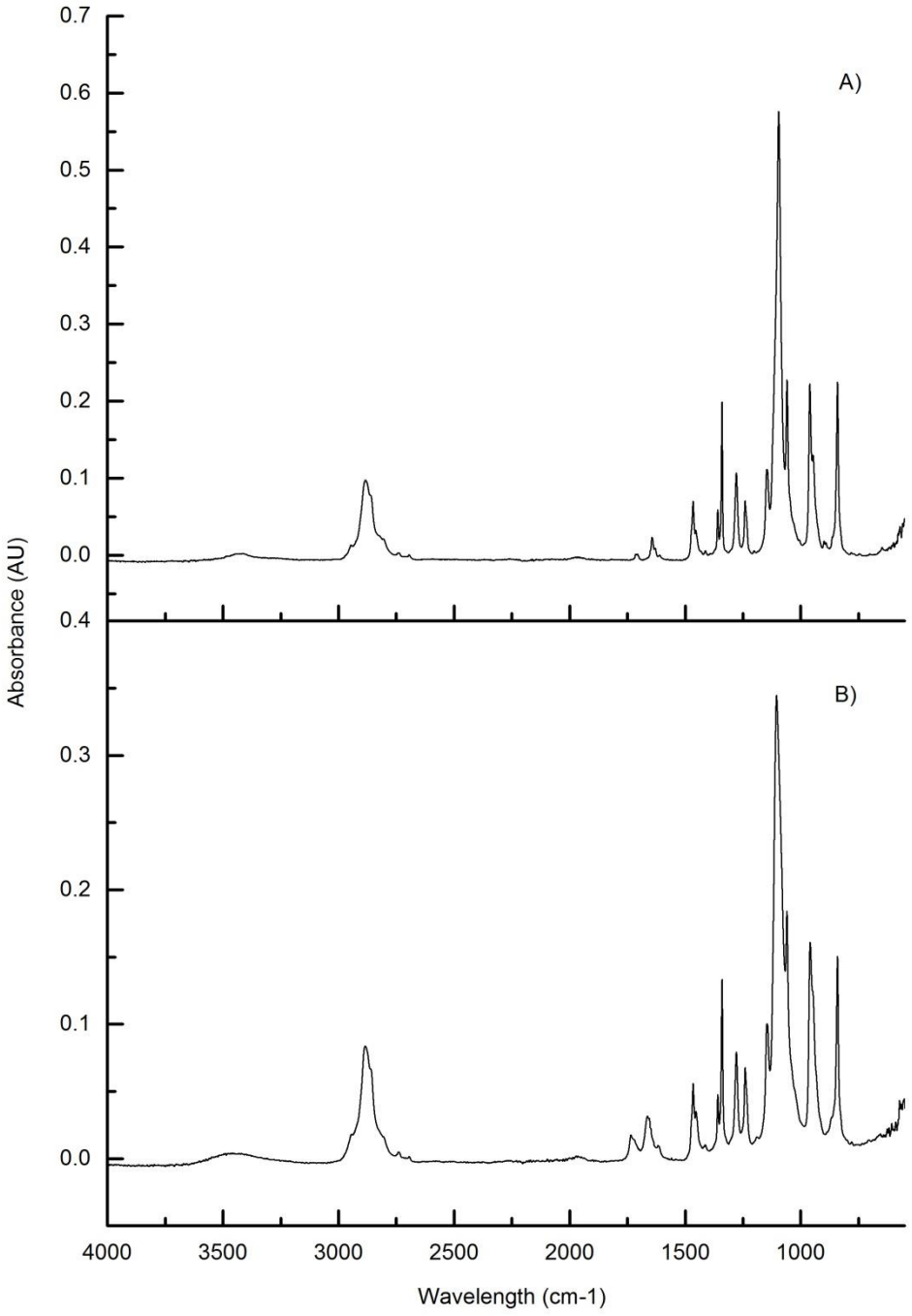


A1.8: Infrared spectra illustrating the effect of DSC treatment on the functional groups of 90:10 PEG:hydrocortisone samples by comparing the spectra A) before and B) after DSC treatment.

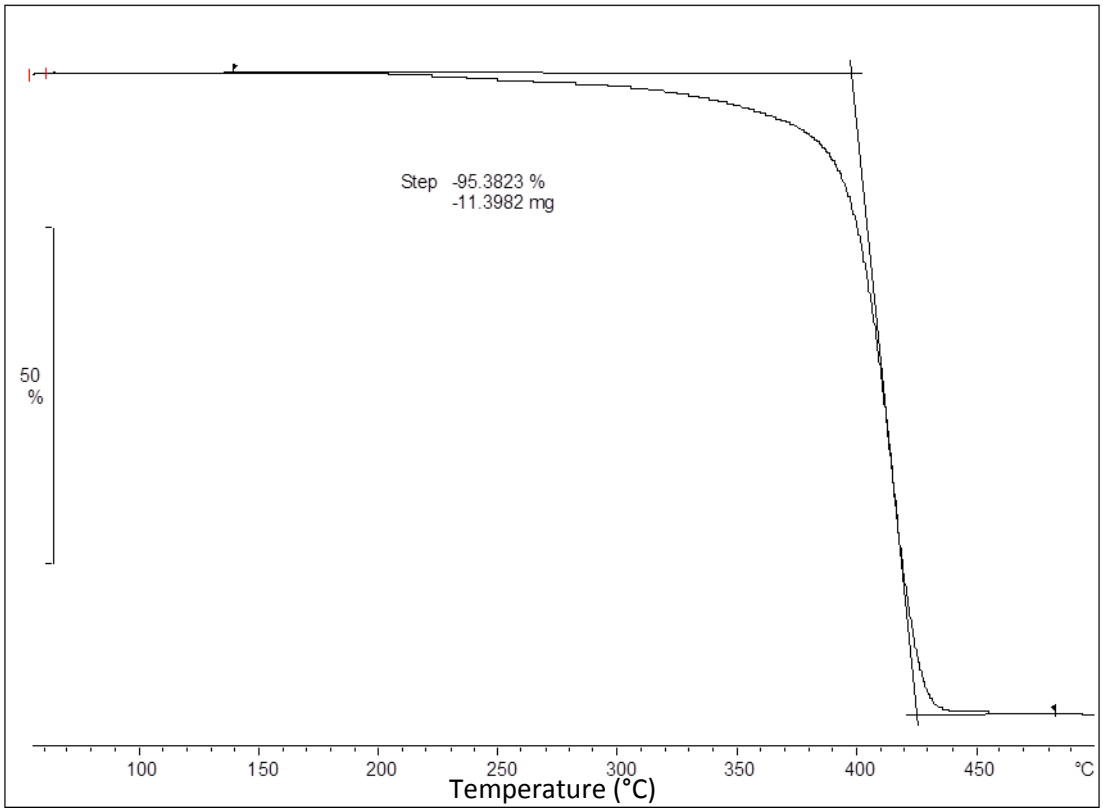


A1.9: Thermogravimetric analyis of the 90:10 PEG:hydrocortisone sample, showing the percentage degradation.

A1.10: Thermogravimetric analysis of 3 replicates of 90:10 PEG:hydrocortisone, giving the mean percentage degradation.

| Sample | Approximate Temperature Range (°C) | Percentage degradation (%) |
|---|---|---|
| 1 | 200-460 | 95.3823 |
| 2 | 200-465 | 95.1172 |
| 3 | 215-455 | 93.2281 |
| Average | 205-460 | 94.58 |
| S.E. | 5 and 2.888751 | 0.678215 |

***Appendix 2: 80:20 PEG:Hydrocortisone Pressure Studies***

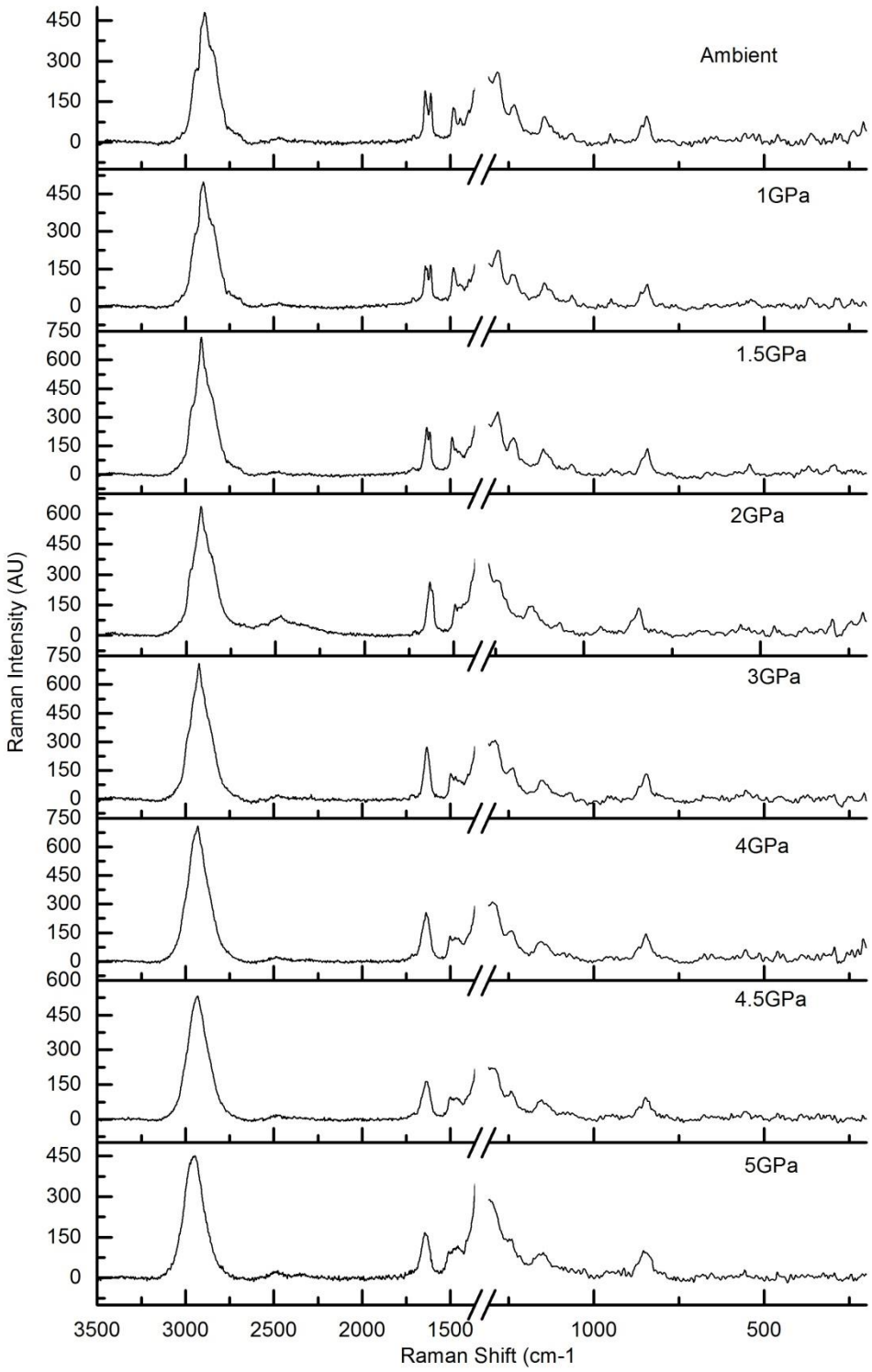


A2.1: Raman spectra of the 90:10 PEG:hydrocortisone blend illustrating the effect of increasing pressure.

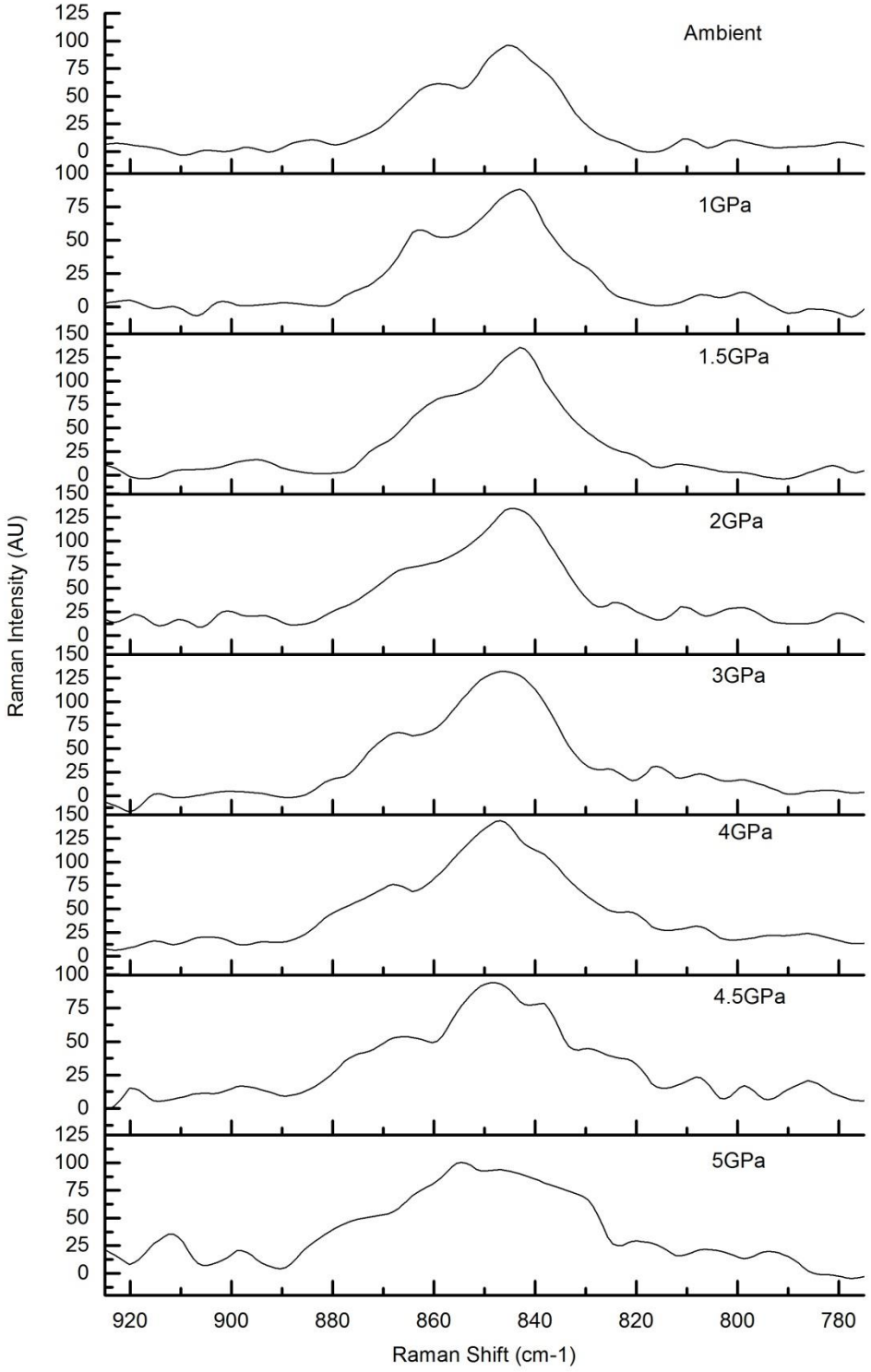


A2.2: Raman spectra of the C-O-C region of the 90:10 PEG:hydrocortisone blend illustrating the effect of increasing pressure.

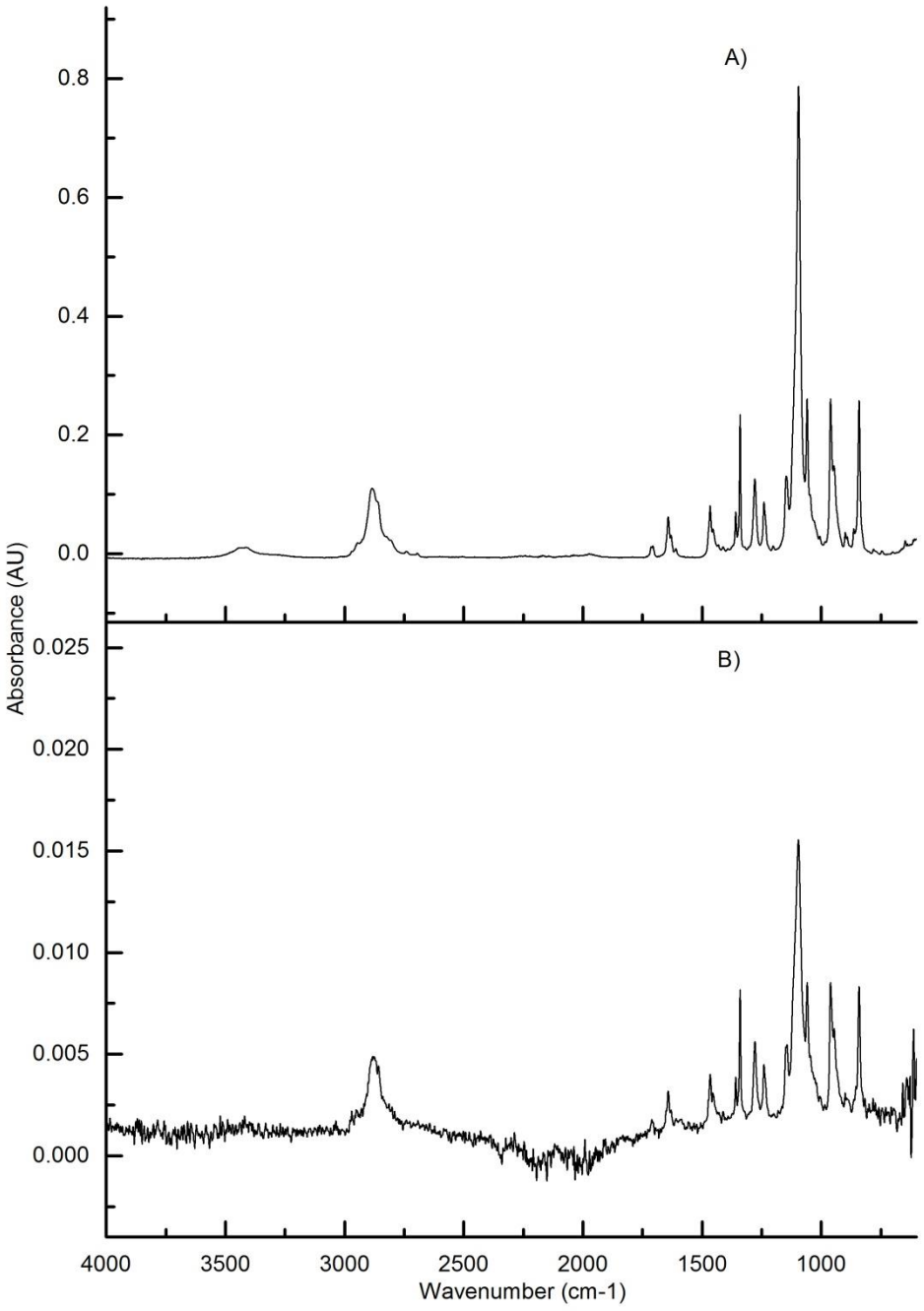


A2.3: Infrared spectra of the 90:10 PEG:hydrocortisone blend illustrating the effect of increasing pressure, comparing the sample at A) ambient and B) after pressure.

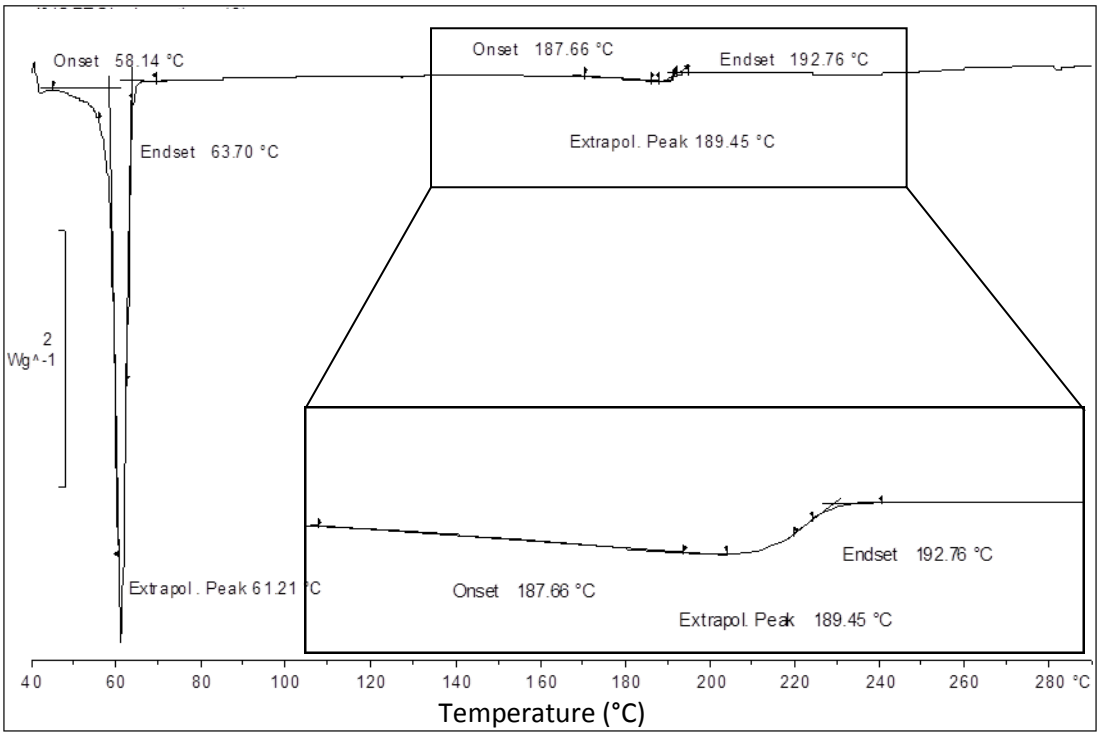


A2.4: Differential scanning calorimetry of the 80:20 PEG:hydrocortisone sample, showing the melting points for PEG and hydrocortisone.

A2.5: Differential scanning calorimetry of 3 replicates of 80:20 PEG:hydrocortisone, with the mean onset, extrapolated peak and endset temperatures.

| | PEG | | | Hydrocortisone | | |
|---|---|---|---|---|---|---|
| Sample | Onset (°C) | Extrapolated Peak (°C) | Endset (°C) | Onset (°C) | Extrapolated Peak (°C) | Endset (°C) |
| 1 | 57.92 | 60.82 | 63.06 | 184.10 | 189.49 | 193.46 |
| 2 | 58.32 | 61.22 | 63.03 | 187.01 | 187.11 | 193.00 |
| 3 | 58.14 | 61.21 | 63.70 | 187.66 | 189.45 | 192.76 |
| Average | 58.13 | 61.08 | 63.26 | 186.26 | 188.68 | 193.07 |
| S.E. | 0.115662 | 0.131698 | 0.218505 | 1.094537 | 0.786751 | 0.205372 |

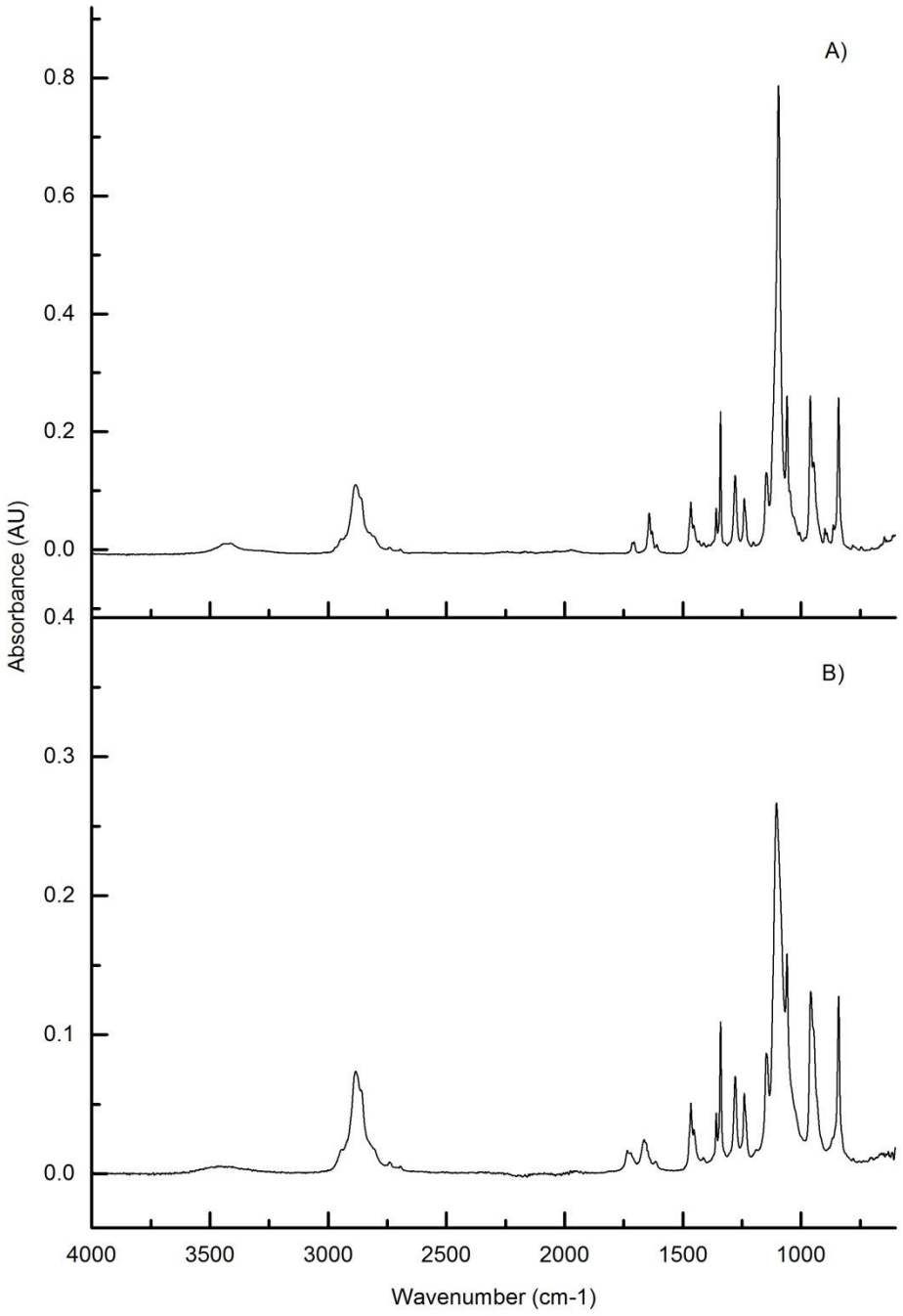


A2.6: Infrared spectra of the 80:20 PEG:hydrocortisone blend illustrating the effect of DSC treatment, by comparison of the sample A) at ambient and B) after DSC.

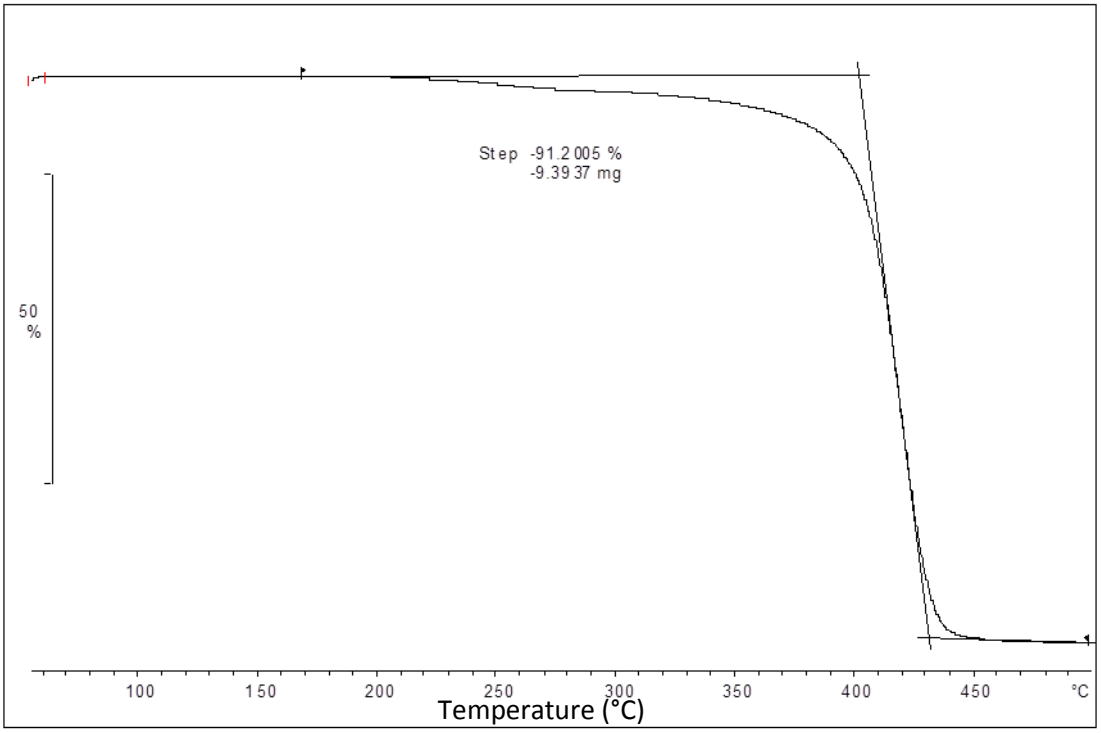


A2.7: Thermogravimetric analysis of the 80:20 PEG:hydrocortisone sample, showing the percentage degradation.

A2.8: Thermogravimetric analysis of 3 replicates of 80:20 PEG:hydrocortisone, giving the mean percentage degradation.

| Sample | Approximate Temperature Range (°C) | Percentage degradation (%) |
|---|---|---|
| 1 | 205-460 | 91.2005 |
| 2 | 210-470 | 91.8904 |
| 3 | 205-465 | 91.1186 |
| Average | 205.67-465 | 91.40 |
| S.E. | 1.67 and 2.886751 | 0.244761 |

***Appendix 3: 50:50 PEG:Hydrocortisone Drug Release***

A3.1: Standard Error (±) of Drug Release from Diamond Anvil Cell Generated Samples as Illustrated by Error Bars in Figure 46

| Time (h) | Simulated Intestinal Fluid (% Drug Release) | | Simulated Gastric Fluid (% Drug Release) | |
|---|---|---|---|---|
| | Pure Hydrocortisone | Hydrocortisone with Derivatives | Pure Hydrocortisone | Hydrocortisone with Derivatives |
| 0 | 0 | 0 | 0 | 0 |
| 0.255 | 1.63 | 9.50 | 1.48 | 1.59 |
| 0.5 | 1.81 | 10.58 | 1.67 | 4.12 |
| 1 | 1.60 | 12.51 | 2.14 | 12.55 |
| 2 | 1.63 | 12.11 | 1.95 | 11.13 |
| 3 | 3.92 | 12.58 | 2.18 | 16.30 |
| 4 | 2.29 | 14.44 | 2.67 | 16.94 |
| 5 | 2.71 | 17.29 | 2.31 | 11.96 |
| 6 | 3.22 | 13.17 | 3.20 | 15.56 |
| 7 | 8.34 | 17.41 | 2.79 | 14.89 |
| 8 | 11.05 | 12.26 | 4.69 | 2.73 |
| 24 | 3.12 | 21.02 | 7.75 | 17.96 |

A3.2: Standard Error (±) of Drug Release in Simulated Intestinal Fluid from Pressure Scale Up as Illustrated by Error Bars in Figure 51

| Time (h) | Pure Hydrocortisone (% Drug Release) | Hydrocortisone with Derivatives (% Drug Release) |
|---|---|---|
| 0 | 0 | 0 |
| 0.25 | 0.16 | 0.18 |
| 0.5 | 0.18 | 0.22 |
| 1 | 1.09 | 1.20 |
| 2 | 1.24 | 1.37 |
| 3 | 1.35 | 1.53 |
| 4 | 1.62 | 1.95 |
| 5 | 1.76 | 2.00 |
| 6 | 1.89 | 2.12 |
| 7 | 1.90 | 2.19 |
| 8 | 2.20 | 2.46 |
| 24 | 1.00 | 2.39 |
| 48 | 4.88 | 6.31 |
| 72 | 7.48 | 8.79 |
| 168 | 14.06 | 13.43 |
| 216 | 9.64 | 5.03 |
| 240 | 10.12 | 5.57 |

A3.3: Standard Error (±) of Drug Release in Simulated Gastric Fluid from Pressure Scale Up as Illustrated by Error Bars in Figure 52

| Time (h) | Pure Hydrocortisone (% Drug Release) | Hydrocortisone with Derivatives (% Drug Release) |
|---|---|---|
| 0 | 0 | 0 |
| 0.25 | 0.07 | 0.16 |
| 0.5 | 0.14 | 0.22 |
| 1 | 0.15 | 0.47 |
| 2 | 0.33 | 0.69 |
| 3 | 0.52 | 0.79 |
| 4 | 0.73 | 0.93 |
| 5 | 0.91 | 1.18 |
| 6 | 1.10 | 1.36 |
| 7 | 1.16 | 1.54 |
| 8 | 1.23 | 1.71 |
| 24 | 3.16 | 11.58 |
| 48 | 3.27 | 11.95 |
| 72 | 11.29 | 6.87 |
| 168 | 22.10 | 14.89 |
| 216 | 27.88 | 17.79 |
| 240 | 28.64 | 17.93 |